An Eigenscrew Analysis of Mechanism Compliance

by

Patricia Leigh McAllister

A thesis submitted to the
Department of Mechanical Engineering
in conformity with the requirements for
the degree of Master of Science (Engineering)

Queen's University
Kingston, Ontario, Canada
December 1998

0-612-36056-3

Abstract

Determination of the magnitudes and directions of the constraints of a mechanical system can be achieved by finding the basis of the system's characteristic compliance or stiffness matrix. When little is known about the geometry of the system, conventional methods cannot be used to calculate the system's compliance or stiffness matrix. A new method has been developed that uses experimental data to calculate a system's compliance matrix, and an eigenvalue decomposition to extract the directions and magnitudes of the system constraints. The system was assumed to be a mechanism in equilibrium. The data were wrenches applied to the system and the mechanism's resulting displacement from equilibrium. Wrenches and displacements were assumed to be linearly related by the system's compliance matrix.

Imperfect data were managed by estimating a symmetric positive semi-definite approximation to the compliance matrix. Eigenscrew decomposition was used to calculate the eigenscrew direction, pitch, and rotational and translational compliance. The eigenscrew pitches and compliances were analyzed to determine the mechanism's compliances and constraints.

Computer simulations suggest that the method reliably finds eigenscrews, pitches, compliances and directions for well-conditioned matrices. Eigenscrew pitches and compliances can be found for ill-conditioned matrices. The analytical technique can

be used to evaluate the static behaviour of a system. It may prove valuable as a design and analysis tool for biomechanics, robotics and automation.

Acknowledgements

I would like to extend sincere thanks to Dr. Randy Ellis for his guidance and support of this work over the past two and a half years. Thanks are also extended to Dr. Tim Bryant and all the members of the Clinical Mechanics Group for their support and encouragement. I would like to thank my friends and family for making the completion of this project both possible and more bearable.

List of Symbols and Abbreviations

Symbols

$\vec{\delta}$ is a column vector of three orthogonal infinitesimal translations.

$\vec{\gamma}$ is a column vector of three orthogonal infinitesimal rotations.

$\vec{\tau}$ is a column vector of three orthogonal torques.

$\vec{f}$ is a column vector of three orthogonal forces.

$\vec{T}$ is a twist vector in axis coordinates.

$\vec{t}$ is a twist vector in ray coordinates.

$\vec{W}$ is a wrench vector in axis coordinates.

$\vec{w}$ is a wrench vector in ray coordinates.

A is the matrix notation for a matrix with columns $\vec{A}_i$.

C is a compliance matrix of a linear passive system in equilibrium in $\mathbb{R}^{6\times 6}$.

S is a stiffness matrix of a linear passive system in equilibrium in $\mathbb{R}^{6\times 6}$.

Spring matrix is a system compliance or stiffness matrix.

$\tilde{\Delta}$ is the matrix that converts twists and wrenches from axis to ray coordinates and *vice versa*.

$\mathbb{S}^n_>$ is the set of symmetric positive definite matrices in $\mathbb{R}^{n\times n}$.

$\mathbb{S}^n_\geq$ is the set of symmetric positive semi-definite matrices in $\mathbb{R}^{n\times n}$.

Abbreviations

SPD Symmetric Positive Definite

SPSD Symmetric Positive Semi-Definite

SVD Singular Value Decomposition

PD Polar Decomposition

DOF Degree of Freedom

Contents

List of Tables

List of Figures

Chapter 1

Introduction

Knowledge of the constraints of a mechanism can be used to understand the behaviour of a mechanism under different loading scenarios. This knowledge can aid in predicting which loading regimes will produce instability of the mechanism or, conversely, which directions must be constrained to prevent failure. The static-loading behaviour of the mechanism can be determined based on its Jacobian matrix, but when there is no geometric information about the mechanism, the Jacobian matrix cannot be determined. A survey of current relevant literature produced no satisfactory method of resolving system constraints for such mechanisms.

The primary goal of this work was to find a method of determining the magnitude and directions of constraint when presented with a system for which there was little or no *a priori* knowledge of the system geometry. Determining the constraints of a system is a statics problem, as it requires knowledge of both the force and displacement behaviour of the system. Any mechanism, in a given pose, can be modeled as a mechanism for which the *spring* matrix (compliance or stiffness matrix) can be used to characterize the force-displacement behaviour. Using a 6×6 spring matrix, it is possible to consider the coupling of 3 orthogonal translations, rotations, forces and torques, and hence determine the directions and magnitudes of constraint by finding the bases of the matrix. Including 6 motion parameters eliminates the need for assumptions regarding the system geometry and the number of degrees of freedom (DOFs) of the system. The methods for determining the spring matrix from experimental force and displacement data, and analyzing the matrix, are the main results presented in this thesis. The experimental method was based on screw theory and the magnitudes and directions of the constraints (or DOFs) were extracted from the resulting spring matrix using eigenvalue decomposition. The analytical method presented in this thesis is equally applicable to mechanical and biological systems that can be locally modeled as a linear spring system in equilibrium.

The remainder of this chapter is dedicated to presenting an overview of screw theory as it was applied in this thesis. The structure of this thesis is:

Chapter 2 contains a review of the literature describing analysis of system DOFs, spring matrix calculation and the symmetric, positive semi-definite (SPSD) matrix approximation.

Chapter 3 contains a detailed description of the experimental approach used to calculate a SPSD spring matrix.

Chapter 4 contains a discussion of the procedure and results of computer simulations used to evaluate the validity of the analysis methods presented in this thesis.

Chapter 5 contains the conclusions drawn from this work and potential future research that may be conducted as a result of this work.

Appendix A lists the diagonal compliance matrices and results obtained for computer simulated experimental data.

1.1 Screw Theory

In order to model the motion of a mechanical system whose constraints are not known *a priori*, it is necessary to acquire 6 DOF force and motion data for the system. Reduction of the acquired data is needed to characterize the system constraints. determine the number of degrees of freedom and investigate the range of motion. Screw theory provides a mathematically concise method of analyzing 6 DOF force and motion data. This section contains a discussion of screw theory as it applies to this thesis.

1.1.1 Screw Theory: Historical Development

In the 1800's the French mathematician, Michel Chasles [6], proved that any small rigid body motion may be represented as the simultaneous rotation about and translation along some axis. Chasles' contemporary, Louis Poinsot [31], proved that any system of forces and torques can be represented by a single force applied along an axis and a single moment about the same axis. At the turn of the century, R. S. Ball [4] unified and expanded upon these theorems in his treatise on screw theory. The term "screw theory" was coined in accordance with the analogy between Chasles' definition of rigid body motion and the motion of a screw. K. H. Hunt further expanded upon screw theory and demonstrated its application to advanced mechanisms in the 1970's [17]. In the early 1980's, Roth applied screw theory to robotic kinematic analysis

[32]. Lipkin and Patterson [29] used screw theory to classify robot compliance based on the concept of eigenscrews and compliant axes in the 1990's. It is the efforts of Lipkin and Patterson that are of primary relevance to the material presented in this thesis.

1.1.2 Twists, Wrenches and Screw Axes

Twists. wrenches and screw axes are the main components of screw theory. Lipkin and Patterson [30], among others. defined these three entities in terms of Plücker ray or line coordinate notation. and Plücker axis coordinate notation. Plücker coordinate notation encodes magnitude, direction and location of the line of action using six parameters. In Plücker line-coordinate notation, the first three components encode the direction of the line of action and the remaining three components encode the location of the line of action with respect to the origin. Hunt [17] explained Plücker line notation in terms of force applied to a rigid body.

Let the force vector be represented as $\vec{F} = [f_x f_y f_z]^T$. Consider a rigid body whose orientation and location may be described by a coordinate system with the origin located at its center of mass. Let $\vec{F}$ be applied at a location $\vec{p} = [xyz]^T$ relative to the origin of the coordinate frame of the rigid body. The location of the force vector is immaterial in determining the reaction *forces* of the body, but it is required for determining the reaction *moments* of the body. The vector $\vec{F}$ acting at point $\vec{p}$ generates a moment $\vec{\tau}$ about the axes of the reference frame that is defined as the cross-product of $\vec{p} \times \vec{F}$. The first three components of the Plücker line coordinates of the wrench represent the line direction, $\vec{F}$. The last three components represent the moment of the force about the origin of the coordinate frame, $\vec{\tau}$, which encodes the location of the line relative to the origin. This definition corresponds to the wrench in Plücker ray coordinates, so

$$\vec{w} = \begin{bmatrix} \vec{f} \\ \vec{\tau} \end{bmatrix} \tag{1.1}$$

where $\vec{f}$ is the force vector and $\vec{\tau}$ is the moment vector.

Twists can be formed from Chasles' description of rigid-body motion. A twist consists of six screw velocities that are approximated by infinitesimal rigid-body displacements (or instantaneous velocities) [30]. Representation of the screw velocity, or twist, in Plücker line notation is analogous to the representation of the wrench. For a twist, the vector of rotational velocities, $\vec{\omega}$ (approximated by $\vec{\gamma}$ a rotational displacement, or instantaneous rotational velocity), yields the direction of the line. The cross product of $\vec{\omega}$ with its location relative to the origin, $\vec{r}$, yields the linear velocity, $\vec{V} = \vec{\omega} \times \vec{r}$ (approximated by a translation $\vec{\delta}$, or instantaneous linear velocity). The first three components of the twist in Plücker line notation are the rotation, which encode the direction, and the final three components are the translation, which encode the location of the line of action, so

$$\vec{t} = \begin{bmatrix} \vec{\gamma} \\ \vec{\delta} \end{bmatrix}$$

where $\vec{\delta}$ represents a vector of instantaneous translational velocities or equivalently an infinitesimal translational displacement, and $\vec{\gamma}$ represents instantaneous rotational velocities, or infinitesimal rotational displacements. In order to correctly interpret the rotational displacement as a vector, the rotation of the rigid body about the orthogonal axes must be independent of order of rotation about the axes. Small angular displacements are nearly independent of the order of rotations.

Screw axes are invariant lines along and about which twists occur and wrenches are applied (see the preceding discussion on Plücker line coordinates). Screw axes are defined by a six-component vector, the first three components of which define the direction of the line and the final three of which provide the moment of the line. or the location of the line with respect to the origin of the coordinate system. This notation corresponds to Plücker ray or line coordinates. Waldron and Hunt [37] explained that normalizing the twist with respect to the angular displacement. or normalizing the wrench with respect to the force, yields the normalized Plücker line coordinates or the screw coordinates of the twist or wrench.

In keeping with the analogy to the motion of screws, the normalized moment of the line encodes the pitch of the screw axis. The pitch, h. of the twist is defined as the ratio of the magnitudes of the translational to rotational motions. so

$$h = \begin{cases} \frac{\vec{\delta} \cdot \vec{\gamma}}{\vec{\gamma} \cdot \vec{\gamma}}, & \text{if } ||\vec{\gamma}|| \neq 0; \\ ||\vec{\delta}||^2, & \text{if } ||\vec{\gamma}|| = 0. \end{cases} \tag{1.2}$$

Here $\vec{\delta}$ represents the translational motion and $\vec{\gamma}$ represents the rotational motion. In the case of a pure translation, the magnitude of the screw is not infinite. but the pitched is assigned the value of the magnitude of the translation. This is necessary to calculate the compliance of the axis as well as to be able to discuss the normalization of the eigenscrew. For wrenches, the pitch is defined similarly as:

$$h = \begin{cases} \frac{\vec{\tau} \cdot \vec{f}}{\vec{f} \cdot \vec{f}}, & \text{if } \|\vec{f}\| \neq 0; \\ \|\vec{\tau}\|^2, & \text{if } \|\vec{f}\| = 0. \end{cases} \tag{1.3}$$

where h is the pitch. $\vec{\tau}$ is the moment vector and $\vec{f}$ is the force vector. If a pure moment is produced. the magnitude of the pitch becomes the magnitude of the moment for the same reasons as the pitch of the twists.

1.2 System Posture Compliance and Stiffness

Twists and wrenches are related to each other by the system compliance matrix $C \in \mathbb{R}^{6\times6}$ and the system stiffness matrix $S \in \mathbb{R}^{6\times6}$. The stiffness matrix S describes the mechanical system's resistance to motion for a particular system configuration. Properties of spring matrices (compliance and stiffness matrices) are discussed in terms of system stiffness due to its familiarity and application to simple systems. but the properties are equally applicable to system compliance. Because the S matrix is representative of a linear passive system in equilibrium. it is symmetric and positive definite.

Symmetry, where $S = S^T$, arises from the assumption that the displacements are small and occur about an equilibrium position. Symmetry of the stiffness matrix implies, for example, that a displacement in the x-direction due to a force in the y-direction will be proportional to a displacement in the y-direction resulting from a force in the x-direction.

A matrix is positive definite if all its eigenvalues, λ_i, are positive and non-zero (i.e.

$\lambda_i > 0$ for all $i = 1$ to n where λ_i of matrix $A \in \mathbb{R}^{m \times n}$). The requirement that the matrix be positive definite arises from the strain-energy condition which implies that energy must be stored by the system when a deformation is imposed. Ang and Andeen [3] gave a clear explanation of the symmetry and positive definite requirements. The strain-energy equation, as it relates to components of screw theory, is

$$\begin{bmatrix} \vec{\delta}^T & \vec{\gamma}^T \end{bmatrix} S \begin{bmatrix} \vec{\delta} \\ \vec{\gamma} \end{bmatrix} > 0 \tag{1.4}$$

In order to guarantee a positive result, the S matrix must be positive definite.

The stiffness relationship between the twists and wrenches is

$$\vec{w} = S\vec{T} \tag{1.5}$$

where $\vec{w}$ is the wrench that results when a twist $\vec{T}$ is imposed on a system with characteristic stiffness matrix $S \in \mathbb{R}^{6 \times 6}$. In this equation, the twist is expressed in axis coordinates and the wrench is expressed in ray coordinates. In Plücker axis coordinate notation the components that encode the location of the line are listed first, followed by the components that encode the direction. Axis notation complies with the relationship between twists and wrenches established by the spring matrix. A twist in axis coordinates is

$$\vec{T} = \begin{bmatrix} \vec{\delta} \\ \vec{\gamma} \end{bmatrix}$$

where $\vec{\delta}$ represents the translational displacement and $\vec{\gamma}$ represents the rotational displacement. The six degree of freedom stiffness equation is analogous to the planar spring equation

$$\vec{F} = k\vec{x} \text{ or } \vec{\tau} = \kappa\vec{\theta} \tag{1.6}$$

where $\vec{x}$ ($\vec{\theta}$) is an imposed displacement collinear with the spring, k (κ) is the spring constant or stiffness and $\vec{F}$ ($\vec{\tau}$) is the resulting force (torque). Stiffness may be regarded as the system's ability to resist an imposed deformation or twist. Conversely, the system compliance may be defined as the system's freedom to move under the action of an applied wrench. The equation of system compliance is

$$\vec{T} = C\vec{w} \tag{1.7}$$

where $\vec{w}$ is the applied wrench in ray coordinates, that causes the twist displacement $\vec{T}$, which is represented in axis coordinates, when applied to a system with compliance matrix C $\in \mathbb{R}^{6\times6}$. This is analogous to the planar spring equation

$$\vec{x} = \frac{1}{k}\vec{F} \tag{1.8}$$

where $\vec{F}$ is the applied force, $1/k$ is the spring compliance constant C and $\vec{x}$ is the resulting displacement.

By solving for $\vec{w}$ in Equation (1.7) and equating the result with Equation (1.5) one can conclude that $S = C^{-1}$. In order to obtain meaningful results with regard to the number of degrees of freedom of a mechanical system and the system constraints, the compliance of the system configuration will be the focus of discussion for the remainder of this thesis.

The $\tilde{\Delta}$ Matrix

In the section on twists, wrenches and screw axes, the twist and wrench vectors were expressed in ray coordinate notation. In the preceding section on the relationship between twists and wrenches, twists were expressed in axis coordinate notation and wrenches were expressed in ray coordinate notation. Both notations are used: one reason is that the matrices that transform twists and wrenches from one coordinate frame to another have the same form when twists and wrenches are written in opposite notations. Also, the compliance and stiffness relationships are most simply expressed when twists and wrenches are written in opposite notations. However, it is often necessary to write the twist and wrench vectors in a consistent coordinate notation. The means of converting between coordinate notation is the $\tilde{\Delta}$ matrix:

$$\tilde{\Delta} = \begin{bmatrix} 0 & 0 & 0 & 1 & 0 & 0 \\ 0 & 0 & 0 & 0 & 1 & 0 \\ 0 & 0 & 0 & 0 & 0 & 1 \\ 1 & 0 & 0 & 0 & 0 & 0 \\ 0 & 1 & 0 & 0 & 0 & 0 \\ 0 & 0 & 1 & 0 & 0 & 0 \end{bmatrix} = \begin{bmatrix} 0 & I \\ I & 0 \end{bmatrix} \tag{1.9}$$

Note that

$$1. \quad \tilde{\Delta}^T = \tilde{\Delta} \tag{1.10}$$

and

$$2.\quad \tilde{\Delta}^{-1} = \tilde{\Delta} \tag{1.11}$$

The effect of the $\tilde{\Delta}$ matrix on twists and wrenches is to reverse the sequence of the rotation and translation components. The conversion of a twist in axis coordinates to a twist in ray coordinates is then:

$$\vec{t} = \tilde{\Delta}\vec{T} = \begin{bmatrix} \vec{\gamma} \\ \vec{\delta} \end{bmatrix} \tag{1.12}$$

Similarly, the conversion of a wrench in ray coordinates to a wrench in axis coordinates is:

$$\vec{W} = \tilde{\Delta}\vec{w} = \begin{bmatrix} \vec{\tau} \\ \vec{f} \end{bmatrix} \tag{1.13}$$

1.2.1 Eigenvalues and Eigenvectors

The mechanical systems considered here may be characterized by eigenvalue and eigenvector decomposition of the compliance matrices.

Any matrix $A \in \mathbb{R}^{n \times n}$ may be considered to be a linear function that maps vectors from one space to another. If A is a nonsingular matrix, there are n nontrivial vectors $\vec{e}$ for which the result of the mapping function is a scalar multiple of $\vec{e}$, that is,

$$\lambda\vec{e} = A\vec{e} \tag{1.14}$$

where $\lambda \in \mathbb{R}$ is a scalar and $\vec{e}$ represents a vector transformed by the function A. For example, consider the case where A is the homogeneous representation of a rigid planar transformation. The pole p is an eigenvector of A corresponding to an eigenvalue of 1, and so it is the instant center of the transformation and remains unchanged under the action of A. (The pole is undefined for pure translation.)

In three-dimensional motion, the pole concept may be extended to an invariant line, or a series of poles in stacked planes. Points on the invariant line are constrained to translate along the line, and points in the body off the line are constrained to rotate about the line and translate in the direction of the line.

In order to find the location of the poles, or invariant lines, Equation (1.14) may be rearranged as

$$\vec{0} = A\vec{e} - \lambda\vec{e} \tag{1.15}$$

and further simplified to obtain

$$\vec{0} = [A - \lambda I]\vec{e} \tag{1.16}$$

where I represents the identity matrix. Taking determinants of Equation (1.16) gives the characteristic equation of matrix A

$$\det[A - \lambda I] = 0 \tag{1.17}$$

Equation (1.17) may be solved for $\lambda_1 \ldots \lambda_n$, which are the eigenvalues of matrix A. The corresponding eigenvectors are those vectors that are mapped to scalar multiples of themselves under the action of A, as shown in Equation (1.14).

The eigenvectors form a linearly independent basis of the matrix A. This implies that the result of the action of A on any vector $\vec{v}$ is a linear combination of scalar multiples of the eigenvectors $\vec{e}$ of A. Equation (1.14) may thus be rewritten as

$$\lambda_i \vec{e}_i = A\vec{e}_i \tag{1.18}$$

where $\vec{e}_i \in \mathbb{R}^n$ is an eigenvector, and $\lambda_i \in \mathbb{R}$ represents the eigenvalues of the matrix $A \in \mathbb{R}^{n \times n}$.

Eigenscrews

The eigenscrews of a compliance matrix C for a system posture are determined in much the same way as for any square matrix. The primary difference is the interpretation of the eigenvector as a screw axis, with three components indicating direction and three components indicating the line moment. Eigenscrews are determined by the characteristic equation (1.19) based on $\vec{t} = \tilde{\Delta} C \vec{w}$, where $\tilde{\Delta}$ ensures consistent coordinate notation, so

$$\lambda_i \vec{e}_i = \tilde{\Delta} C \vec{e}_i \tag{1.19}$$

The eigenscrews are represented by $\vec{e}_i \in \mathbb{R}^6$. When the eigenscrews are normalized with respect to the magnitude of the vector formed by the first three components, as in Equation (1.20), the first three components of the eigenscrew represent the direction and the final three components encode the pitch of the matrix.

$$\begin{aligned}\vec{e}_i &= \frac{\vec{e}_i}{\|\vec{e}_i(1:3)\|} \\ &= \begin{bmatrix} x & y & z & hx & hy & hz \end{bmatrix}^T\end{aligned} \tag{1.20}$$

where $x^2 + y^2 + z^2 = 1$, and $1 \leq i \leq 6$. In this notation, the pitch of the eigenscrew can be found using the method of Lipkin and Patterson [29], as

$$h_i = \frac{1}{2}\vec{e}_i^T \tilde{\Delta} \vec{e}_i \tag{1.21}$$

The pitch is the relative amount of translational and rotational compliance in the direction of the eigenscrew. Values of $|h_i| > 1$ indicate that more units of translation occurs per unit of rotation. Conversely, values of $|h_i| < 1$ indicate more units of rotational deformation occur per unit of translational deformation. The rotational and translational compliance associated with each eigenscrew may be determined by combining the pitches and the eigenvalue corresponding to the eigenscrew. The equations that define translational and rotational compliance are, respectively

$$c_{t_i} = \lambda_i h_i \tag{1.22a}$$

$$c_{r_i} = \frac{\lambda_i}{h_i} \tag{1.22b}$$

When $\vec{e}_i$ is acted upon by $\tilde{\Delta}C$, λ_i represents the scalar multiple by which $\vec{e}_i$ is compressed or extended in the direction of the eigenscrew, $\vec{e}_i$. The pitch h_i represents the ratio of the magnitude of translation to rotation, and λ_i represents the total motion in the direction of $\vec{e}_i$. Thus, λ_i and h_i represent the amount of constraint in the direction of $\vec{e}_i$.

Compliant Axes

Lipkin and Patterson [29] described compliant axes based on the two-system of Hunt [17]. These axes are determined from the eigenvalue/eigenvector decomposition. A compliant axis exists if there are two collinear eigenscrews having eigenvalues and pitches of equal magnitude but opposite sign. These two eigenscrews are *reciprocal*, or dual (i.e. $\vec{e}_i^T \tilde{\Delta} \vec{e}_j = 0$). Lipkin and Patterson [29] define a compliant axis as one on which an applied "force produces a parallel linear deformation, and a rotational deformation about the line of force produces a parallel couple." In essence, the compliant axis behaves like a linear spring when a force is applied, and behaves like a torsional spring when a rotational deformation is applied. The application of forces and rotational deformations coincident with a compliant axis result in *un-coupled* rotational and translational behaviour.

If a compliant axis exists then all other eigenscrews must intersect the compliant axis in a hyperplane orthogonal to it. If two compliant axes exist, then all eigenscrews are grouped in orthogonal pairs. Patterson and Lipkin [29] presented a classification scheme for systems based on the number of compliant axes.

1.3 Summary

The determination of system constraint and compliance characteristics is challenging for mechanical systems for which there is no geometric information. In order to avoid making assumptions regarding the system geometry, a method of experimentally determining the static behaviour of the system has been proposed. A method based on screw theory has been developed to evaluate the characteristic constraints and compliances of systems for which there is no knowledge of the system geometry. Screw theory offers the benefit of concise descriptions of 6-DOF data, incorporation of force and motion data, and easily interpretable eigenscrew results. Methods described in the open literature used to evaluate system DOFs and characteristic spring matrices were reviewed. The following chapter contains a discussion of these methods, and their pros and cons within the context of the goals of this work.

Chapter 2

Literature Review

Characterization of a mechanical system based on its degrees of freedom, as described in the preceding chapter, has three distinct stages: determination of the number of degrees of freedom; determination of the system spring matrix; and optimization of the experimentally determined compliance matrix (ensuring the symmetric, positive-definite requirement).

2.1 Identification of System Degrees of Freedom (DOFs)

Four distinct methods of system DOF identification have been discussed in the robotic and biomedical literature. These methods are characterization of system spring matrices [29], determination of the rank of the Jacobian matrix and screw-system identification ([7], [17], [18], [28], [41]), analysis of configuration space trajectories [27], and principal component analysis [9]. A survey and comparison of methods used to detect the DOFs of a system are presented in the following sections.

2.1.1 Characterization of System Compliance and Stiffness Matrices

The characterization of mechanical systems based on spring matrices was presented by Patterson and Lipkin [29] in 1990. Patterson and Lipkin's method of system analysis used the relationship between the system displacements and forces. the compliance matrix. to determine the system characteristics. The system rotations and translations were represented as twists, and the forces and moments were represented as wrenches in Plücker coordinates. These elements, as well as the system compliance matrix were introduced in the theory section of Chapter 1. Patterson and Lipkin characterized robot manipulators based on the eigenscrews of the compliance matrix and the existence of compliant axes. The eigenscrews were represented in six-component Plücker ray coordinates. A twist resulting from the application of an arbitrary wrench may be calculated as a linear sum of the eigenscrews. The ratio of the eigenvalue to the corresponding eigenscrew pitch yielded the rotational compliance. Multiplication of the eigenvalue with the corresponding eigenscrew pitch resulted in the translational compliance. Small values of compliance indicated directions of constraint. whereas large values indicated directions of compliance. Thus the number of degrees of freedom of the system was determined based on the magnitude of the rotational and translational compliance of the eigenscrews.

Patterson and Lipkin's method offers the opportunity to analyze general systems for which no knowledge of configuration geometry exists, but for which accurate evaluation of the compliance matrix is possible. The directions of the axes of motion can be obtained from the eigenscrews. The system analysis also determines the extent of constraint for each eigenscrew by including the forces required to cause the displacements. For these reasons, Patterson and Lipkin's method of eigenscrew decomposition and system compliance characterization was selected for application to the problem described in Chapter 1.

2.1.2 Rank of the Jacobian Matrix and Screw System Identification

The Jacobian matrix $J(\vec{q})$ relates instantaneous joint velocities, $\dot{\vec{q}}$ (and static generalized forces) to the instantaneous Cartesian velocity of the tip (and to the static force/torque present at the tip). Because the columns of the Jacobian are screws, it can also be interpreted as containing position and direction information for each of the constraints of a system in configuration $\vec{q}$, where $\vec{q}$ is a vector of the actuator positions that specifies the manipulator configuration. System analysis based on evaluation of the rank of the Jacobian matrix is based on linear independence of the screws that are the column vectors. A matrix $A \in \mathbb{R}^{6\times 6}$ is of full rank *iff* its column-space is 6. If each column represents the direction of an actuator axis for a robot manipulator in screw coordinates (i.e., the matrix is the Jacobian $J(\vec{q})$), then a rank of 6 indicates that the manipulator is free to move from its present configuration. If the rank, $r < 6$, the manipulator is constrained in $6 - r$ motions (translations and rotations) from the present configuration, and only r motions are free.

Hunt [18] presented a method of extracting the number of degrees of freedom available to a manipulator based on its Jacobian matrix for a specific configuration. The Jacobian, $J(\vec{q})$, is constructed using the screw coordinate representation of the actuators $\vec{\alpha}$ in ray coordinates as columns of $J(\vec{q})$. Reciprocal screws were found in axis coordinates for the set of screws in $J(\vec{q})$ using:

$$J(\vec{q})^T \vec{\alpha_i^*} = 0 \tag{2.1}$$

where $\vec{\alpha_i^*}$ is a member of the matrix of reciprocal screws, $J^*(\vec{q})$, represented in axis coordinates. The screws in $J(\vec{q})$ represent directions of kinematic freedom, whereas the reciprocal screws represent the directions of constraint of the system (i.e. a force applied to the end effector in the direction of a reciprocal screw produces no motion of the end-effector because this direction is completely constrained). For $\text{rank}(J(\vec{q})) = 6$, there is no solution for $\vec{\alpha_i^*}$ in Equation (2.1) and the end-effector has total kinematic freedom.

Hunt [17] presented a thorough survey of the kinematic interpretations of twenty-seven general and special cases of screw systems. In each case, the effect of loss of degrees of freedom (or increase in size of the reciprocal screw space) on manipulator kinematics was discussed.

Zavatsky [41] used the technique described above to examine the number of degrees of freedom available in a flexed-knee-stance testing rig. Using the parameterized geometry of the simulator's actuators in screw coordinates, Zavatsky found the analytical solution for the rig's determinant. The author used this result to deduce which configuration conditions yield a zero determinant, indicating loss of degrees of freedom at this configuration. He also determined that a zero determinant could be avoided by careful selection of geometric parameters of the rig.

Conlay and Long [7] considered the converse situation: they examined the stability (constraints) of the knee for different degrees of flexion. For each flexion position, they determined the position and orientation of each of the nine constraining structures (ligament, capsule and contact force) of the knee. The screw coordinates of each constraining structure were obtained by modeling each constraint as a prismatic joint. The matrices for any combination of six structures were obtained and the determinant of the matrix was evaluated. A determinant of zero indicated that at least two of the columns representing the constraints were dependent ($r < 6$) and the knee with $r < 6$ was considered unstable, as it would be unconstrained in one or more rotations or translations. The unconstrained direction corresponds to the direction given by the reciprocal screw. The researchers found that no combination of six constraint directions produced a zero determinant. Based on this result, it was concluded that the knee was stable for the range of flexion that they examined.

The work of Murphy and Mann [28] on kinematic freedom of the knee bears several similarities to the work by Conlay and Long. Murphy and Mann modeled ligament and contact force constraints as zero-pitch wrenches corresponding to prismatic joints. Murphy and Mann also recognized that the ligaments exert no force until they are extended beyond their initial length, and exert no force beyond their rupture length. The insertion sites for each ligament on the tibia and femur provided the initial length and origin of each filament. All possible positions and orientations of the femur relative to the tibia were determined separately for each of the filament constraints. The positions and orientations of the femur form an annulus, with the inner radius corresponding to the initial length of the filament and the outer radius corresponding to maximum filamentary extension. The intersection of the annuli for all ligaments was the set of achievable positions and orientations of the femur with respect to the tibia based on ligament constraints. The contact situations were evaluated for each of these positions, as there would be no contact force exerted for the case in which there is lift-off from the tibial plateau. Once the ligament and contact constraints were determined for each tibia-femur configuration, the screw coordinates were calculated for each constraint. A matrix, A, of the screw coordinates was constructed and the rank, r, of the matrix was determined. For $r < 6$, there was a solution to either or both of the repelling and reciprocal screw system configurations. Representing a screw axis as $\vec{\alpha}$, the screw axis is in a repelling configuration if

$$A\alpha \leq 0 \tag{2.2}$$

and it is in a reciprocal configuration if

$$A\alpha = 0 \tag{2.3}$$

A solution for the repelling screw system represents a direction in which the ligaments are shortened and lift-off occurs from the tibial plateau. A solution for the reciprocal screws represents a direction in which no work is done by the constraints, or a direction in which the body is unconstrained. The authors presented one example solution for the model, but cited the need for a complete set of solutions for the configurations of the knee in order to properly characterize the total freedom of the knee.

Although the methods introduced in this section have the advantage of revealing which directions are constrained and which ones are free to move, the methods are unable to provide the *amount* of constraint or freedom about each screw axis because force conditions are not taken into account. This omission could result in incorrect conclusions when using the constraint analysis method of Conlay and Long, and also when using the method of Murphy and Mann. Conclusions drawn from the freedom analysis of the testing rig by Zavatsky could also be challenged on this basis. In all of these cases, the discussion of freedom or constraint is based solely on the geometry of the physical system. Determination of the number of degrees of freedom by examination of the linear independence of the actuator or constraint axes yields the number of directions in which the manipulator may move, but does not consider that some of these directions may be very stiff and highly resistant to motion. Conversely, some of the directions of "constraint" may be very compliant and not provide the "stability" expected from the results of the kinematic analysis. For this reason, the results obtained by Conlay and Long may be questioned: it is possible that for some arrangements of the ligaments and contact forces, the knee may be unstable under certain loading conditions. Zavatsky's analysis may also be questioned if there are geometric configurations for which directions of freedom are very stiff, which would imply that the rig is kinematically free to move in a free direction but would require application of a large force in order to do so.

A second disadvantage of Zavatsky's method is that accurate knowledge of the geometric configuration of the actuators or constraints must be known *a priori*. Thus, the method of screw systems and Jacobian matrix rank may not be applied to mechanical systems for which accurate description of actuator/constraint configuration is not known.

2.1.3 Analysis of Configuration Space Plots

C-space is strongly associated with robot analysis: it is a space which represents all positions and orientations attainable by a manipulator. Operational c-space for

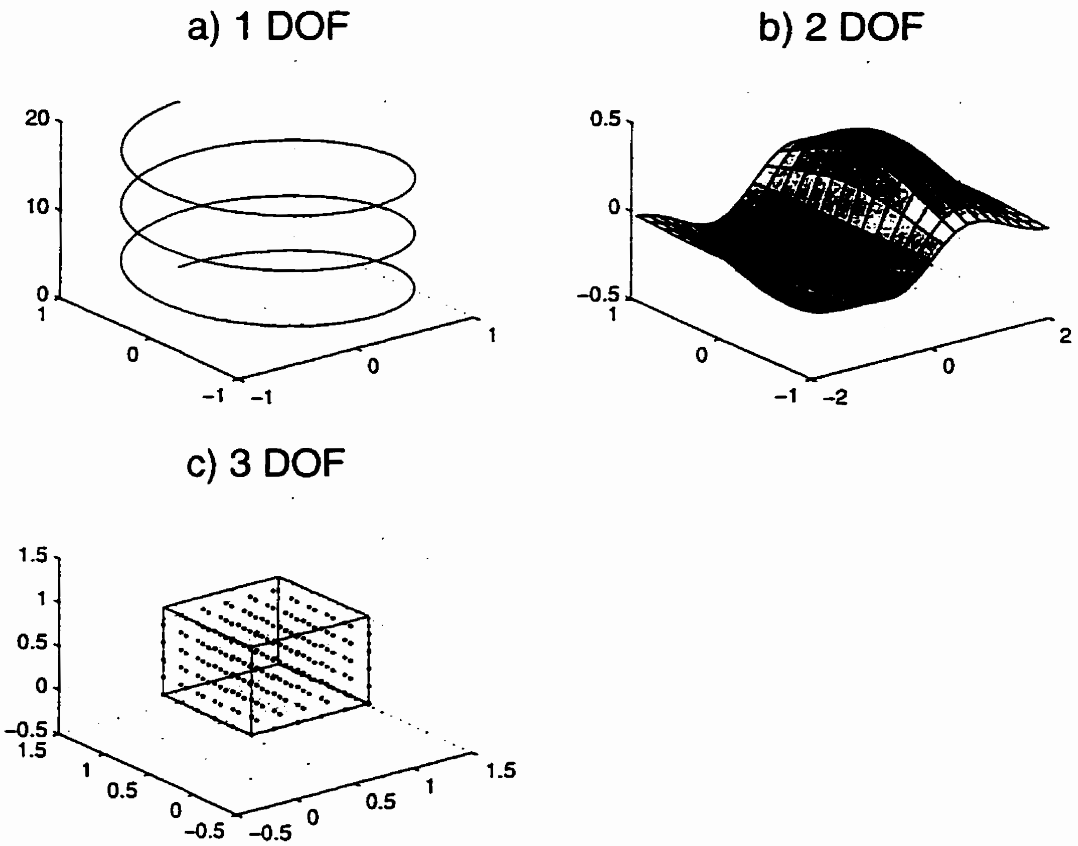

Figure 2.1: C-space trajectories for 1, 2, and 3 DOF systems.

planar motion may be plotted in three dimensions because three parameters (x, y and ϕ about z) are sufficient to fully specify a manipulator's planar position and orientation. The minimum number of DOFs required to achieve a given motion can be estimated from the trajectory in the manipulator's c-space. The c-space for a one-DOF joint will map to a curve, the c-space for a two-DOF manipulator will map to a surface, and the c-space for a three-DOF manipulator will map to a volume (see Figure (2.1)).

In 1993, Moore etál [27] presented a method of determining the number of degrees of freedom required to specify a planar motion of the human wrist. Their method of identifying the number of DOFs consisted of plotting the three c-space parameters in three-dimensional space and fitting the c-space to a curve, surface or volume. The residuals of the fits were calculated and analyzed to determine the number of degrees of freedom necessary to describe the wrist "power" motion. "Large" residuals would indicate a poor fit of the c-space trajectory to a surface, so more DOFs would be required to describe the kinematics of the wrist. Moore etàl determined the c-space for the wrist by observing the relative motion between a coordinate system fixed to the hand and a coordinate system fixed to the arm, as the wrist cycled through the planar "power" motion. After obtaining the c-space for repeated motions, a surface was fit to the c-space and residuals between the c-space and the modeled surface were calculated. Residuals for the surface fit were small and indicated that two degrees of freedom were required to fully specify the "power" motion.

Two advantages of this method of DOF identification are its straightforward application to experimental data, and no *a priori* knowledge of the system geometry was required. Two disadvantages of this technique were that it focused on kinematics of the wrist, and did not yield the directions of the axes that provided the two degrees of freedom. The lack of force data meant that no measure of stiffness or compliance associated with each degree of freedom was determined.

2.1.4 Principal Component Analysis

Jolliffe [19] stated that

> The central idea of principal component analysis (PCA) is to reduce the dimensionality of a data set which consists of a large number of interrelated variables, while retaining as much as possible of the variation present

> in the data set. This is achieved by transforming to a new set of variables, the principal components (PCs), which are uncorrelated, and which are ordered so that the first *few* retain most of the variation present in *all* of the original variables.

The PCs can be obtained by eigenvalue decomposition of the covariance matrix for the set of original variables. The eigenvectors are the PCs and represent linear combinations of the original variables, and the eigenvalues are the variance of the original variables associated with each PC. The largest eigenvalues correspond to those PCs that maximize the variance of the original variables.

PCA has had broad application. Jolliffe [19] cited application of PCA to analyze the correlation of anthropometric measurements, the description of weather factor patterns over large spatial areas, the correlation of life-style factors of the elderly, the correlation of chemical compounds and properties, and correlation between prices of various stocks. PCA has also been applied to signal processing [22], acoustics [21], imaging [23], face recognition [34], speech analysis [35], and many other applications.

Principal Component Analysis (PCA) is being used in current research to identify the axes of freedom of motion. Deluzio [9] has had promising results in using eigenvectors to identify the axes of rotation in simple and double pendulum experiments. As in the work by Moore etàl [27] described above, the data analyzed is kinematic data and neglects forces acting on the system. Another similarity to the c-space method is that PCA requires no *a priori* knowledge of the system geometry. However, in contrast to the work by Moore etàl, PCA does identify the directions of the axes of motion.

PCA does not allow determination of the magnitude of stiffness or compliance about each axis because it neglects forces. It is unclear how such data could be included in PCA while preserving the physical significance of the PCs.

2.2 Determining the Compliance Matrix of a System

The spring matrix of a mechanical system can be calculated using geometrical information, or estimated from experimental data. The majority of the work [26], [37], [12], [20], [33], [38], [10], [3], [36] has been on the calculation of compliance based on the known geometry of the system. The work of Gosselin [12] and Tahmasebi and Tsai [36] are typical examples of the geometrical approach, both defining the stiffness matrix K as

$$K = J(\vec{q})^T \kappa J(\vec{q}) \tag{2.4}$$

where κ is a diagonal matrix representing the stiffness of each of the actuators and $J(\vec{q})$ is the Jacobian of the manipulator for configuration $\vec{q}$. Both Tahmasebi and Tsai, and Gosselin determined the stiffness of parallel manipulators from the Jacobian matrix. For these mechanisms, the forward solution is more complicated than the inverse solution. For this reason, the problem is posed in the inverse form and the Jacobian matrix of the parallel manipulator is defined as the inverse of the Jacobian used in standard practice. This equation is derived from the way that the Jacobian relates (a) infinitesimal displacements, and (b) static forces. The displacement relationship is

$$\delta\vec{q} = J(\vec{q})\delta\vec{x} \tag{2.5}$$

where $\delta\vec{q}$ is the vector whose components are the infinitesimal displacements of the actuators, and $\delta\vec{x}$, is the vector whose components are the infinitesimal displacements of the end-effector, $\delta\vec{x}$. The statics relationship is

$$\vec{F} = J(\vec{q})^T\vec{f} \tag{2.6}$$

$\vec{F}$ is the vector of forces and torques applied at the end effector, and $\vec{f}$ is the vector of generalized forces applied at the actuators. Modeling the actuators as having linear stiffness gives the relation

$$\vec{f} = \kappa\delta\vec{q} \tag{2.7}$$

from which Equation (2.4) can be derived. A consequence of such a formulation is that the accuracy of determining the system's stiffness, depends on the accuracy of the knowledge of the system's geometry. For situations where little is known about the configuration of the system, the Jacobian cannot be reliably determined.

The experimental approach to estimating the spring matrix is not reported in the open literature as frequently as is the geometrical approach. To the best of our knowledge, ElMaraghy and Johns [11] are the only research group that have attempted to experimentally determine the compliance of the end-effector of a manipulator. They attempted to experimentally determine the end-effector compliance in order to validate a model that was previously determined analytically (ElMaraghy and Johns [10]). They were, however, unsuccessful in validating the analytical solution of the compliance matrix of the SCARA robot they studied because they were unable to defeat the active compliance compensation in the manipulator control system. Their reported experimental results for the PUMA 560 did correspond to results obtained by Lozinski [25].

These results confirmed that an experimental approach for determining the compliance was possible. The experimental method was, in essence, estimating the compliance at the end-effector by displacing the end-effector a known amount and measuring the applied force. The particular goal of the work of ElMaraghy and Johns described in [11] was to measure the joint compliances that were calculated using a Jacobian method. The significance of their corresponding paper is as a demonstration of the possibility of experimentally determining end-effector compliances based on measurement of end-effector forces and displacements of a system for which the geometric configuration is unknown.

2.3 Obtaining Symmetric Positive-Definite Matrices from Experimental Data

A typical experiment for estimating the compliance of a mechanical system might be to apply a wrench $\vec{w}$ to the system when it is in equilibrium, and then to measure the resulting twist $\vec{T}$ from equilibrium. Recall that $\vec{w}$ was defined in the previous chapter as a vector of forces/torques in ray coordinates and $\vec{T}$ was defined as a vector of translations/rotations in axis coordinates. The column vectors of repeated measurements can be gathered into matrices, so for a constant compliance matrix C at the equilibrium configuration the wrenches can be assembled into a matrix w and the corresponding displacements can be assembled into a matrix T. The individual relations $\vec{T}_i = C\vec{w}_i$ can thus be expressed as $T = Cw$.

As previously discussed, the compliance matrix C must be symmetric and positive definite. However, when obtaining experimentally measuring twists and wrenches, there will inevitably be noise in the measurements. Estimating C as

$$C = Tw^T(ww^T)^{-1} \tag{2.8}$$

will not necessarily produce an estimated compliance matrix C that is symmetric and positive-definite. Thus in general, a symmetric positive-definite approximation to the experimental matrix must be found. Two approaches have been proposed for the solution of the symmetric positive-definite matrix problem: find the nearest symmetric positive-semidefinite (SPSD) matrix to the given matrix, or find some SPSD matrix that minimizes the residuals of the modeled system (i.e. that minimizes $||Cw - T||_F$). $||\cdot||_F$ represents the Frobenius norm which is calculated as

$$||B||_F = \sqrt{\sum_{i=1}^{n}\sum_{j=1}^{m} b_{ij}^2} \tag{2.9}$$

for matrix B.

Let A be an arbitrary matrix and let P be an SPSD matrix ($P \in \mathbb{S}^n_{\geq}$ where $\mathbb{S}^n_{\geq}$ is the set of SPSD matrices in $\mathbb{R}^{n \times n}$). Higham [16] proposed a method of finding the SPSD matrix P nearest to A by minimizing the Frobenius norm of their difference.

which is finding P such that:

$$\min_{P \in \mathbb{S}^n_{\geq}} \|A - P\|_F \tag{2.10}$$

This method was based on the matrix 2-norm approximation method reported by Halmos [13], which found the matrix 2-norm distance to a set of positive approximants for a given matrix A. The 2-norm of a matrix was defined as the square root of the spectral radius of a given matrix:

$$\|C_{exp}\|_2 = \sqrt{\rho(C_{exp}^T C_{exp})} \tag{2.11}$$

The spectral radius ρ of a matrix B is defined as the maximum magnitude of the eigenvalues of B.

Higham's solution provides a unique solution P for the positive approximation. The approximant is obtained by setting the negative eigenvalues of the matrix A to zero. Higham's approximation method is described in greater detail in Chapter 3. Section 3.2.

Minimization of residuals for a modeled system was first presented by Brock [5] in 1968. Brock proposed a method of minimizing the Frobenius norm of the residuals of a modeled linear system by setting the first-derivative of the function in Equation (2.12) to zero, so that

$$f(C) = \text{tr}[(Cw - T)^T Z(Cw - T)] \tag{2.12}$$

where $C \in \mathbb{S}^n_>$ represents an $n \times n$ symmetric positive-definite matrix. $w \in \mathbb{R}^{n \times m}$ and

$T \in \mathbb{R}^{n \times m}$ represent system force and displacement data respectively, and $Z \in \mathbb{R}^{n \times n}$ is a diagonal scaling matrix. For the solution of system stiffness or compliance, the identity matrix was used for Z. The trace of a matrix "tr" is defined as the sum of the eigenvalues of the matrix. As demonstrated in 1996 by Woodgate [39], this method does not guarantee a positive definite solution for a perturbed system, nor does it guarantee the existence of a solution.

Allwright [1] presented a solution for the minimization problem introduced by Brock that determined a SPSD approximant using an iterative projection method and least-squares approximation. Candidate matrices for the minimization of the residual were constrained to lie in conical hulls to ensure definiteness of the solution.

Woodgate [40], [39] presented two iterative algorithms for minimization of the Frobenius norm of the residuals. The algorithm proposed in his first paper [40] used a least-squares or quasi-Newton iterative approach to solve for a SPSD matrix over a convex solution space. The constraints were specified in order to guarantee a positive semidefinite solution. No measure of efficacy of the algorithm was reported in the paper. He later reported [39] that the efficiency and accuracy of these solutions obtained using the least-squares algorithm depended on the initial estimate for C. In this latter paper an algorithm was presented that used a modified Newton's method to find a positive semi-definite matrix in a non-convex space. This method relied on constraints in the algorithm for convergence. Woodgate claimed this method offered greater efficiency and better convergence properties than did his previous algorithm [40], but these claims remain unsubstantiated.

The most recent reference to the residual-minimization problem in the open literature is by Andersson and Elfving [2]. They presented a survey of the theory and reported a numerical study comparing the convergence properties of gradient-projection algorithms, a modified parallel-tangent method and a method presented by Han and Lou [14]. The gradient-projection algorithms included the methods developed by Woodgate [40] and Allwright [1]. Andersson and Elfving observed that the gradient-projection algorithms exhibited sensitivity to starting-matrix condition values. The residual error decreased monotonically for the gradient-projection methods. although error for the parallel-tangent method was not consistent for high iteration values (i.e. near convergence). The method of Han and Lou proved sensitive to step length and initial conditioning of the problem. Of the three methods investigated in this study, the authors preferred the gradient-projection methods because they were more consistent in convergence and less sensitive to selection of step size than the other methods. However, Andersson and Elfving concluded fast and robust algorithms for convergence of the residual minimization problem have not yet been developed.

Chapter 3

Determining the System Compliance Matrix

This chapter contains a discussion of the process that was used to obtain the system compliance matrix given twist and wrench data for an arbitrary mechanical system. Consideration was given to the situation when experimentally gathered twist and wrench data may be contaminated with noise. When this is the case, the calculated system compliance matrix is rarely symmetric and positive semi-definite. A SPSD matrix approximation method, presented in this chapter, is intended to ensure that the compliance matrix is physically meaningful. Error-corrective measures, which included system over-determination and SPSD approximation, were implemented and evaluated for efficiency in reducing compliance matrix errors. The results of these evaluations are presented at the end of this chapter.

3.1 Determining the Compliance Matrix for a Mechanical System

Given perfect data, the compliance matrix C of a system configuration can be determined given applied force (wrench, w) and resulting displacement (twist, T) data. C can be isolated in $T = \tilde{\Delta}Cw$ to obtain

$$C = \tilde{\Delta}Tw^{-1} \tag{3.1}$$

In Equation (3.1), both T and w must be elements of $\mathbb{R}^{m \times n}, m = n = 6$, and $\tilde{\Delta}$ ensures that twists and wrenches are in consistent notation. In Equation (3.1), the twists T were given in axis coordinates and wrenches w were in ray coordinates. In order to reduce the effect of noise and ensure that w is of full rank, the system is generally over-determined and $n \gg 6$. When $n > 6$, w is not directly invertible. There are two possibilities for obtaining the inverse of w.

3.1.1 Isolating the Compliance Matrix in Over-determined Systems

The simplest means of isolating C entails post-multiplying both sides of Equation (3.1) by w^T to obtain square matrices Tw^T and ww^T. In so doing, square invertible matrices are obtained provided that the matrix is non-singular (i.e. $\det(ww^T) \neq 0$). C can then be estimated as

$$C = \tilde{\Delta}(Tw^T)(ww^T)^{-1} \tag{3.2}$$

If ww^T is not invertible, then the pseudo-inverse of the w matrix can be obtained using singular value decomposition (SVD). The SVD of a matrix $A \in \mathbb{R}^{m \times n}$ is a decomposition of A into three constituent components: two orthogonal matrices $U \in \mathbb{R}^{m \times m}$ and $V \in \mathbb{R}^{n \times n}$, and a diagonal matrix of singular values $\Sigma \in \mathbb{R}^{m \times n}$ as

$$SVD(A) = U\Sigma V^T = A \tag{3.3}$$

One important property of orthogonal matrices is that the transpose is equal to the inverse (i.e., $[U]^{-1} = [U]^T$ and $[V]^{-1} = [V]^T$). The inverse of a diagonal matrix is obtained by taking the reciprocal of the diagonal elements of the matrix, so ${\sigma_{ii}}^{-1} = \frac{1}{\sigma_{ii}}$. In the case where $\sigma_{ii} = 0$, the reciprocal is artificially set to zero. Taking the SVD of w in Equation (3.1), results in

$$T = \tilde{\Delta} C U_w \Sigma_w V_w^T \tag{3.4}$$

C can be estimated as

$$C = \tilde{\Delta} T V_w \Sigma_w^{-1} U_w^T \tag{3.5}$$

3.2 Determining the Compliance Matrix from Experimental Data

Whenever data is collected experimentally, there will be error associated with the measurements. Noise may interfere constructively or destructively with the magnitude of the electrical signal, resulting in increased or decreased magnitude of the measurement. This measurement error can propagate through calculations involving the experimental data and affect the results such that they will not make sense when applied to real systems. The calculation of the compliance matrix based on experimentally acquired twist and wrench data is vulnerable to the propagation of such errors, so the resulting compliance matrix is rarely SPSD.

As discussed in the preceding section, the SPSD requirement must be met for real systems. When a compliance matrix does not meet these conditions, an approximation must be found that preserves the information provided by the experimentally determined compliance matrix C_{exp} but also meets the SPSD criteria. In the preceding chapter, two methods of obtaining a SPSD compliance matrix were presented. Higham's method [16] was selected for SPSD approximation based on its conciseness and its guarantee of a SPSD solution. In Higham's method, the SPSD matrix "nearest" to the experimentally determined matrix was found by minimizing the Frobenius norm of the residuals. This "nearest" matrix can be defined as a linear function C_{app_F} that yields results that are very similar to results obtained with C_{exp} when applied to an arbitrary vector of independent variables, $\vec{X}$ (i.e. $C_{exp}(\vec{X}) \simeq C_{app}(\vec{X})$). The matrix C_{app} is obtained by minimizing the residuals of the elements of the C_{exp} and C_{app_F} matrices in

$$\min_{C_{app_F} \in \mathbf{S}^n_{\geq}} \|C_{exp} - C_{app_F}\|_F \tag{3.6}$$

Higham's method was based on an approximation method presented by Halmos [13] in 1972. Halmos' approximation method resulted in a non-unique solution for the SPSD matrix problem. Halmos used the 2-norm to specify the distance from C_{exp} to a SPSD approximant C_{app_2}. The 2-norm of a matrix was defined as the square-root of the spectral radius of a given matrix:

$$||C_{exp}||_2 = \sqrt{\rho(C_{exp}^T C_{exp})} \tag{3.7}$$

The spectral radius ρ of a matrix B is defined as the maximum magnitude of the eigenvalues of B. Halmos defined the distance from C_{exp} to a symmetric positive semidefinite matrix C_{app_2} as the 2-norm of $(C_{exp} - C_{app_2})$. There is an analogy between the distance between SPSD and non-SPSD matrices, and the distance between a complex number $N = a + bi$ and a positive, real approximant R as illustrated in Figure (3.1). The positive real approximant R of N is the real component a of N. The distance from R to N is the magnitude of the imaginary component $|b|$ of N. The 2-norm distance between C_{exp} and C_{app_2}, is the distance from the C_{exp} matrix to a set of all positive approximants, implying there may be more than one within that distance from C_{exp}. This suggests that the 2-norm method may not locate the "nearest" matrix.

In 1988, Higham [16] presented a method by which a unique. nearest SPSD matrix to a real matrix could be found by using the Frobenius norm to limit the range of the search and identified a unique solution. The Frobenius norm is defined as

$$||C_{exp}||_F = \sqrt{\sum_i \sum_j c_{ij}^2} \tag{3.8}$$

C_{app_F}, the SPSD approximant to C_{exp}, is found by minimizing $||C_{exp} - C_{app}||_F^2$. Higham first decomposed C_{exp} into a symmetric part D

$$D = \frac{C_{exp} + C_{exp}^T}{2} \tag{3.9}$$

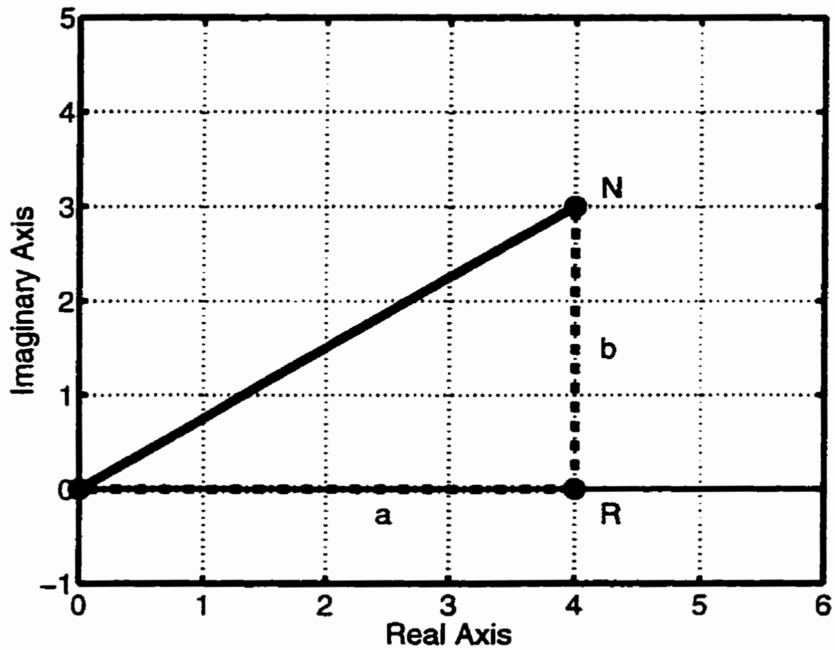

Figure 3.1: Real approximation of an imaginary number.

and a skew-symmetric part E

$$E = \frac{C_{exp} - C_{exp}^T}{2} \tag{3.10}$$

Because $D + E = C_{exp}$,

$$||D + E||_F^2 = ||D||_F^2 + ||E||_F^2 = ||C_{exp}||_F^2 \tag{3.11}$$

The problem is thus reduced to one of finding a symmetric positive semidefinite (SPSD) approximation for the symmetric component, D.

$$||C_{exp} - C_{app_F}||_F^2 = ||D - C_{app_F}||_F^2 + ||E||^2 \tag{3.12}$$

D can be decomposed into constitutive components using the singular-value decomposition, so that

$$\mathrm{SVD}(D) = Z\Lambda Z^T = D \tag{3.13}$$

where Λ is a diagonal matrix with elements $|\lambda_i|$ and Z is an orthogonal matrix. Because Z is orthogonal it can be used to transform a matrix to a similar matrix. This is useful here because if $A = Z^T BZ$ then $\|A\|_F = \|Z^T BZ\|_F$. Applying Z to $D - C_{app_F}$ of Equation (3.12) gives

$$\|D - C_{app_F}\|_F^2 = \|Z^T DZ - Z^T C_{app_F} Z\|_F^2 = \|\Lambda - Y\|_F^2 \tag{3.14}$$

where

$$\Lambda = Z^T DZ \tag{3.15}$$

and

$$Y = Z^T C_{app_F} Z \tag{3.16}$$

The expansion of Equation (3.14) using the definition of the Frobenius norm gives

$$\|\Lambda - Y\|_F^2 = \sum_{i \neq j} y_{ij}^2 + \sum_i (\lambda_i - y_{ii})^2 \geq \sum_{\lambda_i < 0} (\lambda_i - y_{ii})^2 \geq \sum_{\lambda_i < 0} \lambda_i^2 \tag{3.17}$$

and all $y_{ii} \geq 0$ since Y must be symmetric positive semidefinite. There is thus a unique solution for the problem of approximating a diagonal matrix Y which consists of the diagonal elements. λ_i for all $\lambda_i \geq 0$ and 0 for all $\lambda_i < 0$. The rationale for setting $\lambda_i = 0$ for $\lambda_i < 0$ was that 0 is closer to $\lambda_i < 0$ than $|\lambda_i|$. A straightforward means of systematically eliminating the negative diagonal elements is

$$C_{app_F} = \frac{D + F}{2} \tag{3.18}$$

where $F = Z\mathrm{diag}(|\lambda_i|)Z^T$. The eigenvalues of C_{app_F} are $(\lambda_i(D) + \lambda_i(F))/2$. Higham [15] took advantage of the relation of polar decomposition to singular value decomposition to obtain the symmetric SPSD matrix, F. For the square compliance matrix C_{exp} let the symmetric component D have the polar decomposition $D = QF$, where Q is an orthogonal real matrix ($Q^TQ = I$) and F is a symmetric positive-definite matrix ($F \in \mathbb{S}^n_>$). From the relationship between the polar decomposition (PD) and singular value decomposition,

$$\text{SVD} \ : \ D = U\Sigma V^T \tag{3.19}$$

$$\text{PD} \ : \ D = QF \tag{3.20}$$

$D = QF = (UV^T)(V\Sigma V^T) = U\Sigma B^T$, so

$$Q \ = \ UV^T \tag{3.21}$$

$$F \ = \ V\Sigma V^T \tag{3.22}$$

The positive approximant, C_{app_F}, was given in Equation (3.18) as $(D + F)/2$. The eigenvalues of F are $|\lambda_i(D)|$. The averaging effect of Equation (3.18) results in cancellation of the negative eigenvalues of D and the resulting C_{app_F} meets the SPSD requirements.

Positive semidefinite approximation may provide meaningful results for a real system. The following section on error-minimization evaluates the effectiveness of over-determination of the mechanical system, and of SPSD approximation, in reducing the error associated with the experimentally determined compliance matrix. The effectiveness will be further evaluated for specific matrices in the computer simulations contained in the following chapter.

3.3 Minimizing Error

Raw data do not necessarily conform to the requirements of the physical system as was discussed in the preceding section. Inaccuracy of the compliance matrices may arise from noise in force and displacement measurements, non-collocated reference frames, and violation of experimental assumptions. These error sources can provide indefinite and non-symmetric compliance matrices. This section details the procedures implemented to reduce error and contains a discussion of their efficiency.

3.3.1 Agreement with Twist "Small Angle" Requirement

In the section on screw theory in the introduction, the three angles of rotational deformation of the twist were represented by a vector, $\vec{\gamma}$, of rotations about the x, y and z axes. These angles rotate the rigid body from its initial orientation to its final orientation. In order to correctly represent these displacements as a vector, the rotations must be order-independent. Order-independence is true of "small" angular displacements, but how small is "small"? A Matlab function was written to perform a Monte Carlo simulation of angular displacements. The function first randomly generated three angles between 0 and a user-specified maximum value in degrees. These three angles were used to construct a rotation matrix, R, using the x-z-y Euler angle notation. R was then decomposed using six distinct Euler angle notations to obtain the individual rotations about each of the x, y and z axes. The calculated rotational values were then compared with the original values of rotation. The Euler decomposition method most sensitive to error was the y-z-x Euler angle notation, which is the opposite order of the one used to construct the R matrix.

The data were repeatedly examined for increasingly large maximum angular values. It was determined that if all angles were less than 2 degrees the order-independence assumption was valid with a mean error of 0^o and standard deviation of $\pm 0.15^o$ ($\pm 7.5\%$).

3.3.2 Over-determination

In order to investigate the effect of over-determining the system, a Matlab simulation program was written to generate a 6×6 random matrix B from a uniform distribution between zero and one. The singular value decomposition (SVD) of the random matrix was obtained, and a symmetric positive semi-definite matrix C was calculated as

$$C = V_B \Sigma_B V_B^T$$

where V_B was an orthogonal matrix whose columns represent the eigenvectors of $B^T B$ and Σ_B was the diagonal matrix obtained by SVD. Next, a random $6 \times n$ wrench matrix, w, was created, where $6 \leq n \leq 360$. By combining the C and w in Equation (1.7), a corresponding $6 \times n$ twist matrix, T, was obtained. The entries of the w

and T matrices were perturbed by a small amount k that represented noise in the measurements of the wrenches and twists. The maximum amount of noise added to each entry of the twist and wrench matrices was determined by p, the noise measured as a percentage of the signal, as specified by the user. For the computer simulations, $5\% \leq p \leq 20\%$ was used to examine the stability of the estimation process. The value of noise added to the signal was thus

$$k = (p \div 100) \times w_{ij} \times (r \div 2)$$

where r was a random number from a normal distribution with standard deviation of 1 and mean of 0. k_{max} had a value of p percent of the signal. The perturbed twist and wrench matrices were denoted w_{exp} and T_{exp} respectively. Using the perturbed matrices, the compliance matrix, C_{exp}, was calculated to be

$$C_{exp} = \tilde{\Delta}(T_{exp} w_{exp}^T)(w_{exp} w_{exp}^T)^{-1} \tag{3.23}$$

as described in the preceding chapter on determination of the compliance matrix. The relative error of C_{exp} with respect to the original symmetric positive-definite matrix C was calculated as

$$err = \frac{\|C - C_{exp}\|_F}{\|C\|_F} \tag{3.24}$$

where $\|\cdot\|_F$ indicates the Frobenius norm. This error measurement allowed evaluation of the efficacy of over-determinacy for error-reduction.

Figures (3.2)–(3.4) display the results of the simulations with varying percentage of perturbation included in the T and w matrices. Figure (3.2) displays the results obtained for a spectrum of 1000 randomly generated compliance matrices. In Figures (3.3) and (3.4), the results were obtained from a compliance matrix representing systems with one and six DOF's respectively. The abscissa of the graphs refers to the number of twists or wrenches used to calculate the compliance matrix, and the ordinate refers to the corresponding relative error between C_{exp} and the original compliance matrix. For each point on the graph, 1000 repetitions were performed to ensure that the wrench, twist, and perturbation matrices sufficiently sampled the population. The Frobenius norms of the residuals were averaged over these 1000 trials.

The graphs in Figure (3.2) for the randomly generated compliance matrices demonstrate a trend of decreasing error with increasing over-determination of the system. The residual error was decreased to $0.52 \pm 0.09\%$ for 5% noise content: $1.07 \pm 0.19\%$ for 10% noise content; and a mean error of $1.37 \pm 0.75\%$ for 5–20% noise content. Results obtained for controlled ill-conditioned and well-conditioned compliance matrices representing systems with 1 and 6 degrees of freedom respectively were similar to those obtained for the randomly generated matrices. The results for an ill-conditioned (condition value of 250) compliance matrix are shown in Figure (3.3) ; those for the well-conditioned compliance matrix (condition value of 8) are shown in Figure (3.4). This indicates that Higham's SPSD approximation method is reliable regardless of the condition number of the matrix.

In all cases, the Frobenius norm of the residual and the standard deviation decreased with increasing over-determination, which indicated that over-determination was effective in reducing error due to noise. Because residual errors for twenty-five

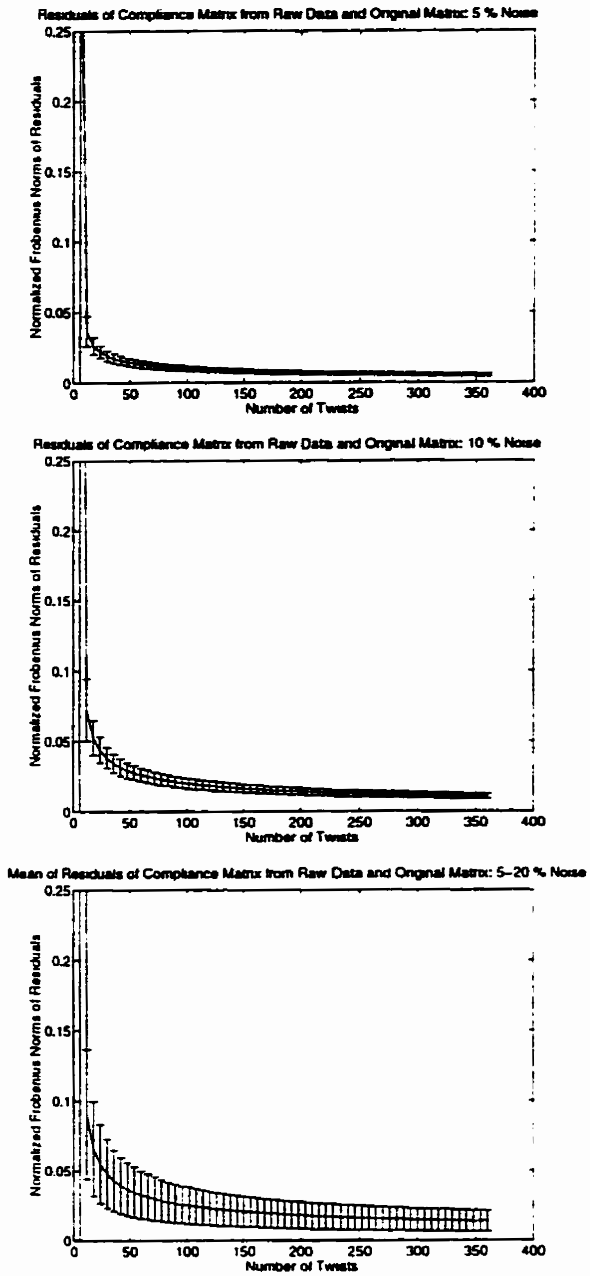

Figure 3.2: Frobenius norm of residuals of the compliance matrix obtained from raw twists and wrenches vs. randomly generated compliance matrices with noise contamination of twists and wrenches of 5%–20% and varying system over-determination.

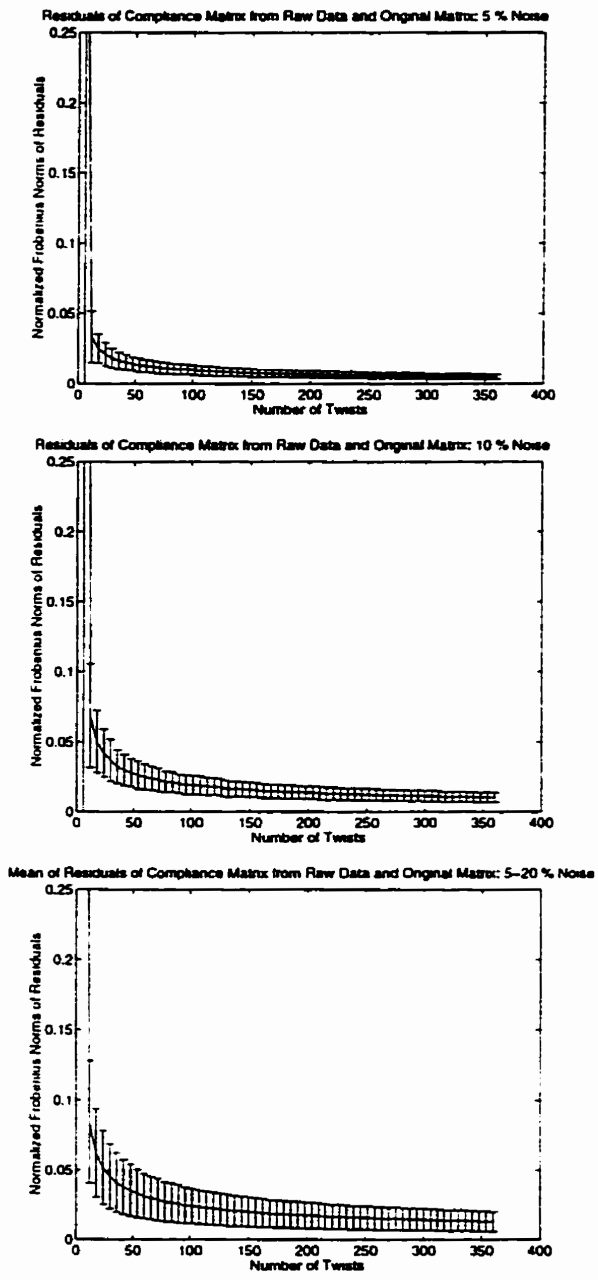

Figure 3.3: Frobenius norm of the compliance matrix obtained from raw twists and wrenches vs. the original compliance matrix for a 1 DOF system with noise contamination of twists and wrenches of 5%–20% and varying system over-determination.

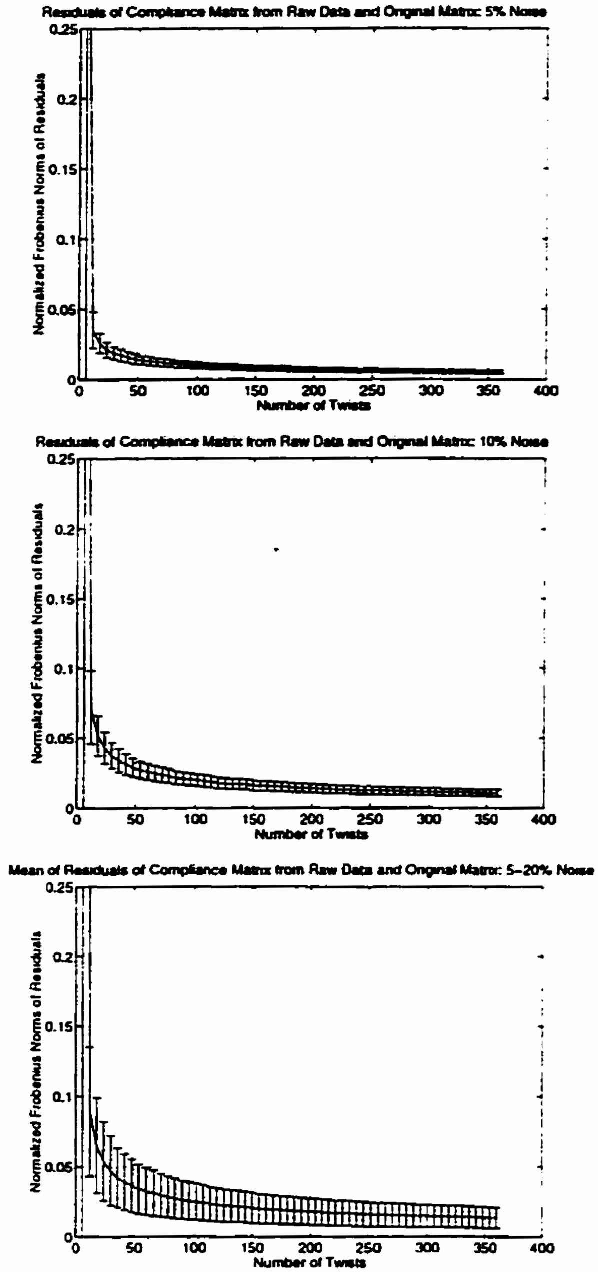

Figure 3.4: Frobenius norm of residuals of the compliance matrix obtained from raw twists and wrenches vs. the original compliance matrix for a 6 DOF system with noise contamination of twists and wrenches of 5%–20% and varying system over-determination.

times over-determined. or 150 observations, corresponded to 2.5% or less for 10% noise content, 25 times over-determined systems were used for all simulations performed in this thesis.

3.3.3 Symmetric Positive Semidefinite Approximation

The third method of error reduction applied to the simulated and experimental results was symmetric, positive semidefinite approximation of C_{exp}. Approximation was done to ensure the compliance matrix conformed to the SPSD requirement of real mechanical systems. The approximation method used here was presented in the preceding chapter.

The efficacy of the SPSD approximation was examined in a similar manner to that discussed in the preceding section on over-determination. Again. simulations were performed in which randomly generated twist and wrench matrices. based on a symmetric positive-definite compliance matrix, were perturbed and a SPSD approximant was calculated. The measure of success of the algorithm was two-fold: first that a SPSD matrix was obtained, and second that the approximation improved the residual error with respect to the original compliance matrix.

Results showed that the SPSD approximation was effective in consistently producing a symmetric positive semidefinite matrix that met the criteria for real systems as outlined in the previous chapter. Results obtained for the residual errors are presented in Figures (3.5)–(3.7). As in the preceding section on over-determination, simulations were performed for one thousand random matrices. one 1DOF matrix and one 6DOF matrix. Approximation of the SPSD matrix was performed as a continuation of the evaluation of over-determination, and the same compliance. twist and wrench matrices were used at this stage.

These graphs are similar to the graphs in Figures (3.2)–(3.4). This result implies that the majority of the error-reduction is achieved by over-determination of the system. For closer examination of the effect of approximating the symmetric positive semidefinite compliance matrix, the percentage difference in error for C_{exp} to C_{app} (equivalent to C_{app_F}) was calculated. The results are reported in Figures (3.8)–(3.10).

As can be seen from Figures (3.8)–(3.10), SPSD approximation of the compliance matrix provides a statistically significant improvement of the residual error obtained for noisy data. These figures also indicate that SPSD approximation consistently improves the estimate of the system compliance matrix.

All three error-reducing methods discussed in this section were implemented in the simulations for real systems described in the following section.

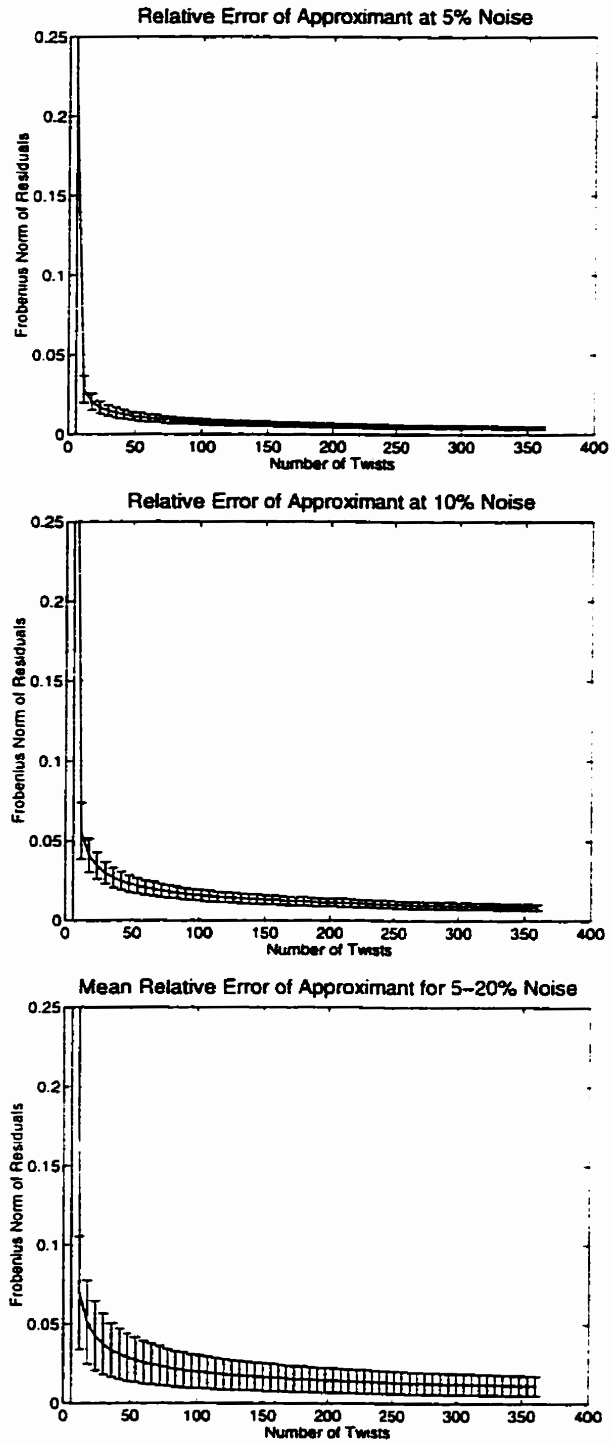

Figure 3.5: Frobenius norm of residuals of the approximant vs. randomly generated compliance matrices with noise contamination of twists and wrenches of 5%–20% and varying system over-determination.

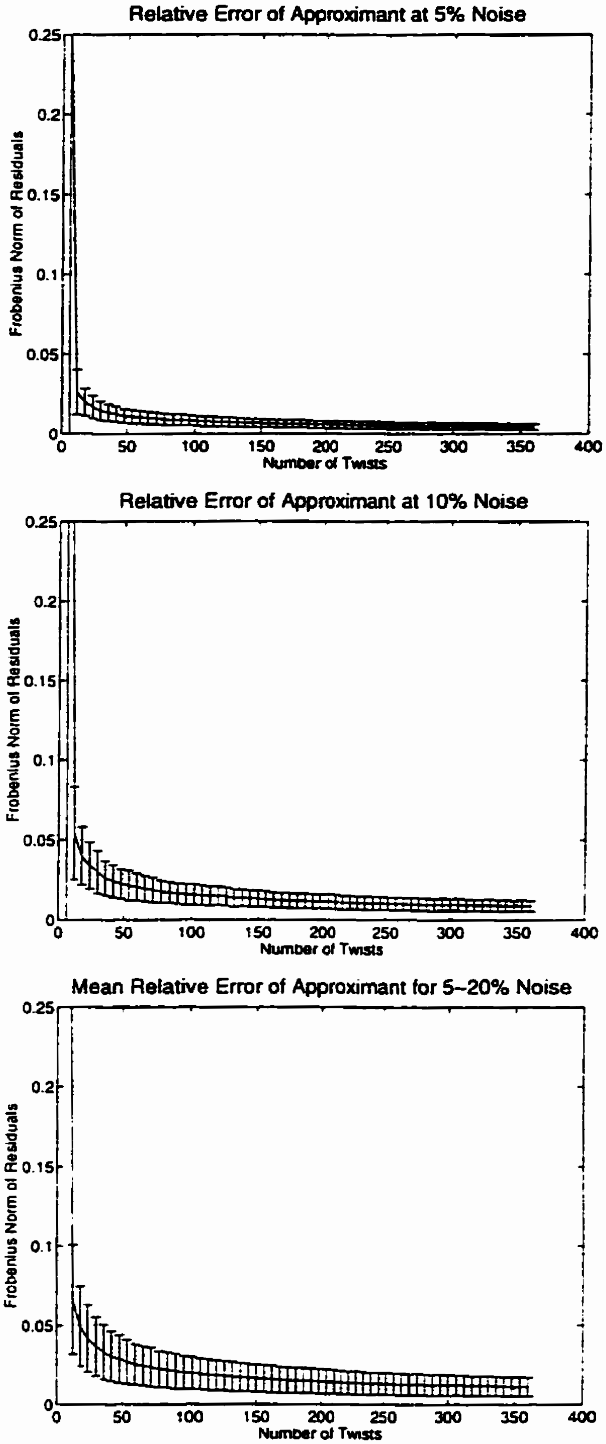

Figure 3.6: Frobenius norm of the approximant vs. the original compliance matrix for a 1 DOF system with noise contamination of twists and wrenches of 5%–20% and varying system over-determination.

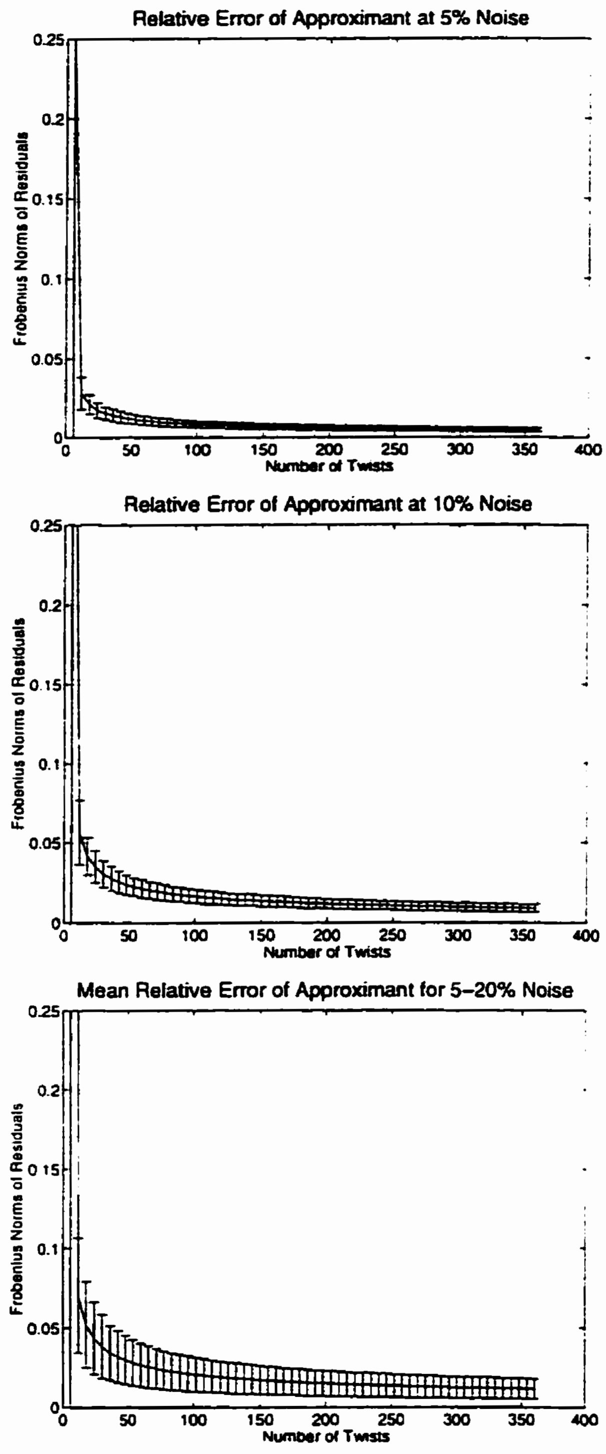

Figure 3.7: Frobenius norm of residuals of the approximant vs. the original compliance matrix for a 6 DOF system with noise contamination of twists and wrenches of 5%–20% and varying system over-determination.

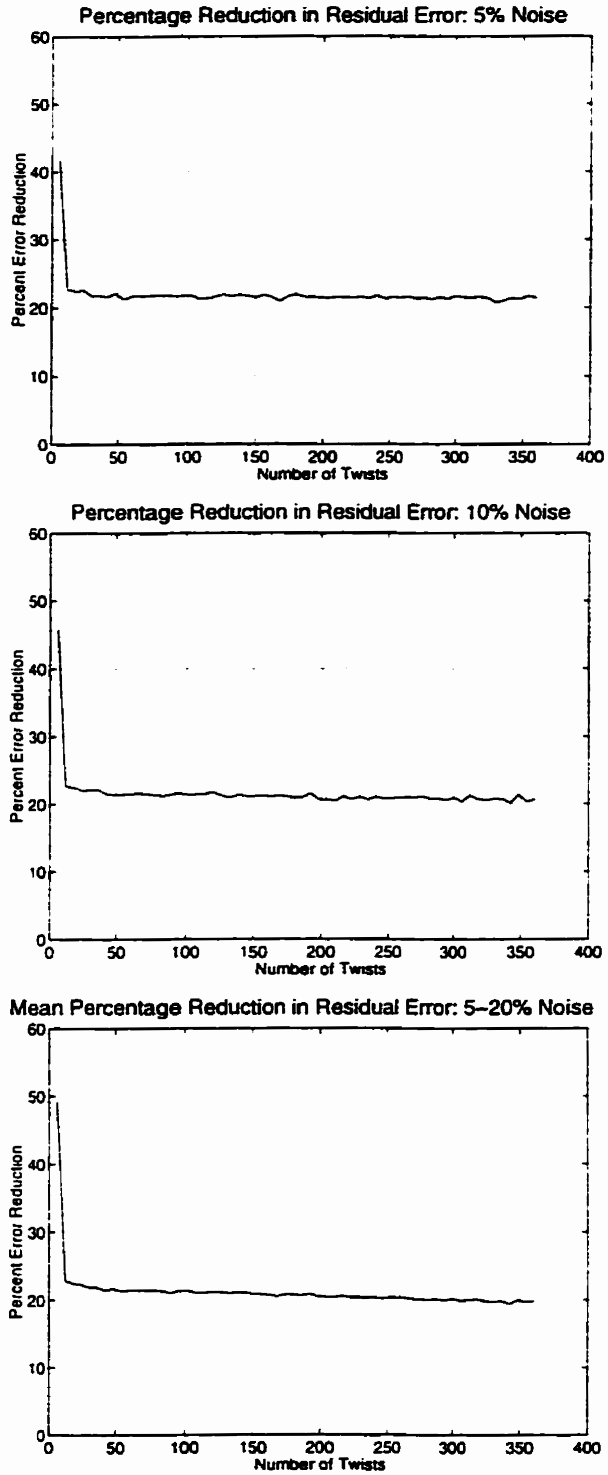

Figure 3.8: Percentage reduction in the Frobenius norms of the residuals for C_{app} vs. C_{exp} for randomly generated compliance matrices with noise contamination of twists and wrenches of 5%–20% and varying system over-determination.

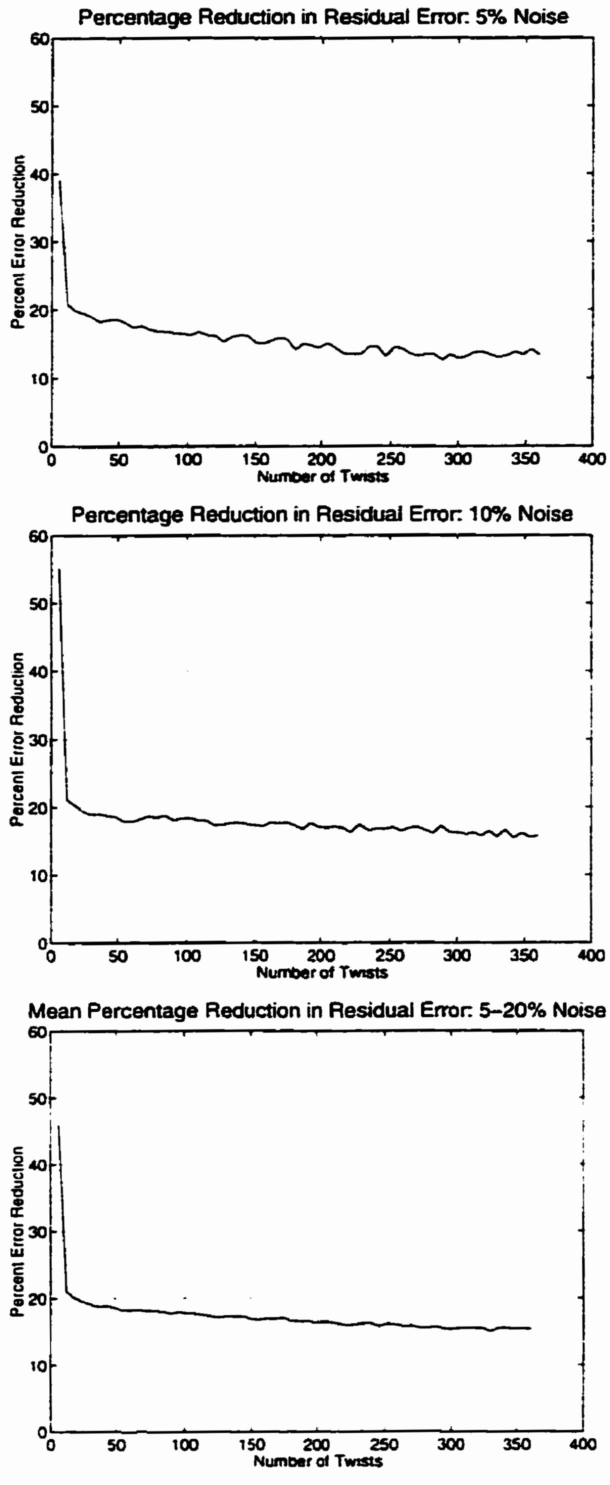

Figure 3.9: Percentage reduction in the Frobenius norm of the residuals for C_{app} vs. C_{exp} for a 1 DOF system with noise contamination of twists and wrenches of 5%–20% and varying system over-determination.

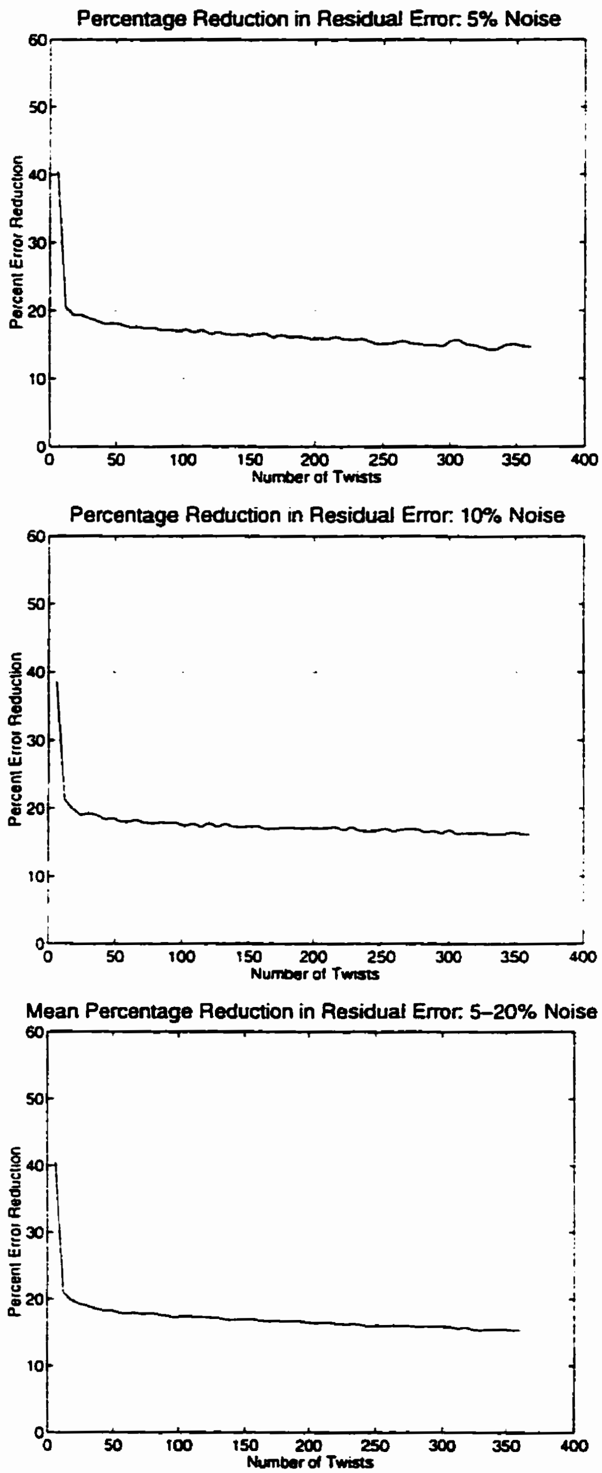

Figure 3.10: Percentage reduction in the Frobenius norm of residuals for C_{app} vs. C_{exp} for a 6 DOF system with noise contamination of twists and wrenches of 5%–20% and varying system over-determination.

Chapter 4

Experimental Procedure and Results

This chapter contains a description of the experimental procedure and the results obtained for the computer simulations conducted to evaluate the viability of using compliance matrices derived from experimental data to characterize mechanical systems.

4.1 Experimental Procedure

Computer simulations were conducted for fifteen system compliance matrices. The majority of the matrices were diagonal matrices constructed to represent systems of varying numbers and magnitudes of DOFs. Four of the matrices were extracted from Patterson and Lipkin [29]. These four matrices represented compliance of a parallel manipulator, a finger of the Stanford/JPL robot hand, an elastically suspended rigid body and a six DOF robot performing a grinding operation. The fifteen compliance matrices varied in conditioning from 4 to 1060. The condition number of the matrix is the ratio of the largest singular value to the smallest singular value obtained from singular value decomposition. The conditioning of a matrix is a measure of its sensitivity to error. Rows and columns associated with the largest values are most susceptible to error arising from noise and other perturbations.

The computer simulation consisted of randomly generating a matrix of 150 wrenches and calculating the corresponding twist matrix using one of the compliance matrices. Noise was added to the twist and wrench matrices. The noise levels used for the simulations were 5%, 10% and 20%. An intermediate compliance matrix was calculated using the perturbed twist and wrench data according to the method described in the preceding chapter. The SPSD approximant was obtained for the intermediate matrix using Higham's method as described in the preceding chapter. At this point, the SPSD approximant was compared to the original system matrix. The error for the approximant was obtained by calculating the Frobenius norm of the residuals of the approximant and the system matrix. and normalizing this value with respect to the Frobenius norm of the system matrix.

Once a SPSD approximant was obtained, eigenscrew decomposition was performed according to the method described in the theory section of the introduction. The eigenscrew directions, pitches and eigenvalues of the approximant were calculated and compared to the eigenscrew directions, pitches and eigenvalues of the system matrix. Because calculation of the rotational and translational compliance is based on ratio and multiplication of the eigenvalues and pitches, it was deemed sufficient to measure the error in the latter two values and the eigenscrew direction in order to evaluate the impact of error in the approximant on conclusions about the system drawn from eigenscrew decomposition.

The simulations were repeated 1000 times at 5%, 10% and 20% for each compliance matrix. All points on the graphs in this chapter represent the mean error value and standard deviation of 1000 trials. Computer simulations were used to evaluate the utility of compliance-matrix analysis in experimental characterization of mechanical systems. The fifteen compliance matrices examined were of three kinds:

- One matrix that represented a hinge joint. The matrix was constructed analytically to have high rotational compliance about a single axis. low translational compliance along the hinge axis, and low compliance along and about all other axes. This was an initial validation matrix, for which the compliant axis was known and results were clearly interpreted.

- Four matrices from literature, all representing physical systems with varying degrees of freedom and compliances. These matrices were secondary validation matrices, for which the compliant axes were established through peer review.

- Ten diagonal compliance matrices, representing systems with varying compliance states. The results could be validated by comparing the estimation with the model, and no other validation was available due to the paucity of the literature on this subject. (See Appendix A.)

The four matrices previously reported were taken from the work of Patterson and Lipkin [29], correcting obvious typographical errors in their article. These four matrices represented the compliances of: a parallel manipulator [26]; a finger of the Stanford/JPL robot hand [8]; a rigid body elastically suspended by a set of six springs; and a six DOF robot performing a grinding operation. Condition numbers of the fifteen compliance matrices varied from 4 to 1060.

In each computer simulation 150 wrenches were generated, with each of the six wrench values drawn from a normal distribution between -1 and +1 and multiplied by a scaling factor which ensured that the small angle condition would not be violated. For each wrench, the ideal twist was calculated as the matrix-vector product of the compliance matrix and the wrench. In order to simulate effects of sensor noise, a "noise" component of magnitude M_w was added to each element of the wrench vector. Each noise component was drawn from a normal distribution between $-M_w$ and $+M_w$, where M_w represented a specified percentage of the element of the wrench vector. The twist vector was similarly and independently contaminated with uniformly distributed variates scaled to the element of the twist vector.

The noise levels used for the simulations were 5%, 10%, and 20% of the relevant wrench element. The vectors were gathered into matrices that simulated time series of measurements, and for each twist/wrench pair the intermediate compliance matrix was calculated from the perturbed twist and wrench data using the method described in the preceding chapter. The SPSD approximant to the compliance matrix was obtained using Higham's method, also described in the preceding chapter.

Each SPSD approximant matrix was compared to the original system matrix. The error for the approximant was obtained by calculating the Frobenius norm of the residuals of the approximant and the system matrix, and then normalizing this value by dividing it by the Frobenius norm of the system matrix. This error value represented an overall measure of the efficacy of the approximation.

For each SPSD approximant the eigenscrew decomposition was also obtained, as described above. The eigenscrew directions, pitches and eigenvalues of the approximant were calculated. Differences in eigenscrew directions between the approximant and the original system were calculated as angles, using the standard definition that the cosine of the angle between two unit vectors is the dot product of the vectors. Because rotational and translational compliances are functions of the eigenvalues and pitches, errors in the elementary values of eigenvalues and pitches were calculated rather than calculating errors in the derived values. These error values represented specific performance criteria of the approximation.

For each compliance matrix, 1000 sets of 150 wrench vectors were generated and the corresponding twist vectors were calculated. Vectors in each set were contaminated with no noise and with 5%, 10%, and 20% noise as described above. Mean errors and standard deviations of errors were calculated for evaluation.

4.2 Results of Computer Simulations

The following four examples were included to help illustrate the procedure described in the preceding section and to present a sample of the results obtained for the fifteen system compliance matrices.

4.2.1 Example 1: A Stiff Hinge

In order to verify that the analysis of rigid-body motions based on screw theory produced useful and accurate information regarding the constraints of real mechanical systems, the results for simulations of real systems were investigated extensively. The following example is a simple diagonal matrix representing the compliance matrix of a stiff hinge with one rotational DOF.

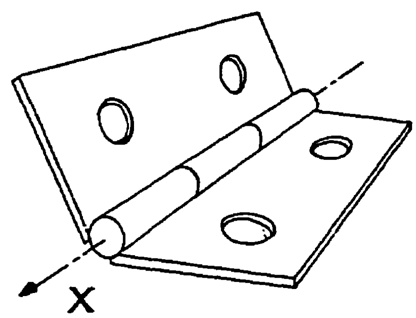

Figure 4.1: The compliance of the stiff hinge in this figure was modeled by C_{hinge}.

The compliance matrix of the hinge was based on the system illustrated in Figure (4.1). The rotational degree of freedom occurred in the direction of the longitudinal axis of the hinge, $\vec{X}$. A compliance matrix for a stiff hinge was calculated as

$$C_{hinge} = \begin{bmatrix} c_{matT_x} & 0 & 0 & 0 & 0 & 0 \\ 0 & c_{matT_y} & 0 & 0 & 0 & 0 \\ 0 & 0 & c_{matT_z} & 0 & 0 & 0 \\ 0 & 0 & 0 & c_{hinge_x} & 0 & 0 \\ 0 & 0 & 0 & 0 & c_{matR_y} & 0 \\ 0 & 0 & 0 & 0 & 0 & c_{matR_z} \end{bmatrix} \qquad (4.1)$$

where c_{matT}, c_{matR} represent the translational and rotational compliance of the hinge material, respectively, and c_{hinge} is the rotational compliance of the hinge. The anticipated results for the eigenvalue and eigenvector decomposition of C_{hinge} were that the largest eigenvalue should correspond to the x-direction and the pitch of the hinge axis should be very small, indicating large rotational compliance and small translational compliance.

The value of c_{hinge_x} was $\frac{1}{200}$, and the values of c_{matT} and c_{matR} in all directions were $\frac{1}{20000}$. The wrench matrix was randomly generated and the twist matrix was obtained from the equation of compliance. Computation of the eigenvectors and eigenvalues of the C_{hinge} matrix was performed for non-noisy and noisy data. 5%, 10% and 20% noise were added to the twist and wrench matrices that were generated for the hinge compliance matrix. The matrix of eigenvectors obtained for data with 0% noise content was

$$e = \begin{bmatrix} 1.00 & 0 & 0 & 0 & 0 & 1.00 \\ 0 & 1.00 & 0 & 0 & 1.00 & 0 \\ 0 & 0 & 1.00 & 1.00 & 0 & 0 \\ -0.10 & 0 & 0 & 0 & 0 & 0.10 \\ 0 & -10.0 & 0 & 0 & 1.00 & 0 \\ 0 & 0 & -1.00 & 1.00 & 0 & 0 \end{bmatrix} \tag{4.2}$$

Each column of the e matrix represents one eigenscrew. The direction of the eigenvector was given by the first three components of the eigenscrew. The corresponding eigenvalues were

$$\vec{\lambda} = \begin{bmatrix} -0.5 & -0.05 & -0.05 & 0.05 & 0.05 & 0.5 \end{bmatrix} \times 10^{-3}$$

The pitches of the eigenscrew axes were

$$\vec{h} = \begin{bmatrix} -0.1 & -1.0 & -1.0 & 1.0 & 1.0 & 0.1 \end{bmatrix}$$

From the eigenvalues and the eigenscrew pitches, the rotational compliances were calculated as

$$\vec{C}_R = \begin{bmatrix} 50.0 & 0.5 & 0.5 & 0.5 & 0.5 & 50.0 \end{bmatrix} \times 10^{-4}$$

The translational compliances were also obtained using the eigenvalue and pitch for each of the eigenscrews. These were

$$\vec{C}_T = \begin{bmatrix} 0.5 & 0.5 & 0.5 & 0.5 & 0.5 & 0.5 \end{bmatrix} \times 10^{-4}$$

From the eigenvalues, eigenscrew directions and eigenscrew pitches it was determined that the system consisted of three orthogonal compliant eigenscrews. Eigenscrew pairs 1 - 6, 2 - 5, and 3 - 4 formed compliant axes. Compliant axes 2 - 5 and 3 - 4 had very small rotational compliance and 1 - 6 had 100 times larger rotational compliance. From the rotational compliance and translational compliances, it was easy to determine that the system had only one degree of rotational compliance and was highly constrained in translation. Compliant axis 1 - 6 corresponded to the x-axis of the hinge as was expected. The pitch of the 1 - 6 axis was calculated to be +/- 0.1 which implies that for every unit of translational motion, there will be 10 units of rotational motion. Combining the pitches with the eigenvalues of the hinge axis, a rotational compliance of 5.0×10^{-3} and a translational compliance of 5.0×10^{-5} were obtained. These results implied that the 1 - 6 compliant axis is resistant to translational motion. The compliance results were in agreement with the model of the hinge. The condition number of the compliance matrix was 100, which is moderately ill-conditioned.

5%, 10% and 20% noise were added to the twist and wrench data and the errors relative to the original compliance matrix, and the eigenscrew decompositions were calculated for 1000 trials. Figure (4.5) presents the error of the approximant relative to the original hinge matrix for each of the 1000 trials. Error reduction of the approximant appears to be effective.

Figure (4.2) contains the results of angular error for each of the eigenvectors for increasing noise levels. Errors for each of the corresponding eigenvalues are presented in Figure (4.3). Errors in the eigenscrew pitches are displayed in Figure (4.4). Each data point in these two figures corresponded to the average of a sample population of 1000. As can be seen from Figure (4.2) the eigenvector directions for 2 - 4 and 3 - 5 compliant axes were very sensitive to noise. However, the eigenvector direction of the 1 - 6 compliant axis was very stable. This suggested that the x-axis of the hinge will be correctly identified to within one degree when 20% was added to the twists and wrenches. The eigenscrew pairs 2 - 4 and 3 - 5 were confined to lie in a plane orthogonal to the 1 - 6 compliant axis, but their directions could not be reliably determined within the plane because these two compliant axes were not distinct. Figure (4.3) shows the computations of the eigenvalues for the compliant axes were robust with respect to added noise. Figure (4.4) indicates that the eigenscrew pitches were reliably determined for each of the compliant axes. Table (4.1) contains the values of the data used to construct these figures.

Table (4.1) presents the mean errors and standard deviations of the results for eigenscrew angular error, eigenvector error and eigenscrew pitch error for each eigenscrew with increasing noise content. The compliant axis had the largest error distribution in pitches. The large errors in direction were attributed to (a) ill-conditioning

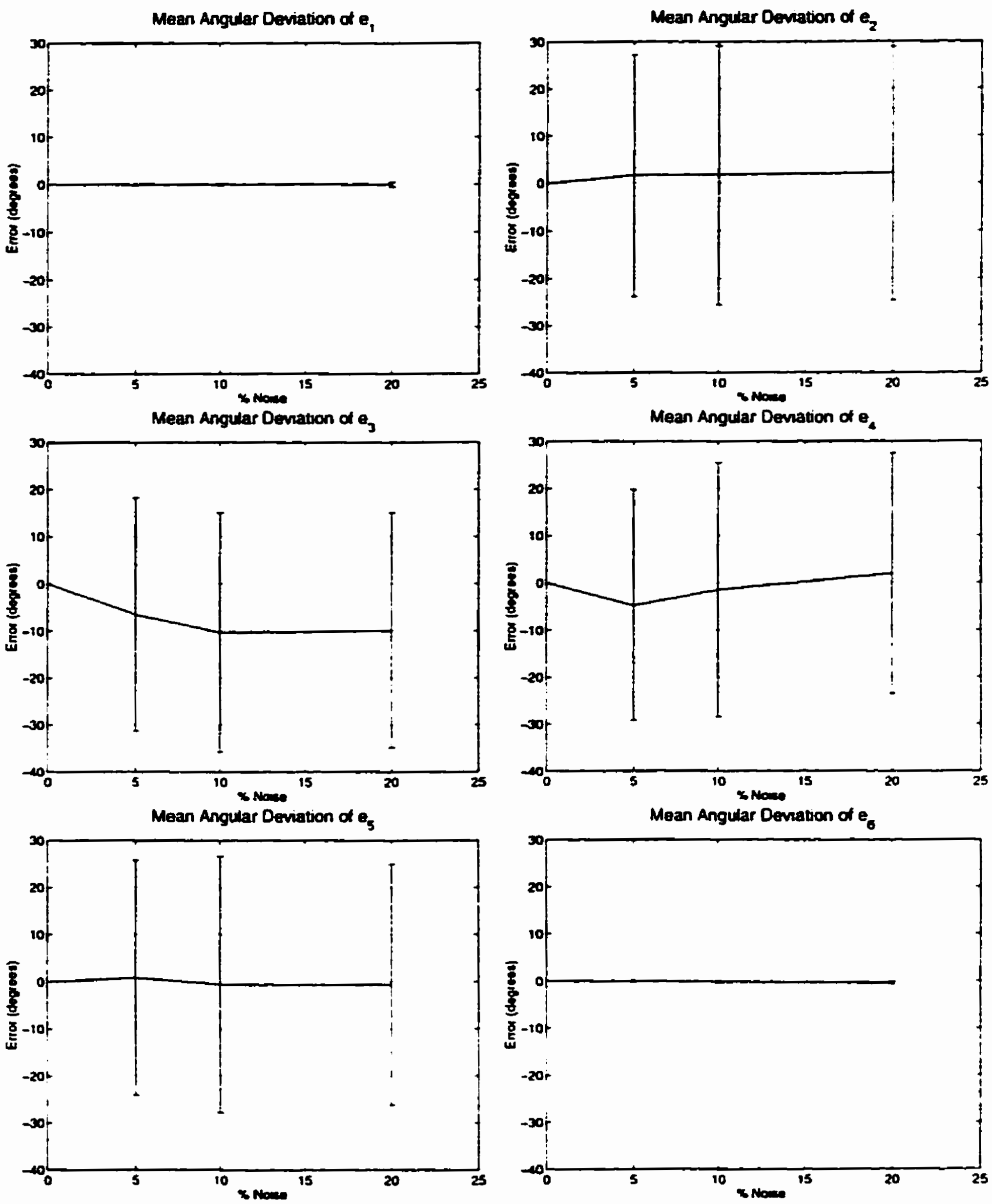

Figure 4.2: Mean errors of eigenscrew directions for hinge model averaged over 1000 trials at 5%, 10% and 20% noise content.

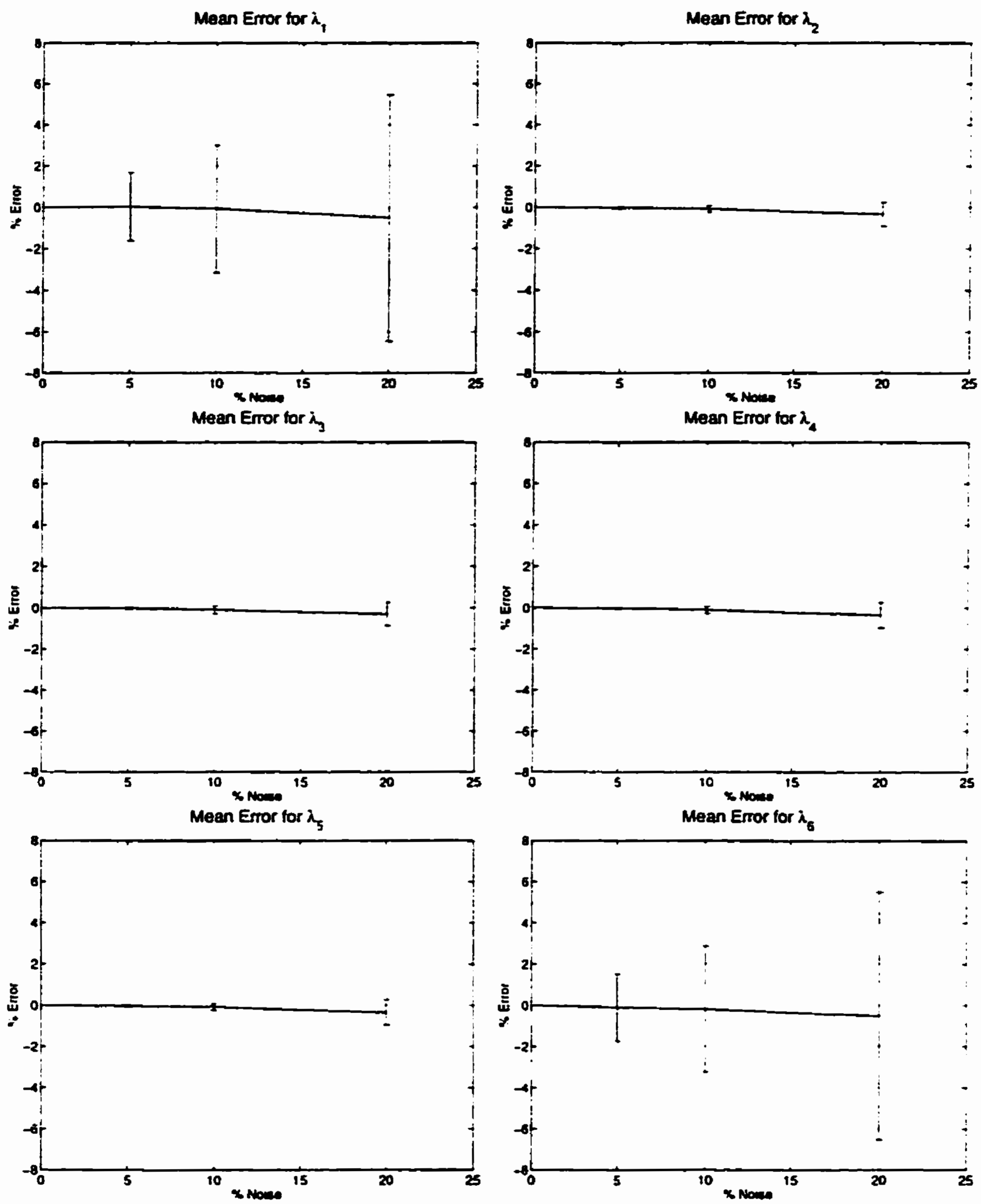

Figure 4.3: Mean errors of eigenvalues for hinge model averaged over 1000 trials at 5%, 10% and 20% noise content.

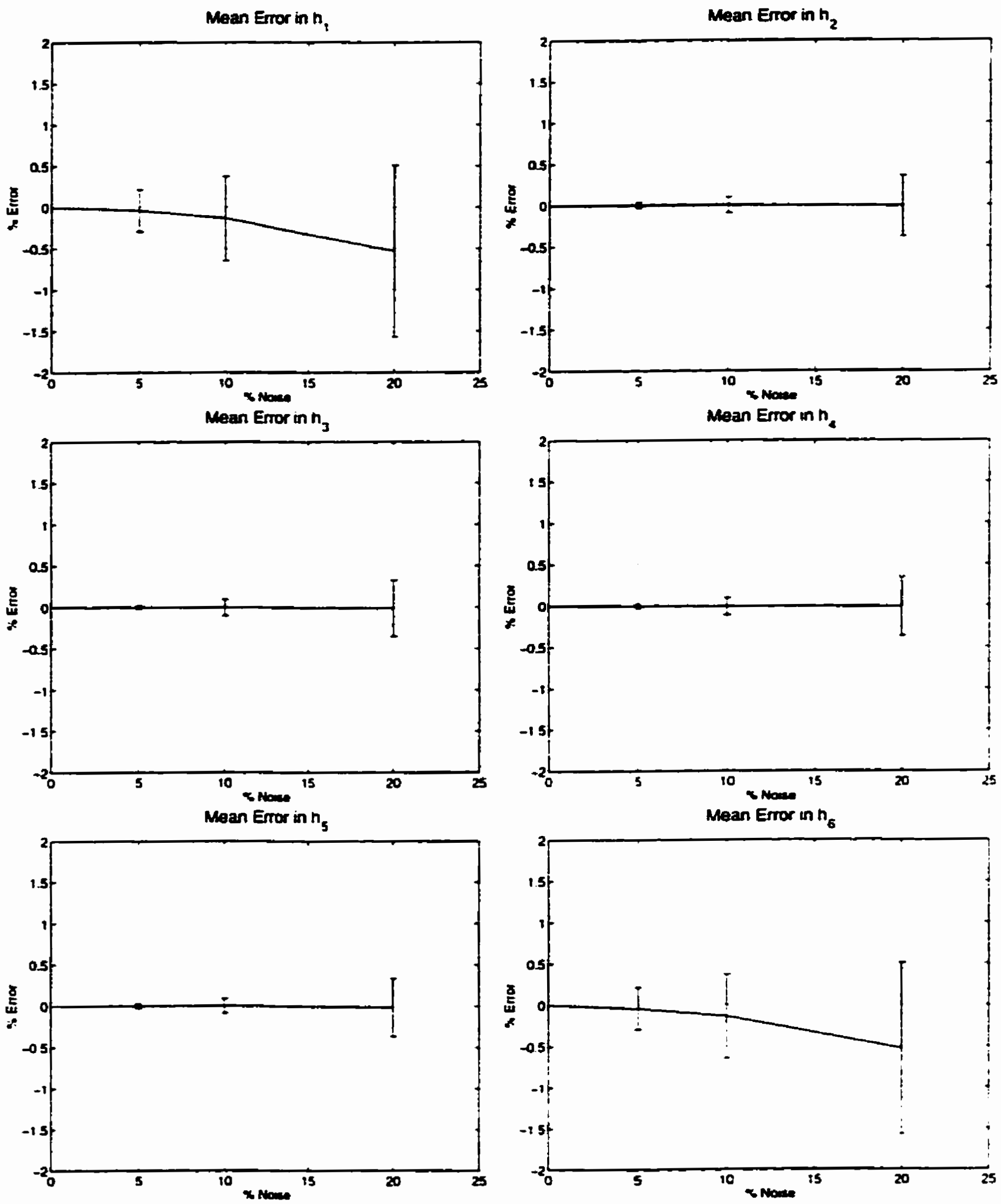

Figure 4.4: Mean errors of pitches for hinge model averaged over 1000 trials at 5%, 10% and 20% noise content.

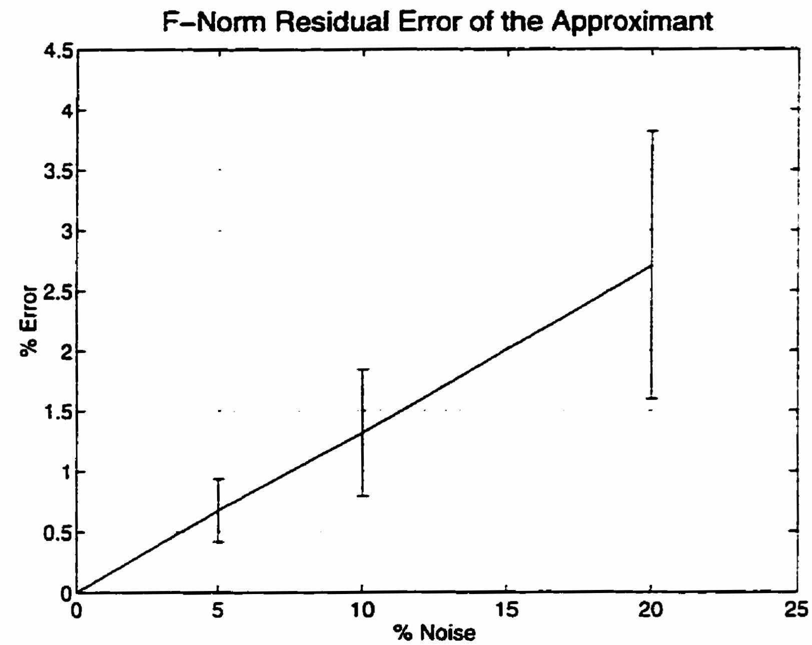

Figure 4.5: Error of the approximant with respect to the hinge compliance matrix.

of the matrix and (b) algebraic multiplicity of the small eigenvalues. It was also observed that, in spite of the large angular error distribution, the eigenscrews corresponding to constrained directions remained in a plane orthogonal to the direction of the most compliant eigenscrew axis. This is to be expected, because eigenvectors with distinct eigenvalues must be orthogonal.

	Noise	1	2	3
Eigen-screw $\text{Dir}^{\text{ns}}(^o)$	5%	0.0±0.1	1.7±25.5	-6.6±24.8
	10%	0.0±0.2	1.8±27.3	-10.4±25.4
	20%	0.0±0.5	2.1±26.7	-9.9±24.9
Eigen-values (%)	5%	0.0±0.0	0.0±0.0	0.0±0.0
	10%	-0.1±3.1	-0.1±0.2	-0.1±0.2
	20%	-0.5±6.0	-0.3±0.6	-0.3±0.6
Pitches (%)	5%	0.0±0.3	0.0±0.0	0.0±0.0
	10%	-0.1±0.5	0.0±0.1	0.0±0.1
	20%	-0.5±1.0	0.0±0.3	0.0±0.3
	Noise	4	5	6
Eigen-screw $\text{Dir}^{\text{ns}}(^o)$	5%	-4.8±24.4	0.8±24.9	0.0±0.1
	10%	-1.5±27.0	-0.6±27.2	-0.2±0.2
	20%	1.9±25.5	-0.6±25.5	-0.4±0.3
Eigen-values (%)	5%	0.0±0.0	0.0±0.0	0.0±0.0
	10%	-0.1±0.2	-0.1±0.2	-0.2±3.1
	20%	-0.3±0.6	-0.4±0.6	-0.5±6.0
Pitches (%)	5%	0.0±0.0	0.0±0.0	0.0±0.3
	10%	0.0±0.1	0.0±0.1	0.1±0.5
	20%	0.0±0.4	0.0±0.4	-0.5±1.0

Table 4.1: Mean errors and standard deviations of eigenscrew direction. pitch and eigenscrew for each of the eigenscrews of the hinge mode at 5%, 10% and 20% noise content.

4.2.2 Example 2: A Finger of the Stanford/JPL Robot Hand

The passive compliance matrix of one finger of the Stanford/JPL robot hand was given by Cutkosky etàl [8] as

$$C = \begin{bmatrix} 0.13 & 0 & -0.02 & 0 & -0.93 & 0 \\ 0 & 0.12 & 0 & 0.50 & 0 & 0.30 \\ -0.02 & 0 & 0.02 & 0 & 0.10 & 0 \\ 0 & 0.50 & 0 & 3.25 & 0 & 2.00 \\ -0.93 & 0 & 0.10 & 0 & 12.00 & 0 \\ 0 & 0.30 & 0 & 2.00 & 0 & 1.25 \end{bmatrix} \times 10^{-3} \tag{4.3}$$

This matrix was ill-conditioned with a condition number of 964. As in the preceding stiff-hinge example, the eigenscrews and eigenvalues were calculated based on the compliance matrix. The normalized eigenscrews were

$$e = \begin{bmatrix} -0.31 & -0.75 & 0 & 0 & -0.75 & -0.31 \\ 0.93 & -0.47 & 0.14 & -0.14 & 0.47 & -0.93 \\ -0.18 & -0.47 & -0.99 & -0.99 & -0.47 & -0.18 \\ -0.06 & 0.15 & -0.65 & 0.65 & -0.15 & 0.06 \\ -0.10 & -0.04 & 0.01 & 0.01 & -0.04 & -0.10 \\ 0.01 & 0 & 1.01 & -1.01 & 0 & -0.01 \end{bmatrix} \tag{4.4}$$

The corresponding eigenvalues were

$$\vec{\lambda} = \begin{bmatrix} -0.98 & -0.33 & -0.02 & 0.02 & 0.33 & 0.98 \end{bmatrix} \times 10^{-3}$$

The eigenscrew pitches were

$$\vec{h} = \begin{bmatrix} -0.08 & -0.09 & -1.00 & 1.00 & 0.09 & 0.08 \end{bmatrix}$$

The rotational compliances of the eigenscrews were

$$\vec{C}_R = \begin{bmatrix} 12.93 & 3.60 & 0.02 & 0.02 & 3.60 & 12.93 \end{bmatrix} \times 10^{-3}$$

The translational compliances of the eigenscrews were

$$\vec{C}_T = \begin{bmatrix} 0.07 & 0.03 & 0.02 & 0.02 & 0.03 & 0.07 \end{bmatrix} \times 10^{-3}$$

Due to the non-collinear eigenscrews, there were no compliant axes for the Stanford/JPL finger in this posture. This result was not expected for this manipulator. The small rotational and translational compliances reveal that the finger was very stiff. The lack of compliant axes could be attributed to the high stiffness of the manipulator that may have made decoupling of the imposed translations and rotations impossible. Past experience indicated that this result may also be attributed to erroneous reporting of the compliance matrix in the literature.

The error of the approximant relative to the compliance matrix in Equation (4.3) was calculated for twists and wrenches containing 5%, 10% and 20% noise. The results of these calculations are presented in Figure (4.6). These results are very similar to those obtained for the hinge example.

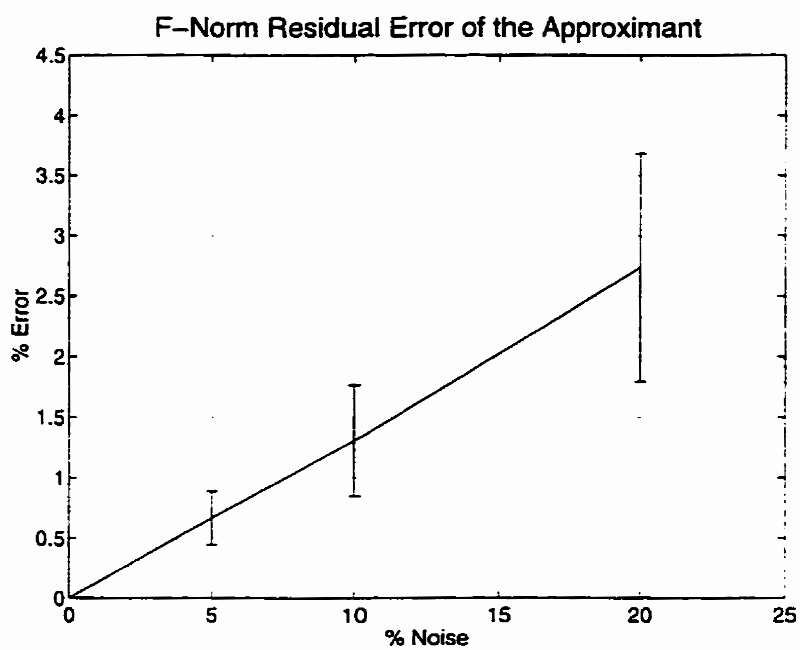

Figure 4.6: Error of the approximant with respect to the compliance matrix of the finger from the Stanford/JPL robot hand.

	Noise	1	2	3
Eigen-screw $Dir^{ns}(^o)$	5%	0.1±0.8	0.0±2.0	-3.3-0.3i±18.9
	10%	0.1±1.7	-0.1±4.0	1.6-.7i±30
	20%	0.1±3.2.	0±7.5	5.5-0.6i±40
Eigen-values (%)	5%	1.2±3.2	-6.4±9.8	-100.0±0.0
	10%	-0.2±5.9	-3.0±13.2	-100.0±0.0
	20%	-0.6±10.2	-2.1±18.9	-88.2±78.7
Pitches (%)	5%	34.3±81.2	33.0±79.5	32.6±84.1
	10%	33.1±85.1	36.9±92.8	33.6±81.5
	20%	33.0±88.8	36.8±76.8	34.3±82.3

	Noise	4	5	6
Eigen-screw $Dir^{ns}(^o)$	5%	15.3-0.2i±13.0	1.6±1.1	0.7±0.5
	10%	21.3+0.1i±23.2	2.6±2.9	1.2±1.1
	20%	21.2+0.1i±35.2	2.0±7.2	1.1±3.1
Eigen-values (%)	5%	-100.0±0.0	-7.0±9.2	-1.0±3.5
	10%	-100.0±0.0	-2.2±13.4	-5.7±0.0
	20%	-86.1±85.3	-3.5±18.6	-0.9±10.4
Pitches (%)	5%	33.6±83.7	36.3±84.8	36.6±82.5
	10%	34.4±82.0	34.7±91.3	33.4±81.8
	20%	36.9±78.9	30.0±87.2	37.0±77.2

Table 4.2: Mean errors and standard deviations of eigenscrew direction, pitch and eigenvalue for each of the eigenscrews of a finger of the Stanford/JPL robot hand at 5%, 10% and 20% noise content.

Angular deviation of the eigenscrew directions, error in the eigenvalues and error in eigenscrew pitches were calculated for each of the eigenscrews for varying noise content. The results of these calculations are presented in Table (4.2). Error distributions were large, especially for the eigenscrews corresponding to the smallest values of compliance, 3 and 4, because of the nearly singular condition of the matrix. Because the compliance values of 3 and 4 were nearly 0, large error offsets and imaginary values in the eigenscrews were occasionally obtained.

4.2.3 Example 3: A Parallel Manipulator

The compliance matrix for a parallel manipulator was given by Patterson and Lipkin [29] as

$$C = \begin{bmatrix} 898 & 0 & 0 & 0 & 0 & 0 \\ 0 & 898 & 0 & 0 & 0 & 0 \\ 0 & 0 & 21.8 & 0 & 0 & 0 \\ 0 & 0 & 0 & 1.04 & 0 & 0 \\ 0 & 0 & 0 & 0 & 1.04 & 0 \\ 0 & 0 & 0 & 0 & 0 & 10.6 \end{bmatrix} \tag{4.5}$$

This matrix is ill-conditioned, with a condition number of 864.

The normalized eigenscrews of the scaled compliance matrix were

$$e = \begin{bmatrix} 1.0 & 0 & 0 & 0 & 0 & 1.0 \\ 0 & 1.0 & 0 & 0 & 1.0 & 0 \\ 0 & 0 & 1.0 & 1.0 & 0 & 0 \\ -29.4 & 0 & 0 & 0 & 0 & 29.4 \\ 0 & -29.4 & 0 & 0 & 29.4 & 0 \\ 0 & 0 & -1.4 & 1.4 & 0 & 0 \end{bmatrix} \tag{4.6}$$

where each column of e represents an eigenscrew. The corresponding eigenvalues were

$$\vec{\lambda} = \begin{bmatrix} -30.5 & -30.5 & -15.2 & 15.2 & 30.5 & 30.5 \end{bmatrix}$$

The pitches of the eigenscrews were

$$\vec{h} = \begin{bmatrix} -29.4 & -29.4 & -1.4 & 1.4 & 29.4 & 29.4 \end{bmatrix}$$

The rotational compliances were

$$\vec{C}_R = \begin{bmatrix} 1.0 & 1.0 & 10.6 & 10.6 & 1.0 & 1.0 \end{bmatrix}$$

The translational compliances were

$$\vec{C}_T = \begin{bmatrix} 898.0 & 898.0 & 21.8 & 21.8 & 898.0 & 898.0 \end{bmatrix}$$

The eigenscrews and eigenvalues presented here were consistent with the results reported by Patterson and Lipkin [29]. The eigenscrews and eigenvalues at 0% noise revealed that the system had three pairs of eigenscrews that met the criteria of compliant axes (eigenscrew pairs 1 - 6, 2 - 5, and 3 - 4). These three compliant axes formed an orthogonal system with axes coinciding with the x-, y- and z-directions of the parallel manipulator's coordinate frame. Calculation of the rotational and translational compliance for each of the eigenscrews revealed that the x-directed and y-directed compliant axes had high translational compliance, whereas the z-directed compliant axis had high rotational compliance. These results suggest that this is a 3-DOF system.

5%, 10% and 20% noise was added to the twists and wrenches. The relative errors in the approximant were comparable to those obtained in the other examples.

Mean errors and standard deviations of errors are presented in Table (4.3). The

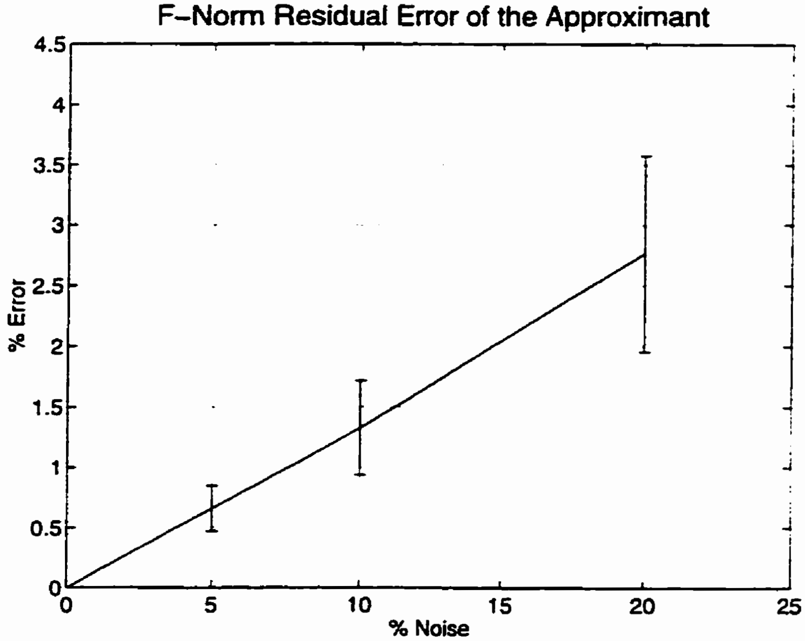

Figure 4.7: Error of the approximant with respect to the compliance matrix of the parallel manipulator.

eigenscrews corresponding to the large diagonal elements were especially susceptible to noise, and poor results were obtained. Again, the two largest eigenvalues were equal and the matrix was ill-conditioned. This is a situation similar to the stiff-hinge example and the results are similar to those obtained for the hinge.

It should be noted that Patterson and Lipkin multiplied the values of the matrix by 10^4. This magnification factor calls into question the effect of scaling on the estimation of the compliance matrix. The original matrix calculated by Merlet [26] used units of Newtons and millimeters, with the matrix having a condition number of 864. These units are inconsistent with SI usage. When units of Newtons and meters were used to calculate C, the condition number was 24 000, which is essentially a singular matrix. When Patterson and Lipkin reported their results in Newtons and millimeters they did not scale angular measurements accordingly, hence the change in the condition number of the matrix. For both the scaled and unscaled compliance matrices the eigenscrew directions and eigenvalues were the same, but the magnitude of the pitch changed substantially because the angles were not reported in milli-radians to ensure consistency between the units. The effect of scaling and unit consistency was not thoroughly investigated in this work, but the decrease in the condition number of Merlet's compliance matrix suggested that a matrix's sensitivity to error, can be improved by astute selection of units. Care must be taken to ensure consistency in the units for a correct eigenscrew decomposition to be obtained.

4.2.4 Example 4: A 6 DOF Robot for a Grinding Operation

The passive compliance matrix for a six-DOF robot used in grinding operations was reported by Patterson and Lipkin [29] as

$$C = \begin{bmatrix} 0.48 & 0 & 0 & 0 & 0 & 0 \\ 0 & 0.59 & 0 & 0 & 0 & 1.20 \\ 0 & 0 & 1.25 & 0 & -4.50 & 0 \\ 0 & 0 & 0 & 100 & 0 & 0 \\ 0 & 0 & -4.50 & 0 & 21.0 & 0 \\ 0 & 1.20 & 0 & 0 & 0 & 3.00 \end{bmatrix} \tag{4.7}$$

	Noise	1	2	3
Eigen-screw Dir^{ns} (^{o})	5%	-3.0±26.4	-2.1±26.5	-0.1±0.3
	10%	-1.6±26.9	0.0±27.1	-0.2±0.6
	20%	0.3±32.1	1.4±39.1	0.0±11.8
Eigen-values (%)	5%	0.0±5.3	-0.1±5.2	-0.1±0.4
	10%	-0.2±10.5	-0.5±10.3	-0.4±0.9
	20%	0.4±18.7	-5.6±24.7	1.4±11.1
Pitches (%)	5%	0.5±0.7	0.4±0.7	0.0±0.4
	10%	1.7±2.6	2.1±2.9	-0.1±0.8
	20%	7.0±8.8	15.7±26.8	-67.3±227.7
	Noise	4	5	6
Eigen-screw Dir^{ns} (^{o})	5%	-0.1±0.3	2.2±26.5	-1.6±26.6
	10%	-0.1±0.6	1.0±27.2	-3.6±26.8
	20%	-0.3±3.0	-0.8±34.4	-2.7±31.7
Eigen-values (%)	5%	-0.1±0.4	-0.1±5.3	-0.2±5.4
	10%	-0.5±0.9	-0.5±10.3	-0.3±10.5
	20%	-2.0±2.1	-3.0±22.0	0.2±19.4
Pitches (%)	5%	-0.0±0.4	0.4±0.7	0.5±0.8
	10%	-0.2±0.9	2.2±3.8	1.8±2.8
	20%	-4.5±38.1	11.8±17.9	7.2±8.7

Table 4.3: Mean errors and standard deviations for eigenscrew direction. pitch and eigenvalue of each eigenscrew of the parallel manipulator at 5%. 10% and 20% noise content.

The system eigenscrews were

$$e = \begin{bmatrix} 1.00 & 0 & 0 & 0 & 0 & 1.00 \\ 0 & -0.96 & -0.79 & 0.79 & -0.96 & 0 \\ 0 & 0.29 & -0.61 & -0.61 & -0.29 & 0 \\ -0.07 & 0 & 0 & 0 & 0 & 0.07 \\ 0 & 0.16 & -0.11 & -0.11 & -0.16 & 0 \\ 0 & 0.17 & 0.45 & -0.45 & 0.17 & 0 \end{bmatrix} \tag{4.8}$$

The corresponding eigenvalues were

$$\vec{\lambda} = \begin{bmatrix} -6.93 & -2.22 & -0.63 & 0.63 & 2.22 & 6.93 \end{bmatrix}$$

The pitches of the eigenscrews were

$$\vec{h} = \begin{bmatrix} -0.07 & -0.11 & -0.19 & 0.19 & 0.11 & 0.07 \end{bmatrix}$$

The rotational compliances were

$$\vec{C_R} = \begin{bmatrix} 100.00 & 20.63 & 3.37 & 3.37 & 20.63 & 100.00 \end{bmatrix}$$

The translational compliances were

$$\vec{C_T} = \begin{bmatrix} 0.48 & 0.24 & 0.12 & 0.12 & 0.24 & 0.48 \end{bmatrix}$$

Eigenscrew decomposition of the compliance matrix in Equation (4.7) revealed the existence of one compliant axis collinear with the x-axis of the system coordinate frame.

The 1 - 6 pair of eigenscrews formed the compliant axis. The other four eigenscrews were perpendicular to the compliant axis. Calculation of the eigenscrew compliance revealed that the compliant axis was predominantly rotationally compliant. Eigenscrews, 2, 5, 3 and 4 were less rotationally compliant. Translational compliance also decreased for the 2, 5, 3 and 4 eigenscrews.

The compliance matrix in Equation (4.7) was calculated from noise contaminated twists and wrenches. The approximant was compared to the original matrix, with the errors presented in Figure (4.8).

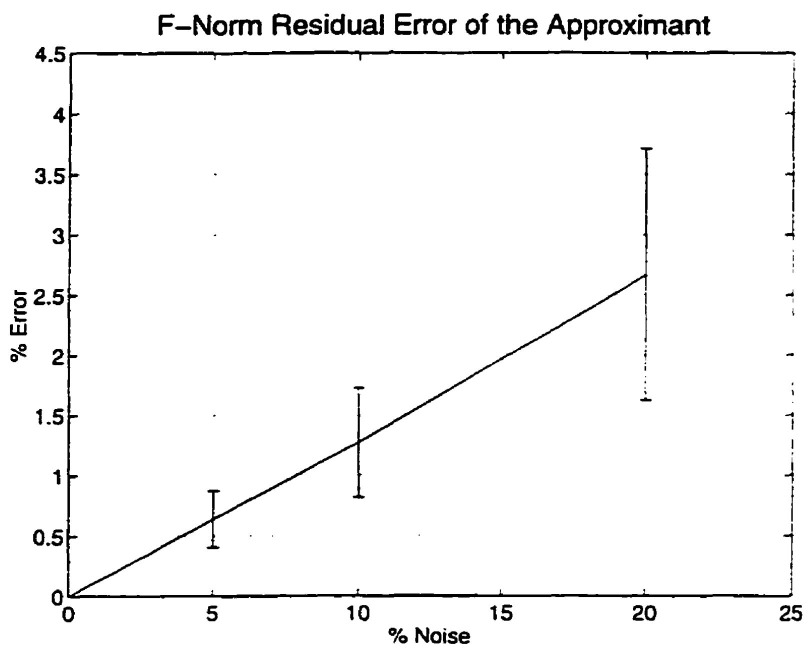

Figure 4.8: Error of the approximant relative to the compliance matrix of the 6 DOF robot for grinding operations.

Eigenscrew directional error, eigenvalue error and eigenscrew pitch error were calculated for 5%, 10% and 20% noise. The results of these trials are presented in Table (4.4). The distribution of the errors in eigenscrew directions were small. The

	Noise	1	2	3
Eigen-screw $\mathrm{Dir}^{\mathrm{ns}}(^o)$	5%	0.1± 0.4	-0.8±0.9	0.5±1.4
	10%	0.2±0.9	-0.1±1.7	0.7±2.9
	20%	0.1±1.9	-0.2±3.8	1.8±6.4
Eigen-values (%)	5%	0.0±2.2	-0.1±2.1	-0.4±4.1
	10%	-0.1±4.3	-0.5±4.3	-1.7±8.0
	20%	-1.3±8.4	-2.1±8.2	-5.1±16.7
Pitches (%)	5%	0.0±0.4	0.1±1.8	0.2±3.5
	10%	0.0±0.7	0.4±3.6	0.8±6.8
	20%	-0.1±1.4	0.9±7.1	3.5±14.6
	Noise	4	5	6
Eigen-screw $\mathrm{Dir}^{\mathrm{ns}}(^o)$	5%	0.1±1.5	-0.1±0.9	-0.1±0.4
	10%	0.3±3.0	-0.1±1.7	-0.2±0.8
	20%	0.9±6.5	-0.2±3.7	-0.3±1.8
Eigen-values (%)	5%	-0.2±4.0	-0.2±2.1	-0.1±2.2
	10%	-1.5±8.0	-0.8±4.2	-0.3±4.3
	20%	-5.4±16.0	-2.0±8.4	-0.3±8.4
Pitches (%)	5%	0.1±3.4	0.1±1.8	-0.0±0.4
	10%	0.8±6.9	0.4±3.5	0.0±0.7
	20%	3.6±14.1	0.8±7.6	-0.1±1.4

Table 4.4: Mean errors and standard deviations of eigenscrew direction, pitch and eigenvalue associated for each of the eigenscrews of the robot performing a grinding operation at 5%, 10% and 20% noise content.

error distribution for the eigenvalues and pitches were larger, as expected for a poorly conditioned matrix. The relatively small errors in eigenscrew directions is because all eigenvalues were distinct.

4.2.5 Example 5: An Elastically Suspended Rigid Body

The compliance matrix of an elastically suspended rigid body was reported by Patterson and Lipkin [29] as

$$C = \begin{bmatrix} 40.40 & 0 & 0 & -16.00 & 0 & 0 \\ 0 & 30.00 & 0 & 0 & -11.80 & 0 \\ 0 & 0 & 31.80 & 0 & 0 & -13.10 \\ -16.00 & 0 & 0 & 56.20 & 0 & 0 \\ 0 & -11.80 & 0 & 0 & 10.50 & 0 \\ 0 & 0 & -13.10 & 0 & 0 & 25.40 \end{bmatrix} \tag{4.9}$$

The normalized eigenscrews of C were

$$e(0) = \begin{bmatrix} 1.00 & 0 & 0 & 0 & 0 & 1.00 \\ 0 & 0 & 1.00 & -1.00 & 0 & 0 \\ 0 & 1.00 & 0.00 & 0.00 & 1.00 & 0 \\ -0.85 & 0 & 0 & 0 & 0 & 0.85 \\ 0 & 0 & -1.69 & -1.69 & 0 & 0 \\ 0 & -1.12 & -0.00 & 0.00 & 1.12 & 0 \end{bmatrix} \tag{4.10}$$

The corresponding eigenvalues were

$$\lambda(0) = \begin{bmatrix} -63.65 & -41.52 & -29.55 & 5.95 & 15.32 & 31.65 \end{bmatrix}$$

The eigenscrew pitches were

$$h(0) = \begin{bmatrix} -0.85 & -1.12 & -1.69 & 1.69 & 1.12 & 0.85 \end{bmatrix}$$

The rotational compliances were

$$C_R(0) = \begin{bmatrix} 75.07 & 37.11 & 17.48 & 3.52 & 13.69 & 37.33 \end{bmatrix}$$

The translational compliances were

$$C_T(0) = \begin{bmatrix} 53.97 & 46.46 & 49.95 & 10.05 & 17.14 & 26.83 \end{bmatrix}$$

There were no compliant axes in this system because there were no equal values of compliance. The eigenscrews formed an orthogonal system and demonstrated that the compliance behaviour of the rigid body could not be decoupled. The errors for eigenscrew direction. pitch and eigenvalue are presented in Table (4.5). The mean errors and standard deviations were small as was expected because of the condition number of 13.4 of the compliance matrix.

4.3 Summary of Results of Computer Simulations

The results for the remaining ten compliance matrices investigated were consistent with the results presented in the examples. Ill-conditioned matrices consistently yielded large error distributions ($\pm 10\%$ to $\pm 25\%$) for eigenvalues and eigenscrew pitches. The eigenvalues were more sensitive to ill-conditioning than the eigenscrew pitches. When matrix ill-conditioning was combined with non-distinct eigenvalues,

	Noise	1	2	3
Eigen-screw $\text{Dir}^{\text{ns}}(^o)$	5%	-0.0±0.3	-0.0±0.4	0.0±0.5
	10%	-0.0±0.6	-0.1±0.9	0.0±1.0
	20%	-0.0±1.1	-0.1±1.7	-0.1±2.0
Eigen-values (%)	5%	-0.1±0.4	-0.1±0.4	-0.1±0.4
	10%	-0.2±0.8	-0.2±0.8	-0.3±0.8
	20%	-1.0±1.5	-1.0±1.6	-0.9±1.6
Pitches (%)	5%	0.0±0.3	-0.0±0.4	0.0±0.4
	10%	-0.0±0.7	-0.0±0.7	-0.0±0.8
	20%	-0.1±1.4	0.0±1.4	-0.0±1.6
	Noise	4	5	6
Eigen-screw $\text{Dir}^{\text{ns}}(^o)$	5%	-0.0±0.3	-0.0±0.4	0.0±0.5
	10%	-0.0±0.6	-0.1±0.9	0.0±1.0
	20%	-0.0±1.1	-0.1±1.7	-0.1±2.0
Eigen-values (%)	5%	-0.1±0.4	-0.1±0.4	-0.1±0.4
	10%	-0.2±0.8	-0.2±0.8	-0.3±0.8
	20%	-1.0±1.5	-1.0±1.6	-0.9±1.6
Pitches (%)	5%	0.0±0.3	-0.0±0.4	0.0±0.4
	10%	-0.0±0.7	-0.0±0.7	-0.0±0.8
	20%	-0.1±1.4	0.0±1.4	-0.0±1.6

Table 4.5: Mean errors and standard deviations for eigenscrew direction. pitch and eigenvalue for each of the eigenscrews of an elastically suspended rigid body at 5%. 10% and 20% noise content.

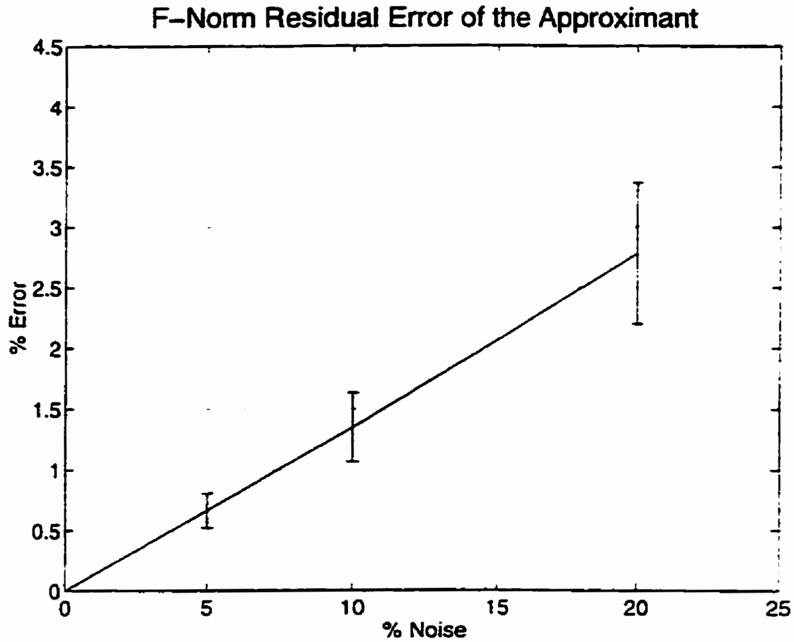

Figure 4.9: Error of the approximant relative to the compliance matrix of the elastically suspended rigid body.

the eigenscrew directions were poorly determined. When a matrix was well conditioned. the error distributions were reduced for all criteria examined. When there were no compliant axes. it was difficult to determine the number of degrees of freedom of the system.

Chapter 5

Conclusions, Recommendations and Future Work

This thesis addressed the question, "Is it possible to determine the number, directions and magnitudes of compliance of a system for which there is no *a priori* knowledge of the system geometry?" While exploring the possible methods of solving this problem, an intermediate goal became the accurate determination of the system compliance matrix. The primary contribution of this thesis was the presentation of a viable solution for describing the static properties of any mechanical or biomechanical system. This chapter contains a discussion of the success of this project in meeting the goals of this thesis, and of remaining work to improve the current solution technique.

5.1 Conclusions

The results of the computer simulations reported in the preceding chapter demonstrated that it was possible to determine the compliance matrix of a system based on the experimental wrench and twist data, regardless of the extent of knowledge of the system geometry. Higham's SPSD approximation method was successful in reducing error incurred by noisy data and obtaining a SPSD matrix. The normalized Frobenius norm of the residuals of the approximant revealed that the compliance matrix could be determined to within 4% of the actual system compliance matrix when 20% noise was added to the twist and wrench data. The success of the eigenscrew decomposition in determining the number, direction and magnitude of the degrees of freedom of the system was difficult to measure, because the accuracy of the information obtained through eigenscrew decomposition was dependent on matrix conditioning and algebraic multiplicity of the compliance matrix.

5.1.1 The Effect of Matrix Conditioning

The condition number of the compliance matrix was a good indicator of the accuracy of the results obtained with eigenscrew decomposition. Ill-conditioned compliance matrices exhibited increased sensitivity to noise when the eigenscrew decomposition was applied. Large errors in eigenvalue and pitch magnitudes were associated with ill-conditioned matrices. When the compliance matrix was ill-conditioned. the results obtained with eigenscrew decomposition were unreliable.

5.1.2 Algebraic Multiplicity

Algebraic multiplicity posed problems in detection of eigenscrew direction when this situation was combined with ill-conditioning. Algebraic multiplicity occurred when two or more compliant axes had equal compliance magnitudes. When four of six eigenscrews had equal magnitude of compliance, these four eigenscrews were constrained to lie in a plane orthogonal to the direction of the remaining two eigenscrews. When noise was added to the twists and wrenches, the directions of the four eigenscrews remained confined to the plane orthogonal to the two remaining eigenscrews, but their directions within the plane could not be reliably determined.

5.1.3 System Coupling in the Compliance Matrix

Non-zero off-diagonal elements of the compliance matrix indicated coupling in the system. When the system was compliant, the compliance matrix was diagonalizable by transforming the system to a new reference frame. However, non-diagonalizable matrices existed (e.g. Example 5 in Chapter 4) in which there was extensive coupling. In these situations, more information about the system could be gained from examination of both the compliance matrix coupling and the eigenscrew analysis. For this reason, it is very important to consider the compliance matrix as well as the eigenscrew decomposition when analyzing system DOFs. Due to the possibility of extensive coupling within the system, all six DOFs of the system must be measured until it is possible to determine that fewer DOFs exist. The extent of coupling may indicate the existence of skew axes.

5.2 Recommendations and Future Work

The work presented in this thesis in no way exhausts the breadth of topics to be investigated with regard to compliance matrices. This section contains a brief description of a few of the topics that remain to be explored.

5.2.1 Improving the Compliance Matrix Approximant: SPD Matrices

Higham's method of obtaining a SPSD matrix approximant was used in this thesis. but a second approach to the problem of obtaining a SPSD matrix was discussed in the review of relevant literature (Chapter 2). This alternate approach was posed as a problem of minimizing residual errors. The error-reducing capabilities of each of these methods should be compared.

One short-coming of Higham's approximation method is that it returns a semi-definite approximant. This approximant can be singular or ill-conditioned. producing difficulties in performing the eigenscrew analysis as discussed above. Restricting the approximant to a symmetric, positive-definite (SPD) solution would improve reliability of the results obtained with the eigenscrew analysis and possibly improve the residual error of the approximant as well.

5.2.2 Optimization of Matrix Conditioning via Scaling

Compliance matrices can be divided into four quadrants. based on the units in each quadrant, so

$$C = \begin{bmatrix} A & B \\ B^T & D \end{bmatrix}$$

where A has units of length over force ($\frac{m}{N}$), B and B^T have units of unity over force ($\frac{1}{N}$), and D has units of unity over force times length ($\frac{1}{N \cdot m}$). By careful selection of the units of length (e.g.. mm, m, km) it is possible to change and improve the condition number of the compliance matrix. This was demonstrated by Merlet [26] for the compliance of a parallel manipulator in Example 2 of Chapter 4. Further investigation into the effect of scaling on matrix conditioning and eigenscrew analysis would be useful. It may be possible to optimize the condition number of the matrix by careful selection of scaling.

5.2.3 Minimization of the System Coupling

It may be possible to select a reference frame that diagonalizes the compliance matrix, or that minimizes the off-diagonal values in the compliance matrix. Loncaric [24] described how to transform stiffness and compliance matrices into other coordinate systems. Finding the optimal transformation (rotation and translation) that diagonalizes the matrix may prove to be challenging.

5.2.4 Application to Mechanical and Biological Systems

The methods of DOF analysis presented in this thesis have not been applied to real systems. The application of compliance matrix evaluation and eigenscrew decomposition to mechanical and biological systems is the next obvious step. The results obtained from the computer simulations were promising for potentially determining the compliance matrix for any multi-body system. According to the computer simulations, it should be possible to analyze the DOFs based on experimental wrench and twist data. It should be noted that care should be taken to collocate the reference frames of the twists and wrenches. The condition and rank of the wrench matrix should also be monitored in order to ensure the richness of the data. Inertial effects within the system should be avoided when measuring the applied wrenches in order to ensure the equilibrium criterion. Finally signal conditioning should be used to eliminate as much noise as possible from the twists and wrenches without compromising the quality of the measurements.

5.3 Summary

This work originated from a biomechanical problem for which the magnitude and direction of the passive constraints of the human knee were required. The knee is a complex three-body system with passive motion constrained by ligamentous soft-tissue and bone-on-bone contact. There is redundancy in the constraints of the knee because the failure of one ligament does not result in an unconstrained range of motion. Each knee is geometrically unique which means that the location of the insertion sites of the ligaments vary slightly from knee to knee. The stiffness of the ligaments and the density of the bone also vary depending on the age of the tissue, and quality of the tissue which degrades in the presence of joint disease such as arthritis. For these reasons, finding the constrained directions of motion of the knee and the amount of constraint are not easily determined using conventional methods where geometry and material properties are known and constant.

The results of this work suggest that the number, directions and magnitudes of constraint can be determined for any mechanical system. The methods of analysis here could be useful as a tool for design and analysis of prosthetic joints, the diagnosis of human joint instabilities and the detection of unwanted constraint or compliance in robot manipulators as they interact with their environments.

Bibliography

[1] J.C. Allwright. Positive semidefinite matrices: Characterizatoin via conical hulls and least-squares solution of a matrix equation. *SIAM Journal on Control and Optimization*, 26(3):537–556, May 1988.

[2] L.-E. Andersson and T. Elfving. A constrained procrustes problem. *SIAM Jounal on Matrix Analysis and Applications*, 18(1):124–139, January 1997.

[3] M. H. Ang, Jr. and G. B. Andeen. Specifying and achieving passive compliance based on manipulator structure. *IEEE Transactions on Robotics and Automation*, 11(4):504–515, August 1995.

[4] R. S. Ball. *The theory of screws.* Cambridge University Press, 1900.

[5] J.E. Brock. Optimal matrices describing linear systems. *AIAA Journal*, 6(7):1292–1296, July 1968.

[6] M. Chasles. Note sur les propriétés générales du système de deux corps semblables entre eux, placés d'une manière quelconque dans l'espace; et sur le déplacement fini, ou infiniment petit d'un corps solide libre,. *Bulletin des Sciences Mathématiques de Férrusac*, 14:321–326, 1831.

[7] M.D. Conlay and G. L. Long. Ligament forces, condyle reactions, line geometry, screw theory and human knee stability. In *Advances in Bioengineering*, volume 28, pages 169–170. ASME. ASME. 1994.

[8] M. Cutkosky, P. Akella, R. Howe, and I. Kao. Grasping as a contact sport. In *Proceedings Fourth International Symposium on Robotics Research*, pages 199–206, Cambridge, MA, 1988. MIT Press.

[9] K. Deluzio. Personal communication, re: PCA. Department of Mechanical Engineering, Queen's University, Kingston, Ontario, Canada. K7L 3N6. 1998.

[10] H.A. ElMaraghy and B. Johns. An investigation into the compliance of SCARA robots. Part i: Analytical model. *Journal of Dynamic Systems, Measurement, and Control*, 110:18–22, March 1988.

[11] H.A. ElMaraghy and B. Johns. An investigation into the compliance of SCARA robots. Part ii: Experimental and numerical validation. *Journal of Dynamic Systems, Measurement, and Control*, 110:23–30. March 1988.

[12] C. Gosselin. Stiffness mapping of parallel manipulators. *IEEE Transactions on Robotics and Automation*, 6(3):377–382, June 1990.

[13] P.R. Halmos. Positive approximants of operators. *Indiana University Mathematics Journal*, 21(10):951–960, 1972.

[14] S.-P. Han and G. Lou. A parallel algorithm for a class of convex programs. *SIAM Journal on Control and Optimization*, 26:345–355, 1988.

[15] N. J. Higham. Computing the polar decomposition – with applications. *SIAM Journal on Science and Statistical Computing*, 7(4):1160–1174, October 1986.

[16] N.J. Higham. Computing a nearest symmetric positive semidefinite matrix. *Linear Algebra and its applications*, 103:103–118, 1988.

[17] K. H. Hunt. *Kinematic geometry of mechanisms*. Oxford University Press, 1978.

[18] K. H. Hunt. Special configurations of robot-arms via screw theory (Part 1). *Robotica*, 4:171–179, 1986.

[19] I.T. Jolliffe. *Principal Component Analysis*. Springer-Verlag, 1986.

[20] D.R. Kerr. Analysis, properties, and design of a stewart-platform transducer. *Journal of Mechanisms, Transmissions, and Automation in Design*. 111:25–28, March 1989.

[21] P.H. Kraeutner and J.S. Bird. Principal components array processing for swath acoustic mapping. In *Proceedings of the 1997 Oceans Conference*. volume 2, pages 1246–1254. IEEE, 1997.

[22] D.H. Lange and G.F. Inbar. Variable single-trial evoked potential estimation via principal component identification. In *Proceedings of the 18th Annual International Conference of the IEEE Engineering in Medicine and Biology Society*, volume 3, pages 954–955, 1996.

[23] Y.T. Lin. Y.K. Chen. and S.Y. Kung. Principal component clustering approach to object-oriented motion segmentation and estimation. *Journal of VLSI Signal Processing Systems for Signal, Image and Video Technology*, 17(2-3):163–187. November 1997.

[24] J. Loncaric. Normal forms of stiffness and compliance matrices. *IEEE Jounal of Robotics and Automation*, RA-3(6):567–572. December 1987.

[25] C.A. Lozinsky. Robot calibration: Method and results. Master's thesis. Massachusetts Institue of Technology, June 1984.

[26] J-P. Merlet. Force-feedback control of parallel manipulators. In *IEEE International Conference on Robotics and Automation*. volume 3. pages 1484–1489. April 1988.

[27] J.A. Moore, R.E. Ellis, D.R. Pichora, and A. M. Hollister. A kinematic technique for describing wrist joint motion: Analysis of configuration space plots. *Proceedings of the Institution of Mechanical Engineers. Part H: Journal of Engineering and Medicine*, 207:211–218, 1993.

[28] M.C. Murphy and R. W. Mann. A method for estimating the total freedom of the knee. In *Modelling and Control Issues in Biomechanical Systems*. pages 55–65. The American Society of Mechanical Engineers, 1988.

[29] T. Patterson and H. Lipkin. A classification of robot compliance. In *Cams. Gears. Robot and Mechanism Design*, volume 26. pages 307–314. ASME. ASME Design Technical Conferences, September 1990.

[30] T. Patterson and H. Lipkin. Structure of robot compliance. In *Cams. Gears, Robot and Mechanism Design*, volume 26, pages 315–322. ASME, ASME Design Technical Conferences, September 1990.

[31] L. Poinsot. Sur la composition des moments et la composition des aires. *J. école Polyt., Paris*, 6:182–205. 1806.

[32] B. Roth. Screws, motors and wrenches that cannot be bought in a hardware store. In M. Brady and R. Paul, editors, *Robotics Research: The First International Symposium*, pages 679–693. MIT Press, 1984.

[33] J.M. Schimmels and M.A. Peshkin. Synthesis and validation of non-diagonal accommodation matrices for error-corrective assembly. In *IEEE International Conference on Robotics and Automation (Proceedings)*, pages 714–719. 1990.

[34] L.J. Shen and H.C. Fu. Principal component based bdnn for face recognition. In *Proceedings of the 1997 IEEE International Congerence on Neural Networks*, volume 3, pages 1368–1372, 1997.

[35] M. Stone. M.H. Goldstein, Jr., and Y. Zhang. Principal component analysis of cross sections of tongue shapes in vowel production. *Speech Communication*, 22(2-3):173–184, August 1997.

[36] F. Tahmasebi and L.-W. Tsai. On the stiffness of a novel six-degree-of-freedom parallel minimanipulator. *Journal of Robotic Systems*, 12(12):845–856, 1995.

[37] K.J. Waldron and K.H. Hunt. Series-parallel dualities in actively coordinated mechanisms. *International Journal of Robotics Research*, 10(5):473–479. October 1991.

[38] W. Wang, R. N. K. Loh, and E.Y. Gu. Passive compliance versus active compliance in robot-based automated assembly systems. *Industrial Robot*, 25(1):48–57. 1998.

[39] K. G. Woodgate. Optimal stiffness matrix estimation for elastic structures. Department of Aeronautics, Imperial College of Science, Technology and Medicine, London, SW7 2BY, England., November 1996.

[40] K.G. Woodgate. Least-squares solution of F=PG over positive semidefinite symmetric P. *Linear Algebra and its applications*, 245:171–190, 1996.

[41] A. B. Zavatsky. A kinematic-freedom analysis of a flexed-knee-stance testing rig. *Journal of Biomechanics*, 30(3):277–280, 1997.

Appendix A

Ten Diagonal Compliance Matrices

The results of the computer simulations for ten different diagonal compliance matrices are summarized in this appendix. The matrices were constructed to simulate the compliance matrices of stiff mechanical systems with varying numbers and magnitudes of DOFs. For each matrix, 1000 trials were performed at 3 noise levels (5%, 10% and 20 %). For each trial, 150 samples of twists and wrenches were generated and contaminated with noise. The compliance matrix was reconstructed from the twists and wrenches, and the SPSD approximant was calculated. The eigenscrew decomposition of the compliance matrix was performed in which the eigenscrew direction and pitch, the eigenvalues, and the rotational and translational compliance were calculated. Mean errors and standard deviations of the eigenscrew directions, eigenvalues and eigenscrew pitches are presented in the tables for each matrix. The results were discussed in Chapter 4.

A.1 One Rotational DOF System

The compliance matrix is

$$C_1 = \begin{bmatrix} 0.02 & 0 & 0 & 0 & 0 & 0 \\ 0 & 0.03 & 0 & 0 & 0 & 0 \\ 0 & 0 & 0.03 & 0 & 0 & 0 \\ 0 & 0 & 0 & 5.00 & 0 & 0 \\ 0 & 0 & 0 & 0 & 0.10 & 0 \\ 0 & 0 & 0 & 0 & 0 & 0.05 \end{bmatrix} \times 10^{-3}$$

The normalized eigenscrews of C_1 were

$$e = \begin{bmatrix} 1.00 & 0 & 0 & 0 & 0 & 1.00 \\ 0 & 1.00 & 0 & 0 & 1.00 & 0 \\ 0 & 0 & 1.00 & 1.00 & 0 & 0 \\ -0.06 & 0 & 0 & 0 & 0 & 0.06 \\ 0 & -0.55 & 0 & 0 & 0.55 & 0 \\ 0 & 0 & -0.78 & 0.78 & 0 & 0 \end{bmatrix}$$

The corresponding eigenvalues were

$$\vec{\lambda} = \begin{bmatrix} -0.32 & -0.06 & -0.04 & 0.04 & 0.06 & 0.32 \end{bmatrix} \times 10^{-3}$$

The eigenscrew pitches were

$$h = \begin{bmatrix} -0.06 & -0.55 & -0.78 & 0.78 & 0.55 & 0.06 \end{bmatrix}$$

The rotational compliances were

$$\vec{C_R} = \begin{bmatrix} 5.00 & 0.10 & 0.05 & 0.05 & 0.10 & 5.00 \end{bmatrix} \times 10^{-3}$$

The translational compliances were

$$\vec{C_T} = \begin{bmatrix} 0.02 & 0.03 & 0.03 & 0.03 & 0.03 & 0.02 \end{bmatrix} \times 10^{-3}$$

The compliance matrix had three orthogonal compliant axes, two of which were very stiff. The condition number of the matrix was 250 which is moderately ill-conditioned. There was no algebraic multiplicity. Figure A.1 summarizes the results obtained for the residual error of the approximant. Table A.1 contains a summary of the errors obtained for the eigenscrew directions, the eigenvalues and the eigenscrew pitches for increasing noise level.

	Noise	1	2	3
Eigen-screw $\mathrm{Dir}^{\mathrm{ns}}(^{o})$	5%	0.0±0.1	0.0±0.3	-0.1±0.2
	10%	0.0±0.3	0.0±0.6	-0.1±0.5
	20%	0.0±0.5	0.0±1.5	-0.1±1.5
Eigen-values (%)	5%	0.0±2.6	0.0±0.0	0.0±0.1
	10%	0.2±4.7	-0.1±0.1	-0.1±0.2
	20%	-0.8±9.8	-0.5±1.0	-0.5±0.7
Pitches (%)	5%	0.0±0.3	0.0±0.0	0.0±0.0
	10%	-0.1±0.5	0.0±0.1	0.0±0.1
	20%	-0.5±1.0	0.1±1.0	0.2±0.6
	Noise	4	5	6
Eigen-screw $\mathrm{Dir}^{\mathrm{ns}}(^{o})$	5%	0.0±0.2	0.0±0.3	0.0±0.1
	10%	0.0±0.6	0.0±0.6	0.0±0.3
	20%	0.0±1.5	0.0±1.5	0.0±0.5
Eigen-values (%)	5%	0.0±0.0	0.0±0.0	-0.1±2.7
	10%	-0.1±0.2	-0.1±0.1	-0.4±4.7
	20%	-0.5±0.7	-0.5±1.1	-0.1±9.8
Pitches (%)	5%	0.0±0.0	0.0±0.0	0.0±0.3
	10%	0.0±0.1	0.1±0.1	-0.1±0.5
	20%	0.2±0.6	0.1±1.0	-0.5±1.0

Table A.1: Mean errors and standard deviations for eigenscrew direction. pitch and eigenvalue for each of the eigenscrews of C_1 at 5%, 10% and 20% noise content.

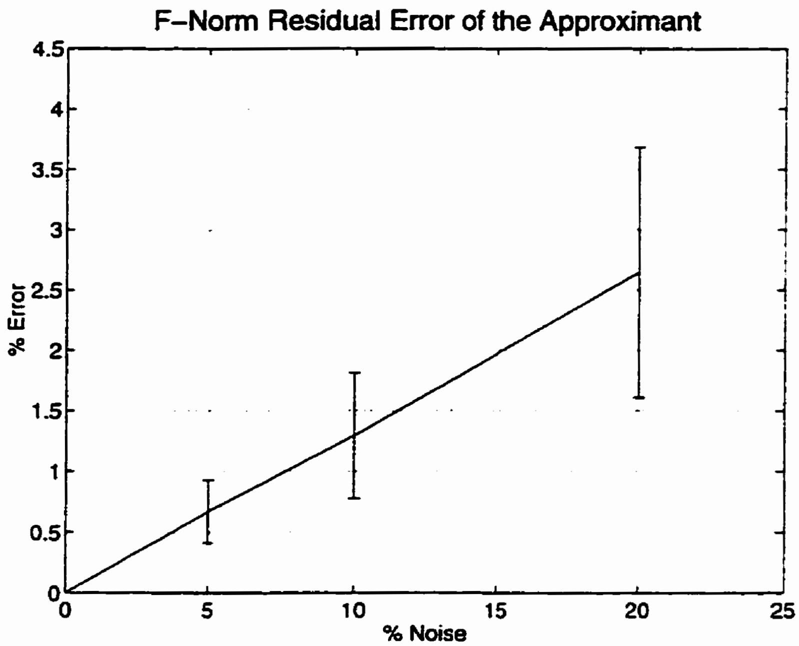

Figure A.1: Error of the approximant relative to compliance matrix C_1.

A.2 Two DOFs System: Collinear Rotational and Translational

The system compliance matrix was

$$C_2 = \begin{bmatrix} 2.50 & 0 & 0 & 0 & 0 & 0 \\ 0 & 0.03 & 0 & 0 & 0 & 0 \\ 0 & 0 & 0.03 & 0 & 0 & 0 \\ 0 & 0 & 0 & 5.00 & 0 & 0 \\ 0 & 0 & 0 & 0 & 0.10 & 0 \\ 0 & 0 & 0 & 0 & 0 & 0.05 \end{bmatrix}$$

The normalized eigenscrews of C_2 were

$$e = \begin{bmatrix} 1.00 & 0 & 0 & 0 & 0 & 1.00 \\ 0 & 1.00 & 0 & 0 & 1.00 & 0 \\ 0 & 0 & 1.00 & 1.00 & 0 & 0 \\ -0.71 & 0 & 0 & 0 & 0 & 0.71 \\ 0 & -0.55 & 0 & 0 & 0.55 & 0 \\ 0 & 0 & -0.78 & 0.78 & 0 & 0 \end{bmatrix}$$

The corresponding eigenvalues were

$$\vec{\lambda} = \begin{bmatrix} -3.53 & -0.06 & -0.04 & 0.04 & 0.06 & 3.53 \end{bmatrix} \times 10^{-3}$$

The eigenscrew pitches were

$$\vec{h} = \begin{bmatrix} -0.71 & -0.55 & -0.78 & 0.78 & 0.55 & 0.71 \end{bmatrix}$$

The rotational compliances were

$$\vec{C_R} = \begin{bmatrix} 5.00 & 0.10 & 0.05 & 0.05 & 0.10 & 5.00 \end{bmatrix} \times 10^{-3}$$

The translational compliances were

$$\vec{C_T} = \begin{bmatrix} 2.50 & 0.03 & 0.03 & 0.03 & 0.03 & 2.50 \end{bmatrix} \times 10^{-3}$$

The system had three compliant axes and no algebraic multiplicity. The condition number was 167. Two of the directions were very stiff. The translational and rotational compliance of the x-direction was correctly identified. Figure A.2 presents the residual errors of the approximant for increasing noise. Table A.2 presents a summary of the errors in eigenscrew direction, eigenvalues and eigenscrew pitches.

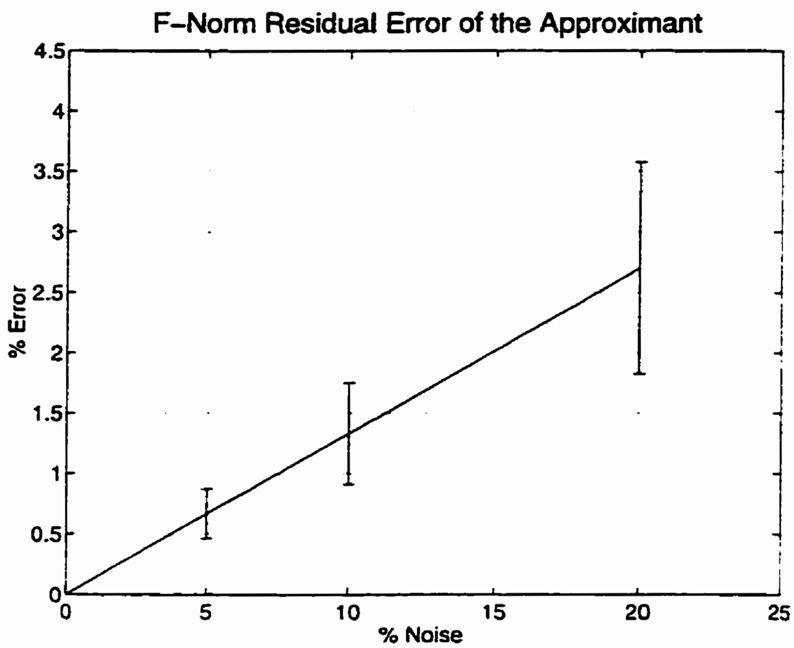

Figure A.2: Error of the approximant relative to compliance matrix C_2.

	Noise	1	2	3
Eigen-screws $\text{Dir}^{\text{ns}}(^o)$	5%	0±0.2	0±0.1	0±0.1
	10%	-0.1±0.3	0±0.3	-0.1±0.4
	20%	-0.2±0.6	0±0.8	-0.2±1.1
Eigen-values (%)	5%	-0.1±0.4	0.0±0.1	-0.1±0.1
	10%	-0.2±0.8	-0.1±0.2	-0.2±0.2
	20%	-0.9±1.7	-0.7±1.0	-0.7±0.7
Pitches (%)	5%	0.0±0.4	0.0±0.0	0.0±0.0
	10%	0.0±0.7	0.1±0.1	0.1±0.2
	20%	-0.1±1.5	0.2±0.9	0.2±0.6

	Noise	4	5	6
Eigen-screws $\text{Dir}^{\text{ns}}(^o)$	5%	0.0±0.1	0.0±0.1	0.1±0.1
	10%	0.0±0.4	0.0±0.3	0.1±0.3
	20%	0.0±1.2	0.0±0.8	0.3±0.5
Eigen-screw (%)	5%	-0.1±0.1	0.0±0.1	-0.1±0.4
	10%	-0.2±0.2	-0.2±0.2	-0.3±0.8
	20%	-0.7±0.8	-0.7±1.1	-0.9±1.7
Pitches (%)	5%	0.0±0.0	0.0±0.0	0.0±0.4
	10%	0.1±0.2	0.1±0.	0.0±0.7
	20%	0.2±0.6	0.2±0.9	-0.1±1.5

Table A.2: Mean errors and standard deviations for eigenscrew direction, pitch and eigenvalue for each of the eigenscrews of C_2 at 5%. 10 % and 20% noise content.

A.3 Two DOFs System: Non-collinear Rotational and Translational

The system compliance matrix was

$$C_3 = \begin{bmatrix} 0.02 & 0 & 0 & 0 & 0 & 0 \\ 0 & 2.50 & 0 & 0 & 0 & 0 \\ 0 & 0 & 0.03 & 0 & 0 & 0 \\ 0 & 0 & 0 & 5.00 & 0 & 0 \\ 0 & 0 & 0 & 0 & 0.10 & 0 \\ 0 & 0 & 0 & 0 & 0 & 0.05 \end{bmatrix}$$

The normalized eigenscrews of C_3 were

$$e = \begin{bmatrix} 0 & 1.00 & 0 & 0 & 1.00 & 0 \\ 1.00 & 0 & 0 & 0 & 0 & 1.00 \\ 0 & 0 & 1.00 & 1.00 & 0 & 0 \\ 0 & -0.06 & 0 & 0 & 0.06 & 0 \\ -5.00 & 0 & 0 & 0 & 0 & 5.00 \\ 0 & 0 & -0.78 & 0.78 & 0 & 0 \end{bmatrix}$$

The corresponding eigenvalues were

$$\vec{\lambda} = \begin{bmatrix} -0.50 & -0.32 & -0.04 & 0.04 & 0.32 & 0.50 \end{bmatrix} \times 10^{-3}$$

The eigenscrew pitches were

$$\vec{h} = \begin{bmatrix} -5.00 & -0.06 & -0.78 & 0.78 & 0.06 & 5.00 \end{bmatrix}$$

The rotational compliances were

$$\vec{C_R} = \begin{bmatrix} 0.10 & 5.00 & 0.05 & 0.05 & 5.00 & 0.10 \end{bmatrix} \times 10^{-3}$$

The translational compliances were

$$\vec{C_T} = \begin{bmatrix} 2.50 & 0.02 & 0.03 & 0.03 & 0.02 & 2.50 \end{bmatrix} \times 10^{-3}$$

Again, there were three compliant axes and no algebraic multiplicity. The condition value of the matrix was 250. Eigenscrew decomposition identified the non-collinear translational and rotational compliance. The residual errors of the approximant are summarized in Figure A.3. Table A.3 summarizes the errors in the eigenscrew directions, the eigenvalues, and the eigenscrew pitches. The stiff axis had large errors in eigenscrew pitch values.

	Noise	1	2	3
Eigen-screw $\text{Dir}^{\text{ns}}(^o)$	5%	0.3±10.7	0.0±0.2	0.0±0.3
	10%	-0.2±19.5	0.0±5.3	-0.1±0.5
	20%	-1.0±25.8	1.3±24.7	-0.2±1.2
Eigen-values (%)	5%	0.0±0.9	-0.1±2.5	0.0±0.1
	10%	-0.2±2.4	0.4±8.1	-0.2±0.2
	20%	-3.8±11.8	14.8±26.9	-0.7±0.8
Pitches (%)	5%	3.3±5.0	-0.1±0.3	76.4±97.2
	10%	9.9±11.3	-0.3±0.6	100.8±100.0
	20%	24.7±22.7	-1.0±1.6	98.4±99.8
	Noise	4	5	6
Eigen-screw $\text{Dir}^{\text{ns}}(^o)$	5%	0.0±0.3	0.0±0.2	-0.3±10.6
	10%	-0.1±0.5	-0.1±7.2	-0.5±18.5
	20%	-0.3±1.2	-0.7±38.7	0.8±20.2
Eigen-values (%)	5%	-0.1±0.1	-0.1±2.5	0.0±0.9
	10%	-0.2±0.2	0.4±7.2	-0.6±4.6
	20%	-0.7±0.8	4.2±18.7	-10.0±16.9
Pitches (%)	5%	76.4±97.2	-0.1±0.3	3.3±5.1
	10%	100.8±100.0	-0.3±0.6	10.1±11.8
	20%	98.4±99.8	-1.0±1.5	23.8±21.5

Table A.3: Mean errors and standard deviations for eigenscrew direction, pitch and eigenvalue for each of the eigenscrews of C_3 at 5%, 10 % and 20% noise content.

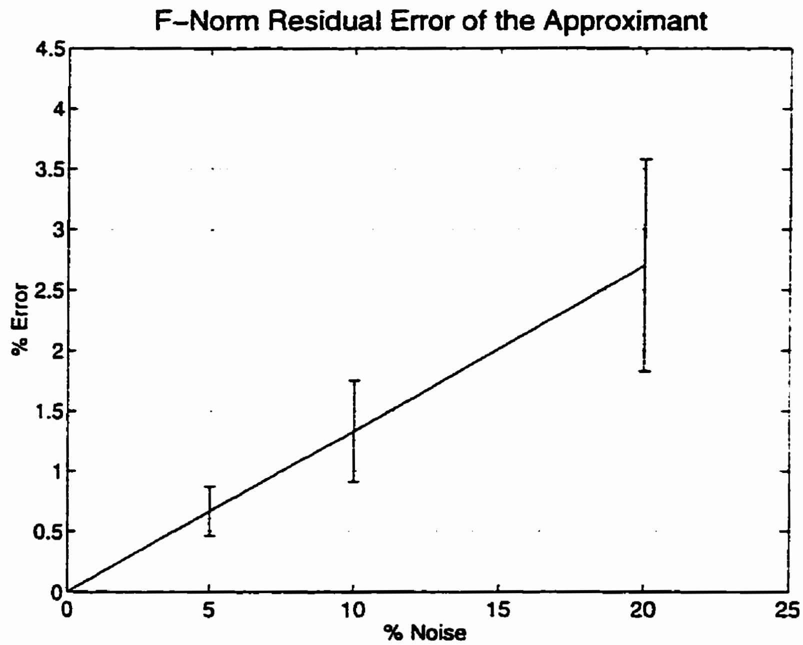

Figure A.3: Error of the approximant relative to compliance matrix C_3.

A.4 Two Rotational DOFs System

The compliance matrix was

$$C_4 = \begin{bmatrix} 0.02 & 0 & 0 & 0 & 0 & 0 \\ 0 & 0.03 & 0 & 0 & 0 & 0 \\ 0 & 0 & 0.03 & 0 & 0 & 0 \\ 0 & 0 & 0 & 5.00 & 0 & 0 \\ 0 & 0 & 0 & 0 & 2.5 & 0 \\ 0 & 0 & 0 & 0 & 0 & 0.05 \end{bmatrix} \times 10^{-3}$$

The normalized eigenscrews of C_4 were

$$e = \begin{bmatrix} 1.00 & 0 & 0 & 0 & 0 & 1.00 \\ 0 & 1.00 & 0 & 0 & 1.00 & 0 \\ 0 & 0 & 1.00 & 1.00 & 0 & 0 \\ -0.06 & 0 & 0 & 0 & 0 & 0.06 \\ 0 & -0.11 & 0 & 0 & 0.11 & 0 \\ 0 & 0 & -0.78 & 0.7746 & 0 & 0 \end{bmatrix}$$

The corresponding eigenvalues were

$$\vec{\lambda} = \begin{bmatrix} -0.32 & -0.27 & -0.04 & 0.04 & 0.27 & 0.32 \end{bmatrix} \times 10^{-3}$$

The eigenscrew pitches were

$$\vec{h} = \begin{bmatrix} -0.06 & -0.11 & -0.78 & 0.78 & 0.11 & 0.06 \end{bmatrix}$$

The rotational compliances were

$$\vec{C_R} = \begin{bmatrix} 5.00 & 2.50 & 0.10 & 0.10 & 2.50 & 5.00 \end{bmatrix} \times 10^{-3}$$

The translational compliances were

$$\vec{C_T} = \begin{bmatrix} 0.02 & 0.03 & 0.03 & 0.03 & 0.03 & 0.02 \end{bmatrix} \times 10^{-3}$$

The rotational compliance in the x-direction and in the y-direction were correctly identified by eigenscrew decomposition. There were three compliant axes, of which one was very stiff. The condition number of the matrix was 250. The residual errors of the approximant are summarized in Figure A.4. Table A.4 presents a summary of the errors resulting from increasing noise level in the eigenscrew decomposition.

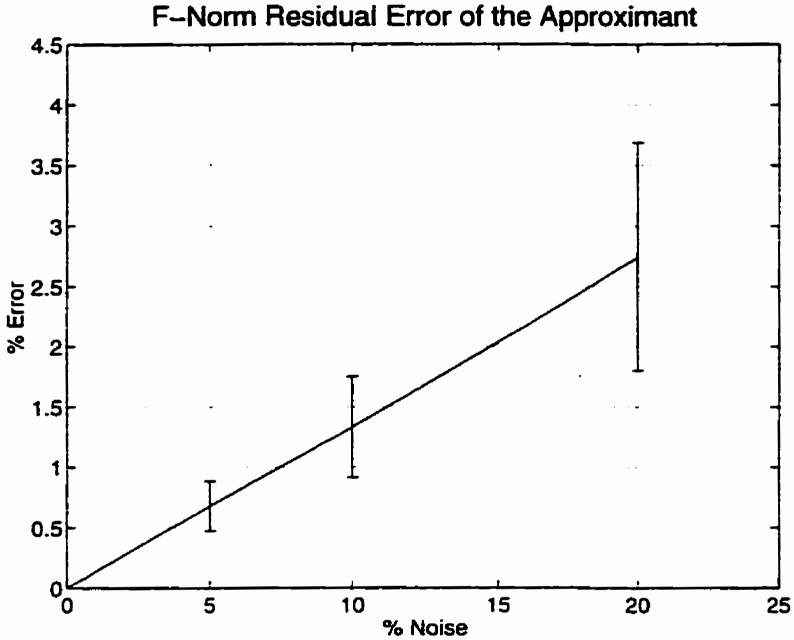

Figure A.4: Error of the approximant relative to compliance matrix C_4.

	Noise	1	2	3
Eigen-screw Dir^{ns}(^{o})	5%	0.0±4.0	0.2±6.9	-0.1±0.3
	10%	0.3±9.2	0.7±15.0	-0.1±0.6
	20%	1.0±16.0	1.1±25.0	-0.3±1.4
Eigen-values (%)	5%	-0.1±2.5	-0.1±1.5	-0.1±0.1
	10%	0.2±4.7	-0.7±2.9	-0.2±0.2
	20%	0.9±9.4	-1.4±7.0	-0.7±0.8
Pitches (%)	5%	-0.4±0.7	0.6±1.1	0.0±0.0
	10%	-1.9±3.3	2.6±4.0	0.1±0.2000
	20%	-5.7±7.2	6.5±8.0	0.2±0.6000
	Noise	4	5	6
Eigen-screw Dir^{ns}(^{o})	5%	0.0±0.3	-0.1±6.9	0.2±4.2
	10%	-0.1±0.6	-0.5±15.1	-1.2±9.4
	20%	-0.3±1.5	0.3±25.2	-1.1±16.2
Eigen-values (%)	5%	-0.1±0.1	-0.2±1.5	0.2±2.5
	10%	-0.2±0.2	-0.6±2.8	0.4±4.8
	20%	-0.7±0.8	-2.1±6.2	-0.1±10.5
Pitches (%)	5%	0.0±0.0	0.6±1.2	-0.4±1.3
	10%	0.1±0.2	2.6±4.2	-2.0±3.8
	20%	0.2±0.6	6.6±7.9	-5.8±7.4

Table A.4: Mean errors and standard deviations for eigenscrew direction, pitch and eigenvalue for each of the eigenscrews of C_4 at 5%. 10 % and 20% noise content.

A.5 Two Rotational DOFs System: Equal Magnitude

The compliance matrix was

$$C_5 = \begin{bmatrix} 0.02 & 0 & 0 & 0 & 0 & 0 \\ 0 & 0.03 & 0 & 0 & 0 & 0 \\ 0 & 0 & 0.03 & 0 & 0 & 0 \\ 0 & 0 & 0 & 5.00 & 0 & 0 \\ 0 & 0 & 0 & 0 & 5.00 & 0 \\ 0 & 0 & 0 & 0 & 0 & 0.05 \end{bmatrix} \times 10^{-3}$$

The normalized eigenscrews of C_5 were

$$e = \begin{bmatrix} 0 & 1.00 & 0 & 0 & 1.00 & 0 \\ 1.00 & 0 & 0 & 0 & 0 & 1.00 \\ 0 & 0 & 1.00 & 1.00 & 0 & 0 \\ 0 & -0.06 & 0 & 0 & 0.06 & 0 \\ -0.08 & 0 & 0 & 0 & 0 & 0.08 \\ 0 & 0 & -0.78 & 0.78 & 0 & 0 \end{bmatrix}$$

The corresponding eigenvalues were

$$\vec{\lambda} = \begin{bmatrix} -0.39 & -0.32 & -0.04 & 0.04 & 0.32 & 0.39 \end{bmatrix} \times 10^{-3}$$

The eigenscrew pitches were

$$\vec{h} = \begin{bmatrix} -0.08 & -0.06 & -0.78 & 0.78 & 0.06 & 0.08 \end{bmatrix}$$

The rotational compliances were

$$\vec{C_R} = \begin{bmatrix} 5.00 & 5.00 & 0.05 & 0.05 & 5.00 & 5.00 \end{bmatrix} \times 10^{-3}$$

The translational compliances were

$$\vec{C_T} = \begin{bmatrix} 0.03 & 0.02 & 0.03 & 0.03 & 0.02 & 0.03 \end{bmatrix} \times 10^{-3}$$

The compliances of the rotational DOFs were correctly identified by the eigenscrew decomposition. The eigenscrew decomposition yielded three orthogonal compliant axes for the system. This matrix approaches the condition of algebraic multiplicity for the x-direction and the y-direction. The condition number of the matrix was 250. The residual errors for the approximant are summarized in Figure A.5. The errors for the eigenscrew directions, the eigenvalues and the eigenscrew pitches for the trials including noise are summarized in Table A.5.

	Noise	1	2	3
Eigen-screw $\text{Dir}^{\text{ns}}(^o)$	5%	0.2±5.0	0.0±4.1	0.0±0.3
	10%	0.3±10.1	-0.6±8.4	-0.1±0.6
	20%	-0.1±18.8	-1.8±16.5	-0.4±1.5
Eigen-values (%)	5%	0.1±2.0	-0.3±2.4	-0.1±0.1
	10%	0.2±4.0	-0.8±4.7	-0.2±0.2
	20%	-1.0±9.5	-0.5±12.0	-0.9±1.0
Pitches (%)	5%	0.1±0.3	-0.1±0.3	0.0±0.0
	10%	0.5±1.0	-0.5±0.9	0.1±0.2
	20%	1.0±2.8	-1.3±2.7	0.3±0.7

	Noise	4	5	6
Eigen-screw $\text{Dir}^{\text{ns}}(^o)$	5%	0.0±0.3	0.3±4.1	-0.2±5.0
	10%	-0.1±0.6	0.8±8.6	0.6±10.3
	20%	-0.3±1.6	-0.9±16.7	0.0±18.8
Eigen-values (%)	5%	-0.1±0.1	-0.1±2.5	0.1±2.0
	10%	-0.2±0.2	-0.5±4.6	0.2±3.8
	20%	-1.0±1.0	-0.4±11.6	-0.6±10.0
Pitches (%)	5%	0.0±0.0	-0.1±0.3	0.1±0.3
	10%	0.1±0.2	-0.5±1.0	0.5±1.0
	20%	0.3±0.8	-1.3±2.8	0.9±2.8

Table A.5: Mean errors and standard deviations for eigenscrew direction, pitch and eigenvalue for each of the eigenscrews of C_5 at 5%, 10 % and 20% noise content.

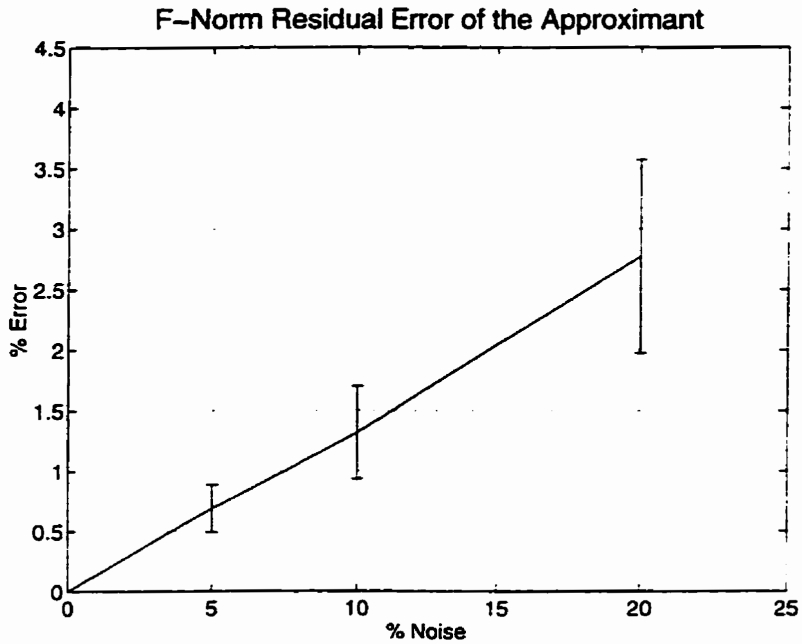

Figure A.5: Error of the approximant relative to compliance matrix C_5.

A.6 Two Translational DOFs System

The compliance matrix was

$$C_6 = \begin{bmatrix} 5.00 & 0 & 0 & 0 & 0 & 0 \\ 0 & 2.50 & 0 & 0 & 0 & 0 \\ 0 & 0 & 0.02 & 0 & 0 & 0 \\ 0 & 0 & 0 & 0.03 & 0 & 0 \\ 0 & 0 & 0 & 0 & 0.10 & 0 \\ 0 & 0 & 0 & 0 & 0 & 0.05 \end{bmatrix}$$

The normalized eigenscrews of C_6 were

$$e = \begin{bmatrix} 0 & 1.00 & 0 & 0 & 1.00 & 0 \\ 1.00 & 0 & 0 & 0 & 0 & 1.00 \\ 0 & 0 & 1.00 & 1.00 & 0 & 0 \\ 0 & -12.91 & 0 & 0 & 12.91 & 0 \\ -5.00 & 0 & 0 & 0 & 0 & 5.00 \\ 0 & 0 & -0.63 & 0.63 & 0 & 0 \end{bmatrix} \times 10^{-3}$$

The corresponding eigenvalues were

$$\vec{\lambda} = \begin{bmatrix} -0.50 & -0.39 & -0.03 & 0.03 & 0.39 & 0.50 \end{bmatrix} \times 10^{-3}$$

The eigenscrew pitches were

$$\vec{h} = \begin{bmatrix} -5.00 & -12.91 & -0.63 & 0.63 & 12.91 & 5.00 \end{bmatrix}$$

The rotational compliances were

$$\vec{C_R} = \begin{bmatrix} 0.10 & 0.03 & 0.05 & 0.05 & 0.03 & 0.10 \end{bmatrix} \times 10^{-3}$$

The translational compliances were

$$\vec{C_T} = \begin{bmatrix} 2.50 & 5.00 & 0.02 & 0.02 & 5.00 & 2.50 \end{bmatrix} \times 10^{-3}$$

There were three compliant axes identified for the system. The translational DOFs were correctly identified using eigenscrew decomposition. The condition value of the matrix was 250. The residual errors for the approximant are presented in Figure A.6. The errors in eigenscrew directions, pitches and eigenvalues are summarized in Table A.6.

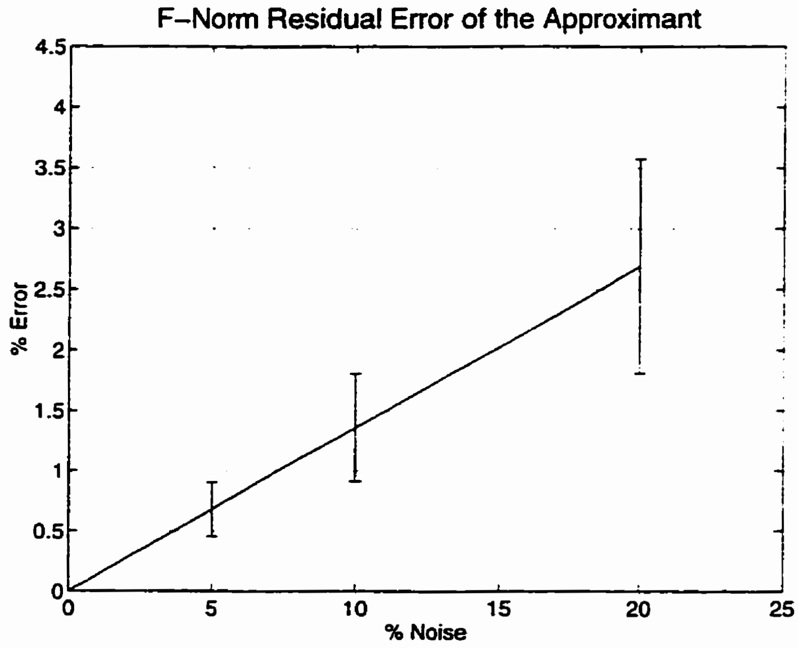

Figure A.6: Error of the approximant relative to compliance matrix C_6.

	Noise	1	2	3
Eigen-screw $Dir^{ns}(^o)$	5%	0.1±1.3	0.2±3.5	0.0±0.1
	10%	0.0±2.9	-0.2±7.4	-0.1±0.3
	20%	0.0±6.3	-0.6±13.7	-0.2±0.5
Eigen-values (%)	5%	0.0±0.8	-0.2±2.0	-0.1±0.1
	10%	0.0±1.7	-0.5±4.0	-0.2±0.2
	20%	-0.3±3.9	-0.7±7.9	-0.9±1.0
Pitches (%)	5%	0.0±0.3	0.3±0.5	0.0±0.1
	10%	-0.2±0.7	1.2±1.4	0.1±0.2
	20%	-0.6±3.3	4.0±4.4	0.4±0.8
	Noise	4	5	6
Eigen-screw $Dir^{ns}(^o)$	5%	0.0±0.2	0.3±3.5	-0.1±1.4
	10%	-0.1±0.3	0.0±7.6	0.0±3.0
	20%	-0.2±0.	-1.4±14.0	0.0±6.4
Eigen-values (%)	5%	-0.1±0.1	0.0±2.0	0.0±0.9
	10%	-0.2±0.3	-0.1±4.0	0.0±1.7
	20%	-0.9±1.0	-1.1±7.6	-0.4±3.6
Pitches (%)	5%	0.0±0.1	0.3±0.5	0.0±0.3
	10%	0.1±0.2	1.2±1.4	-0.2±0.7
	20%	0.4±0.8	3.8±6.4	-0.6±3.2

Table A.6: Mean errors and standard deviations for eigenscrew direction. pitch and eigenvalue for each of the eigenscrews of C_6 at 5%, 10 % and 20% noise content.

A.7 Two Translational DOFs System: Equal Compliance

The compliance matrix was

$$C_7 = \begin{bmatrix} 5.00 & 0 & 0 & 0 & 0 & 0 \\ 0 & 5.00 & 0 & 0 & 0 & 0 \\ 0 & 0 & 0.02 & 0 & 0 & 0 \\ 0 & 0 & 0 & 0.03 & 0 & 0 \\ 0 & 0 & 0 & 0 & 0.10 & 0 \\ 0 & 0 & 0 & 0 & 0 & 0.05 \end{bmatrix}$$

The normalized eigenscrews of C_7 were

$$e = \begin{bmatrix} 0 & 1.00 & 0 & 0 & 1.00 & 0 \\ 1.00 & 0 & 0 & 0 & 0 & 1.00 \\ 0 & 0 & 1.00 & 1.00 & 0 & 0 \\ 0 & -12.91 & 0 & 0 & 12.91 & 0 \\ -7.07 & 0 & 0 & 0 & 0 & 7.07 \\ 0 & 0 & -0.63 & 0.63 & 0 & 0 \end{bmatrix} \times 10^{-3}$$

The corresponding eigenvalues were

$$\vec{\lambda} = \begin{bmatrix} -0.71 & -0.39 & -0.03 & 0.03 & 0.39 & 0.71 \end{bmatrix} \times 10^{-3}$$

$$\vec{h} = \begin{bmatrix} -7.07 & -12.91 & -0.63 & 0.63 & 12.91 & 7.07 \end{bmatrix}$$

$$\vec{C_R} = \begin{bmatrix} 0.10 & 0.03 & 0.05 & 0.05 & 0.03 & 0.10 \end{bmatrix} \times 10^{-3}$$

$$\vec{C_T} = \begin{bmatrix} 5.00 & 5.00 & 0.02 & 0.02 & 5.00 & 5.00 \end{bmatrix} \times 10^{-3}$$

The system had three orthogonal compliant axes. Eigenscrew decomposition correctly identified the two translationally compliant axes. The third compliant axis was stiff. The condition number of the matrix was 250. The compliance matrix approaches algebraic multiplicity. The residual errors for the approximant were presented in Figure A.7. A summary of the errors in the eigenscrew directions. the eigenvalues and the eigenscrew pitches is presented in Table A.7.

	Noise	1	2	3
Eigen-screw $Dir^{ns}(^o)$	5%	0.1±1.2	0.0±2.2	0.0±0.1
	10%	0.4±2.2	0.4±4.0	-0.1±0.3
	20%	-0.1±4.3	-0.1±7.9	-0.2±0.6
Eigen-values (%)	5%	0.0±1.2	0.0±2.1	-0.1±0.1
	10%	-0.1±2.1	-0.4±4.1	-0.3±0.3
	20%	-0.2±4.3	-0.9±7.3	-1.3±1.4
Pitches (%)	5%	0.0±0.3	0.1±0.3	0.0±0.1
	10%	0.1±0.5	0.4±0.6	0.1±0.3
	20%	0.4±1.3	1.6±1.5	0.6±1.0
	Noise	4	5	6
Eigen-screw $Dir^{ns}(^o)$	5%	0.0±0.1	-0.3± 2.1	-0.2±1.1
	10%	-0.1±0.3	0.1±4.1	-0.3±2.2
	20%	-0.2±0.6	0.2±7.8	-0.2±4.3
Eigen-values (%)	5%	-0.1±0.1	-0.1±2.1	0.0±1.2
	10%	-0.3±0.3	-0.1±4.1	-0.1±2.2
	20%	-1.2±1.3	-1.1±7.3	-0.6±4.3
Pitches (%)	5%	0.0±0.1	0.1±0.3	0.0±0.3
	10%	0.1±0.3	0.4±0.6	0.1±0.5
	20%	0.6±1.0	1.6±1.4	0.4± 1.3

Table A.7: Mean errors and standard deviations for eigenscrew direction, pitch and eigenvalue for each of the eigenscrews of C_7 at 5%, 10 % and 20% noise content.

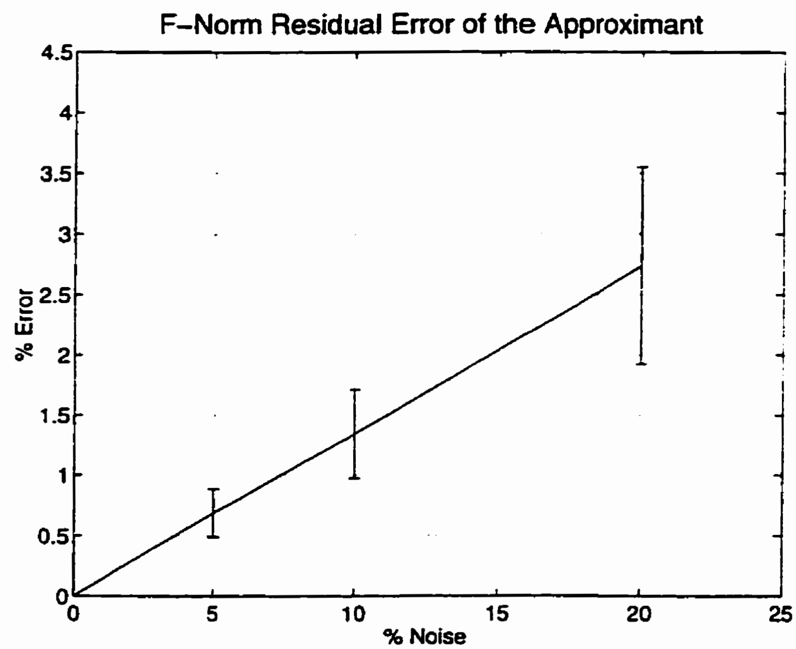

Figure A.7: Error of the approximant relative to compliance matrix C_7.

A.8 Three Rotational DOFs System: Two Equal Compliances

The compliance matrix was

$$C_8 = \begin{bmatrix} 0.02 & 0 & 0 & 0 & 0 & 0 \\ 0 & 0.03 & 0 & 0 & 0 & 0 \\ 0 & 0 & 0.03 & 0 & 0 & 0 \\ 0 & 0 & 0 & 5.00 & 0 & 0 \\ 0 & 0 & 0 & 0 & 5.00 & 0 \\ 0 & 0 & 0 & 0 & 0 & 2.50 \end{bmatrix}$$

The normalized eigenscrews of C_8 were

$$e = \begin{bmatrix} 0 & 1.00 & 0 & 0 & 1.00 & 0 \\ 1.00 & 0 & 0 & 0 & 0 & 1.00 \\ 0 & 0 & 1.00 & 1.00 & 0 & 0 \\ 0 & -0.06 & 0 & 0 & 0.06 & 0 \\ -0.08 & 0 & 0 & 0 & 0 & 0.08 \\ 0 & 0 & -0.11 & 0.11 & 0 & 0 \end{bmatrix}$$

The corresponding eigenvalues were

$$\vec{\lambda} = \begin{bmatrix} -0.39 & -0.32 & -0.27 & 0.27 & 0.32 & 0.39 \end{bmatrix} \times 10^{-3}$$

The eigenscrew pitches were

$$\vec{h} = \begin{bmatrix} -0.08 & -0.06 & -0.11 & 0.11 & 0.06 & 0.08 \end{bmatrix}$$

The rotational compliances were

$$\vec{C_R} = \begin{bmatrix} 5.00 & 5.00 & 2.50 & 2.50 & 5.00 & 5.00 \end{bmatrix} \times 10^{-3}$$

The translational compliances were

$$\vec{C_T} = \begin{bmatrix} 0.03 & 0.02 & 0.03 & 0.03 & 0.02 & 0.03 \end{bmatrix} \times 10^{-3}$$

Again the system has three compliant axes and approaches the condition of algebraic multiplicity. Eigenscrew decomposition correctly identified the compliant axes and the magnitudes of rotational and translational compliance. The condition number of the matrix was 250. The residual errors of the approximant are summarized in Figure A.8. The errors in eigenscrew directions, pitches and eigenvalues are presented in Table A.8.

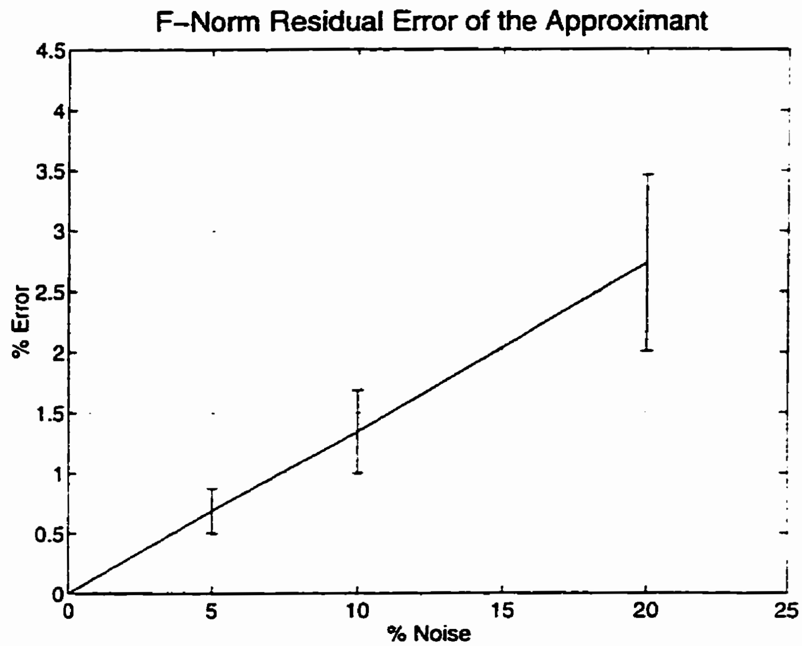

Figure A.8: Error of the approximant relative to compliance matrix C_8.

	Noise	1	2	3
Eigen- screw $Dir^{ns}(^o)$	5%	-0.1±5.6	0.1±6.1	-0.7±7.7000
	10%	-0.3±11.2	-0.8±15.0	-1.9±17.5
	20%	0.4±22.0	0.3±30.3	-2.7±32.4
Eigen- values (%)	5%	0.1±2.0	-0.1±2.4	-0.3±1.5
	10%	-0.4±5.5	0.1±5.9	-0.4±5.2
	20%	-6.4±13.0	6.1±14.3	0.2±13.5
Pitches (%)	5%	0.1±0.3	-0.6±0.8	0.7±1.2
	10%	0.0±2.7	-2.0±2.7	2.9±4.5
	20%	-3.6±8.3	-3.1±5.6	7.8±8.3
	Noise	4	5	6
Eigen- screw $Dir^{ns}(^o)$	5%	-0.8±7.8	-0.1±6.1	0.1±5.5
	10%	0.0±17.7	0.6±15.4	-0.5±11.5
	20%	-1.4±31.0	0.5±29.0	0.3±22.3
Eigen- values (%)	5%	-0.2±1.5	0.1±2.4	0.2±2.0
	10%	-0.4±5.5	0.1±5.7	-0.1±5.5
	20%	0.1±12.5	6.2±15.2	-7.3±14.4
Pitches (%)	5%	0.7±1.2	-0.6±0.8	0.1±0.3
	10%	2.9±4.6	-2.0±2.7	-0.2±3.8
	20%	7.4±8.0	-3.0±5.3	-3.5±8.5

Table A.8: Mean errors and standard deviations for eigenscrew direction, pitch and eigenvalue for each of the eigenscrews of C_8 at 5%, 10 % and 20% noise content.

A.9 Three Rotational DOFs System: Equal Magnitude

The compliance matrix was

$$C_9 = \begin{bmatrix} 0.02 & 0 & 0 & 0 & 0 & 0 \\ 0 & 0.03 & 0 & 0 & 0 & 0 \\ 0 & 0 & 0.03 & 0 & 0 & 0 \\ 0 & 0 & 0 & 5.00 & 0 & 0 \\ 0 & 0 & 0 & 0 & 5.00 & 0 \\ 0 & 0 & 0 & 0 & 0 & 5.00 \end{bmatrix}$$

The normalized eigenscrews of C_9 were

$$e = \begin{bmatrix} 0 & 0 & 1.00 & 1.00 & 0 & 0 \\ 1.00 & 0 & 0 & 0 & 0 & 1.00 \\ 0 & 1.00 & 0 & 0 & 1.00 & 0 \\ 0 & 0 & -0.06 & 0.06 & 0 & 0 \\ -0.08 & 0 & 0 & 0 & 0 & 0.08 \\ 0 & -0.08 & 0 & 0 & 0.08 & 0 \end{bmatrix} \times 10^{-3}$$

The corresponding eigenvalues were

$$\vec{\lambda} = \begin{bmatrix} -0.39 & -0.39 & -0.32 & 0.32 & 0.39 & 0.39 \end{bmatrix} \times 10^{-3}$$

The eigenscrew pitches were

$$\vec{h} = \begin{bmatrix} -0.08 & -0.08 & -0.06 & 0.06 & 0.08 & 0.08 \end{bmatrix}$$

The rotational compliances were

$$\vec{C_R} = \begin{bmatrix} 5.00 & 5.00 & 5.00 & 5.00 & 5.00 & 5.00 \end{bmatrix} \times 10^{-3}$$

The translational compliances were

$$\vec{C_T} = \begin{bmatrix} 0.03 & 0.03 & 0.02 & 0.02 & 0.03 & 0.03 \end{bmatrix} \times 10^{-3}$$

There were three compliant axes in the system. The rotational degrees of freedom were correctly identified by the eigenscrew decomposition. This system contains algebraic multiplicity. The condition number of the matrix was 250. The residual errors of the approximant are presented in Figure A.9. A summary of the errors in the eigenscrew directions, the eigenvalues and the eigenscrew pitches are presented in Table A.9.

	Noise	1	2	3
Eigen-screw $Dir^{ns}(^o)$	5%	-0.3±11.6	-0.1±27.1	-3.5±25.0
	10%	-0.6±17.0	-0.8±28.3	-4.3±25.0
	20%	-0.9±23.2	-0.6±32.4	-3.8±30.2
Eigen-values (%)	5%	-11.9±10.0	-0.1±2.6	14.3±10.5
	10%	-10.8±11.5	0.2±4.7	12.1±11.6
	20%	-13.5±14.6	0.6±9.7	15.4±15.3
Pitches (%)	5%	-0.1±0.4	0.1±0.3	0.0±0.40
	10%	-0.5±1.2	0.5±0.9	0.0±1.3
	20%	-2.2±3.4	1.6±2.6	0.4±2.9
	Noise	4	5	6
Eigen-screw $Dir^{ns}(^o)$	5%	-1.4±25.2	-0.7±27.1	-0.2±11.4
	10%	-1.2±24.7	-1.7±28.4	-0.3±16.8
	20%	0.6±30.0	-0.1±33.6	-0.3±23.4
Eigen-values (%)	5%	16.0±11.7	-1.3±2.1	-11.7±10.0
	10%	15.3±13.6	-2.3±3.8	-10.6±11.8
	20%	17.3±16.8	-3.6±9.8	-15.0±14.7
Pitches (%)	5%	0.0±0.4	0.1±0.3	-0.1±0.4
	10%	-0.1±1.1	0.5±1.1	-0.4±1.2
	20%	0.4±2.7	1.8±2.9	-2.3±3.4

Table A.9: Mean errors and standard deviations for eigenscrew direction, pitch and eigenvalue for each of the eigenscrews of C_9 at 5%, 10 % and 20% noise content.

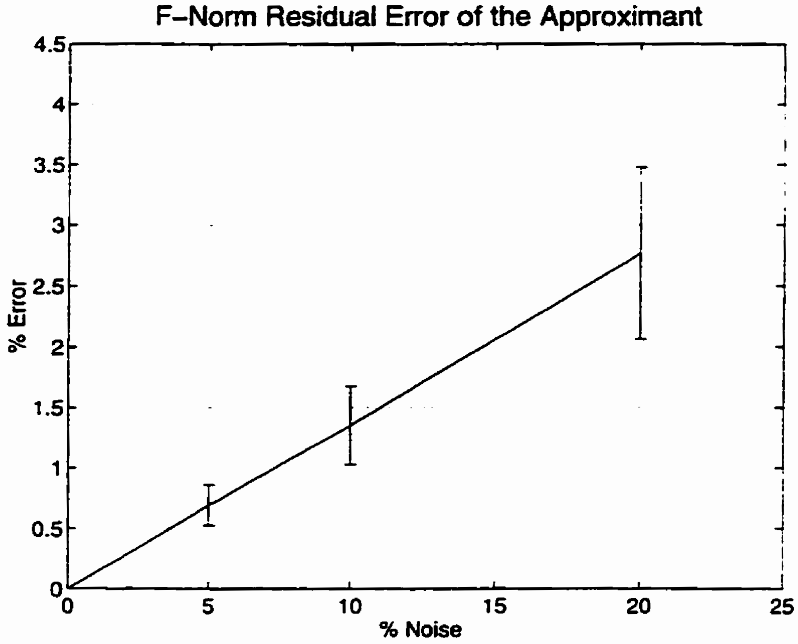

Figure A.9: Error of the approximant relative to compliance matrix C_9.

A.10 Six DOFs System

The compliance matrix was

$$C_{10} = \begin{bmatrix} 10.00 & 0 & 0 & 0 & 0 & 0 \\ 0 & 5.00 & 0 & 0 & 0 & 0 \\ 0 & 0 & 2.50 & 0 & 0 & 0 \\ 0 & 0 & 0 & 5.00 & 0 & 0 \\ 0 & 0 & 0 & 0 & 2.50 & 0 \\ 0 & 0 & 0 & 0 & 0 & 1.25 \end{bmatrix} \times 10^{-3}$$

The normalized eigenscrews of C_{10} were

$$e = \begin{bmatrix} 1.00 & 0 & 0 & 0 & 0 & 1.00 \\ 0 & 1.00 & 0 & 0 & 1.00 & 0 \\ 0 & 0 & 1.00 & 1.00 & 0 & 0 \\ -1.41 & 0 & 0 & 0 & 0 & 1.41 \\ 0 & -1.41 & 0 & 0 & 1.41 & 0 \\ 0 & 0 & -1.41 & 1.41 & 0 & 0 \end{bmatrix}$$

The corresponding eigenvalues were

$$\vec{\lambda} = \begin{bmatrix} -7.10 & -3.50 & -1.80 & 1.80 & 3.50 & 7.10 \end{bmatrix} \times 10^{-3}$$

The eigenscrew pitches were

$$\vec{h} = \begin{bmatrix} -1.41 & -1.41 & -1.41 & 1.41 & 1.41 & 1.41 \end{bmatrix}$$

The rotational compliances were

$$\vec{C_R} = \begin{bmatrix} 5.00 & 2.50 & 1.25 & 1.25 & 2.50 & 5.00 \end{bmatrix}^{-3}$$

The translational compliances were

$$\vec{C_T} = \begin{bmatrix} 10.00 & 5.00 & 2.50 & 2.50 & 5.00 & 10.00 \end{bmatrix}$$

The compliance matrix had three compliant axes. All six DOFs were correctly identified by eigenscrew decomposition. The condition number of the matrix was 8. The residual errors for the approximant are summarized in Figure A.10. The errors in the eigenscrew directions, the eigenvalues and the eigenscrew pitches are presented in Table A.10.

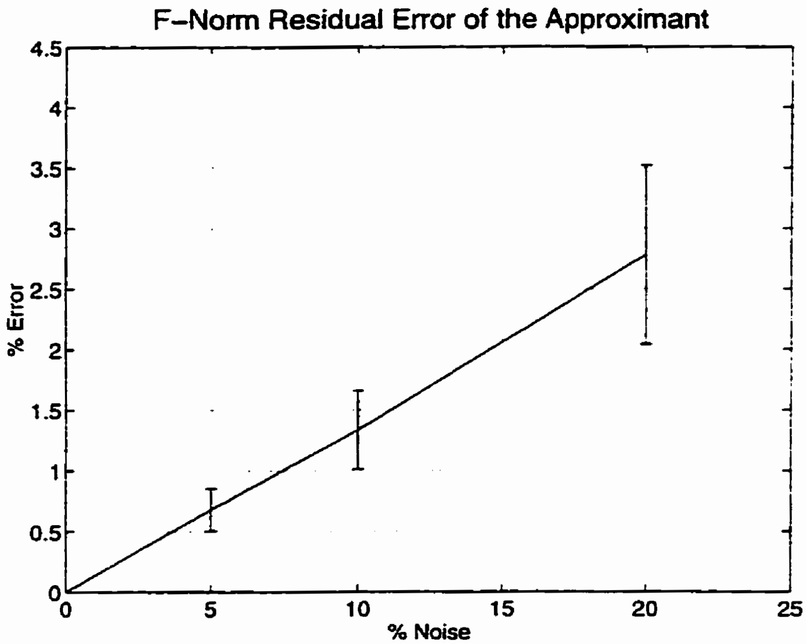

Figure A.10: Error of the approximant relative to compliance matrix C_{10}.

	Noise	1	2	3
Eigen-screw $\mathrm{Dir}^{\mathrm{ns}}(^o)$	5%	0.0±0.3	0.0±0.3	0.0±0.3
	10%	0.0±0.6	0.0±0.7	-0.2±0.5
	20%	-0.1±1.1	0.0±1.3	-0.2±1.1
Eigen-values (%)	5%	0.0±0.4	0.0±0.5	0.0±0.5
	10%	-0.2±0.8	-0.2±0.9	-0.3±0.9
	20%	-0.9±1.7	-1.0±1.7	-1.0±1.7
Pitches (%)	5%	0.0±0.4	0.0±0.4	0.0±0.4
	10%	0.0±0.7	0.0±0.7	0.0±0.7
	20%	0.1±1.4	0.0±1.4	0.0±1.4
	Noise	4	5	6
Eigen-screw $\mathrm{Dir}^{\mathrm{ns}}(^o)$	5%	0.0±0.3	0.0±0.3	0.0±0.3
	10%	0.0±0.6	0.0±0.7	0.0±0.6
	20%	-0.1±1.1	0.0±1.2	0.1±1.1
Eigen-values (%)	5%	-0.1±0.5	0.0±0.4	0.0±0.4
	10%	-0.3±0.9	-0.3±0.9	-0.3±0.8
	20%	-1.0±1.7	-1.0±1.6	-0.9±1.6
Pitches (%)	5%	0.0±0.4	0.0±0.4	0.0±0.4
	10%	0.0±0.7	0.0±0.7	0.0±0.7
	20%	0.0±1.4	0.0±1.4	0.1±1.4

Table A.10: Mean errors and standard deviations for eigenscrew direction, pitch and eigenvalue for each of the eigenscrews of C_{10} at 5%, 10 % and 20% noise content.

IMAGE EVALUATION TEST TARGET (QA-3)

150mm

6"

APPLIED IMAGE, Inc
1653 East Main Street
Rochester, NY 14609 USA
Phone: 716/482-0300
Fax: 716/288-5989